JYVÄSKYLÄ STUDIES IN BIOLOGICAL AND ENVIRONMENTAL SCIENCE
307

Leena Meriläinen

Characterization and Immunological Aspects of *Borrelia Burgdorferi* Pleomorphic Round Bodies

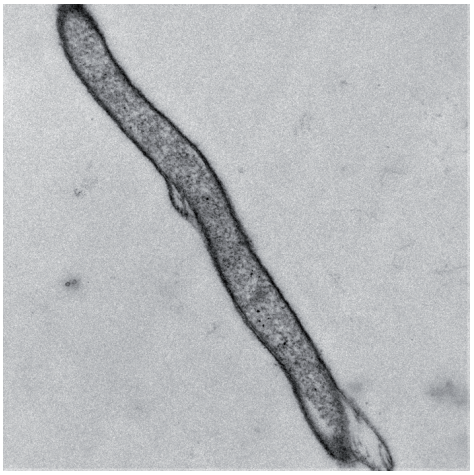

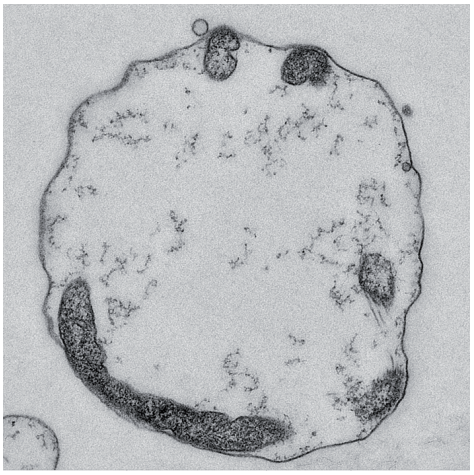

JYVÄSKYLÄN YLIOPISTO

JYVÄSKYLÄ STUDIES IN BIOLOGICAL AND ENVIRONMENTAL SCIENCE 307

Leena Meriläinen

Characterization and Immunological Aspects of *Borrelia Burgdorferi* Pleomorphic Round Bodies

Esitetään Jyväskylän yliopiston matemaattis-luonnontieteellisen tiedekunnan suostumuksella
julkisesti tarkastettavaksi yliopiston Ylistönrinteellä salissa YAA303
lokakuun 23. päivänä 2015 kello 12.

Academic dissertation to be publicly discussed, by permission of
the Faculty of Mathematics and Science of the University of Jyväskylä,
in Ylistönrinne, hall YAA303, on October 23, 2015 at 12 o'clock noon.

UNIVERSITY OF JYVÄSKYLÄ

JYVÄSKYLÄ 2015

Characterization and Immunological Aspects of *Borrelia Burgdorferi* Pleomorphic Round Bodies

JYVÄSKYLÄ STUDIES IN BIOLOGICAL AND ENVIRONMENTAL SCIENCE 307

Leena Meriläinen

Characterization and Immunological Aspects of *Borrelia Burgdorferi* Pleomorphic Round Bodies

UNIVERSITY OF JYVÄSKYLÄ

JYVÄSKYLÄ 2015

Editors
Varpu Marjomäki
Department of Biological and Environmental Science, University of Jyväskylä
Pekka Olsbo, Sini Tuikka
Publishing Unit, University Library of Jyväskylä

Jyväskylä Studies in Biological and Environmental Science
Editorial Board

Jari Haimi, Anssi Lensu, Timo Marjomäki, Varpu Marjomäki
Department of Biological and Environmental Science, University of Jyväskylä

Cover pictures: Transmission electron microscopy illustrations of Borrelia burgdorferi spirochete (left) and round body (right). Images by Leena Meriläinen.

URN:ISBN:978-951-39-6335-4
ISBN 978-951-39-6335-4 (PDF)

ISBN 978-951-39-6334-7 (nid.)
ISSN 1456-9701

Jyväskylä University Printing House, Jyväskylä 2015

ABSTRACT

Meriläinen, Leena
Characterization and immunological aspects of *Borrelia burgdorferi* pleomorphic round bodies.
Jyväskylä: University of Jyväskylä, 2015, 64 p.
(Jyväskylä Studies in Biological and Environmental Science
ISSN 1456-9701; 307)
ISBN 978-951-39-6334-7 (nid.)
ISBN 978-951-39-6335-4 (PDF)
Yhteenveto: *Borrelia burgdorfin* pleomorfisten muotojen karakterisointi ja immunologinen merkitys
Diss.

Borrelia burgdorferi sensu lato–bacteria causes the most common tick-borne infection, Lyme disease. *B. burgdorferi* is pleomorphic and can change the morphology dramatically as a response to environmental conditions to avoid immune response of the host or to promote adherence and dissemination in the host. The role of these pleomorphic variants in Lyme disease pathogenesis has been unclear and debated. This thesis focused on the characterization and immune reactions initiated by spherical round body forms (RBs) of *B. burgdorferi*. The aim was to study induction, cell envelope morphology and components, bioactivity, and phagocytosis of RBs. In addition, the immune response stimulated by RBs was analyzed *in vitro* and the suitability of RBs as a candidate for Lyme disease diagnosis was evaluated. Different culturing condition such as the presence of human serum induced pleomorphic forms. RBs displayed low metabolic activity; however, they were able to revert back to parental spirochetes. The analysis of the outer envelope revealed that RBs are not cell wall deficient as previously suggested, and they have different biochemical signature compared to spirochetes. We also presented the different protein expression between the RBs and spirochetes. Interestingly, results provided evidence that RBs are phagocytosed and processed differently in macrophages. Furthermore, RBs stimulated higher production of MCP-1 chemokine and diminished the production of IL-1β, IL-1ra, IL-6, MIF, MIP-1β and RANTES when compared to spirochetes. The immune response seen in Lyme disease patients was stronger against RBs in some cases. ELISA experiments indicated that incorporation of RBs could improve sensitivity and specificity of Lyme diagnosis and that RBs are a good antigen candidate in Lyme diagnostic tools.

Keywords: *Borrelia burgdorferi*, pleomorphism, round bodies, phagocytosis, immune response.

Leena Meriläinen, University of Jyväskylä, Department of Biological and Environmental Science, P.O. Box 35, Fi-40014 University of Jyväskylä, Finland

Author's address Leena Meriläinen
Department of Biological and Environmental Science
P.O. Box 35
FI-40014 University of Jyväskylä
leena.m.merilainen@jyu.fi

Supervisor Adjunct Professor, Docent Leona Gilbert
Department of Biological and Environmental Science
P.O. Box 35
FI-40014 University of Jyväskylä

Reviewers MD, Horst Maxeiner
Borreliose Centrum Augsburg
Morellstraße 33
86159 Augsburg
USA

PhD, Jyotsna Shah,
IGeneX Inc.
795 San Antonio Road
Palo Alto, CA 94303
USA

Opponent Assistant Professor Monica Embers
Tulane University
18703 Three Rivers Road
Covington, LA 70433-8915
USA

CONTENTS

LIST OF ORIGINAL PUBLICATIONS

The thesis is based on the following original articles, which are referred in the text by Roman numerals I–III.

I Meriläinen L., Herranen A., Schwarzbach A., Gilbert L. 2015. Morphological and biochemical features of *Borrelia burgdorferi* pleomorphic forms. *Microbiology.* 161:516–527.

II Meriläinen L., Brander H., Herranen A., Schwarzbach A., Gilbert L. 2015. Pleomorphic forms of *Borrelia burgdorferi* induce distinct immune responses. Submitted manuscript.

III Puttaraksa K., Meriläinen L., Campillo A., Schwarzbach A., Garcia-Nogales P., Gilbert L. 2015. An Improved and Novel Multiplex ELISA for Lyme Disease diagnosis. Submitted manuscript.

RESPONSIBILITIES IN THE ARTICLES

I The original ideas for analysis of pleomorphic forms were developed by me, Armin Schwarzbach and Leona Gilbert. I designed the experiments together with Leona Gilbert except the composition analysis together with Anni Herranen and Leona Gilbert. I conducted the induction, quantification, reversion and ATP determination of pleomorphic forms as wells as morphology analysis using TEM including data analysis. I wrote the article together with Leona Gilbert.

II The experiments were designed together with all coauthors. I performed the phagocytosis index studies, cytokine analysis and most of the colocalization experiments and data analysis. The Western blot analysis was conducted with Anni Herranen. I wrote the article together with Leona Gilbert.

III The experimental planning was performed together with all coauthors. I was responsible for the pleomorphic round body part of the ELISA experiments. I wrote the article together with Kanoktip Puttaraksa and Leona Gilbert.

ABBREVIATIONS

ACA	*acrodermatitis chronicum migrans*
ATP	adenosine triphosphate
BFL	biofilm-like aggregation
BODIPY	boron-dipyrromethene
BSK-II	Barbour-Stoenner-Kelly II medium
CDC	US Center for disease Control and Prevention
CRASP	complement regulator-acquiring surface protein
CSF	cerebrospinal fluid
CWD	cell wall deficient
C6	highly conserved 25-amino acid peptide from the sixth region of VslE
DIC	differential interference contrast microscopy
EIA	enzyme immunoassay
ELISA	enzyme-linked immunosorbent assay
EM	*erythema migrans*
EPS	extracellular polymeric substance
EUCALB	European Concerted Action On Lyme Borreliosis
FlaB	flagellar protein B
GluNAc	N-acetylglucosamine polysaccharide
HS	human serum
IDSA	Infectious Disease Society of America
IFA	immunofluorescence assay
Ig	immunoglobulin
IRF	interferon regulatory factor
IL	interleukin
ILADS	International Lyme and Associated Diseases Society
i.v.	intravenous
LPS	lipopolysaccharides
MARCO	macrophage receptor with collagenous structure
MHC	major histocompatibility complex
MyD88	myeloid differentiation primary response protein
Osp	outer surface protein
PH	phase contrast microscopy
PhI	phagocytic index
PI	propidium iodide
PMA	phorbol 12-myristate 13-acetate
PTLDS	post-treatment Lyme disease syndrome
PRR	pattern recognition receptor
RB	round body
RND	resistance-nodulation-cell division
TEM	transmission electron microscopy
THP-1	human acute monocytic leukemia cell line
TNF	tumor necrosis factor
TLR	toll-like receptor
VslE	variable surface lipoprotein E
WB	Western blot (immunoblot)
WGA	wheat germ agglutinin

1 INTRODUCTION

Currently, Lyme disease is one of the emerging infectious diseases in the world. Due to the climate change ticks, that transmit the disease causing agent bacteria *Borrelia burgdorferi*, have spread in the new areas and the incidence of disease has increased in the northern hemisphere (Lindgren and Jaenson 2006). The history of Lyme disease goes back to 1883 when Alfred Buchwald described the skin condition *acrodermatitis chronicum atropicans* in Germany (Buchwald 1883). At the time the connection of this skin rash to microbial infection was not understood. In 1909 Arvid Afzelius reported on patients with the skin rash *erythema migrans* and thought already back then that the infection causing agent may be tick-transmitted (Afzelius 1910). Since the first reports, it took almost a century to find the pathogen behind these skin manifestations. In 1975, two concerned mothers reported an outbreak of juvenile rheumatoid arthritis in small towns Lyme, Old Lyme and East Haddam in Connecticut. After extensive investigation led by Dr. Allan Steere, researchers found that skin lesions and tick bites often precede the arthritis symptoms. They came to a conclusion that the disease seen in the area was not normal juvenile arthritis and it was named Lyme disease. In 1981, Willy Burgdorfer finally discovered the spirochete bacterium *Borrelia burgdorferi* as a cause for Lyme disease.

Since the discovery of *B. burgdorferi*, the basic characteristics of this bacterium, pathogenic mechanisms, immunological consequences as well as mechanism for immune evasion are quite well known. Furthermore, several immunological and molecular diagnostic methods have been developed for diagnosis of the disease. Despite this, diagnosis of Lyme disease is sometimes difficult because it is a multisystem disorder with varying disease symptoms. There are still many unresolved questions such as why some patients suffer from Lyme disease symptoms after antibiotic treatment? Or how is the ability of bacteria to take different forms related to the disease pathogens and should these forms be considered when developing new diagnostic tools and treatment protocols? As the disease has become a communal health problem there is a lot of public debate regarding how the disease should be handled.

The aim of this study was to increase basic knowledge about pleomorphic forms of *B. burgdorferi* and investigate the immune response against these variants. These results indicated that pleomorphic round bodies have different biochemical characteristics compared to spirochetes. Albeit that round bodies are dormant they can recruit metabolic and motility components and revert to mobile spirochetes in favorable conditions. Furthermore, round bodies induce distinct immune response compared to spirochetes *in vitro* and Lyme disease patients react differently against these forms.

2 REVIEW OF THE LITERATURE

2.1 *Borrelia burgdorferi*

The tick-transmitted *Borrelia burgdorferi* is a corkscrew shaped spirochete, which is about 10–30 μm long and 0.25–0.5 μm wide. *B. burgdorferi* belongs to the family of *Spirochaetaceae.* Further, it is part of a *Borrelia* genus, a unique branch remarkably different to any other bacteria and other spirochetes in the family (Paster *et al.* 1991). The genus of *Borrelia* consists of two main branches: spirochetes causing either Lyme disease or relapsing fever. Currently, 20 subspecies belong to the Lyme disease causing *B. burgdorferi sensu lato* group (Wang *et al.* 2014); however, all the subspecies are not pathogenic, or their pathogenicity potential is not known. The three genospecies including *B. burgdorferi sensu stricto*, *B. garinii*, and *B. afzelii* are the most common causative agents of Lyme disease. All these three genospecies are common in Europe while only *B. burgdorferi sensu stricto* cause infections in USA (Rudenko *et al.* 2011).

2.1.1 Genome

The genome of *B. burgdorferi sensu stricto* strain B31 was sequenced mostly in 1997 (Fraser *et al.* 1997) and completed in 2000 (Casjens *et al.* 2000). It consists of about 900-kbp linear chromosome and nine linear and 12 circular plasmids that comprise together about 612-kbp. The linear chromosome is conserved within the genus and contains important genes for metabolism and replication. The number of plasmids and their content varies between the species and strains. Plasmids carry a large number of genes encoding for surface lipoproteins and proteins that bacterium requires when interacting between the arthropod and vertebrate host environments (Casjens *et al.* 2010). *B. burgdorferi* is an exceptional bacterium because it lacks genes for the biosynthesis of amino acid, fatty acids, enzyme cofactors, and nucleotides. The biosynthetic disability makes it very dependent on nutrients from the host (Toledo 2011).

2.1.2 The unique morphology and structure

B. burgdorferi has a planar, sinusoidal flat-wave morphology (Goldstein *et al.* 1994, Wolgemuth *et al.* 2006). The fluorescence microscopy image (Fig. 1) demonstrates the typical shape of the *B. burgdorferi*. The morphology is very similar to another pathogenic spirochete *Treponema pallidum*, the cause of syphilis (Izard *et al.* 2009). In addition to the motility function, flagella have an important role defining the cell shape (Motaleb *et al.* 2000). *B. burgdorferi* has 7-11 flagella attached to the other pole of the cell and extend and rotate towards the center (Barbour and Hayes 1986, Charon *et al.* 2009).

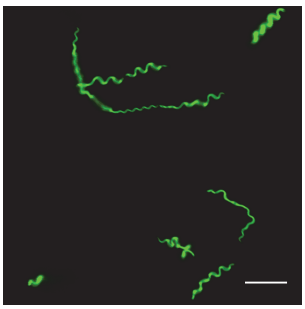

FIGURE 1 Fluorescence microscopy image of green fluorescent *B. burgdorferi* strain GCB726 spirochetes. Scale bar 10 μm.

The cell envelope of *B. burgdorferi* consists of two lipid membranes (Fig. 2). The inner membrane covers the protoplasmic cylinder that entails the cytoplasm and genetic material. Inner membrane has a high density of integral membrane proteins, which mostly are transporters. Periplasmic space with the cell wall (peptidoglycan layer) and flagellar filaments are located between the outer and inner membranes (Barbour and Hayes 1986, Kudryashev *et al.* 2009). *B. burgdorferi* has flagella inside the cell, whereas flagella are extracellular components of many other bacteria. Peptidoglycan wall defines the cell shape and provides mechanical strength in osmotic pressure (Vollmer *et al.* 2008). It is a mesh-like layer composed of β1,4-linked N-acetylglucosamine and N-acetylmuramic acid chains crosslinked by short peptides (Schleifer and Kandler 1972). Outer membrane also has an amorphous slime layer around it (Barbour and Hayes 1986). *B. burgdorferi* has transmembrane resistance-nodulation-cell division (RND)-type efflux system that is involved with antibiotic resistance and infectivity in mice (Bunikis *et al.* 2008).

Because of the double membrane structure, typical to Gram-negative bacteria, *B. burgdorferi* is often classified mistakenly as Gram-negative. In fact, it has several significant differences to Gram-negative bacteria that make this bacterium very exceptional. *B. burgdorferi* does not have lipopolysaccharides (LPS) on the outer membrane (Takayama *et al.* 1987) that usually elicit a strong immune response in eukaryotic species. Instead, the outer membrane has immunogenic glycolipids that stimulate antibody production (Ben-Menachem *et al.* 2003). The

another striking difference to gram-negative bacteria is the huge number and variation of lipoproteins on the *B. burgdorferi* cell surface (Brandt *et al.* 1990). They aid in transmission to the host, persistence, and trigger immune response. The outer membrane displays also a low density of proteins that have transmembrane domains such as porins (Bergström and Zückert 2010). Outer membrane porins have also been reported as reviewed in Bunikis *et al.* 2008. Furthermore, the flagella are in the periplasmic space (Barbour and Hayes 1986) while usually bacteria have them on the outside of the cell.

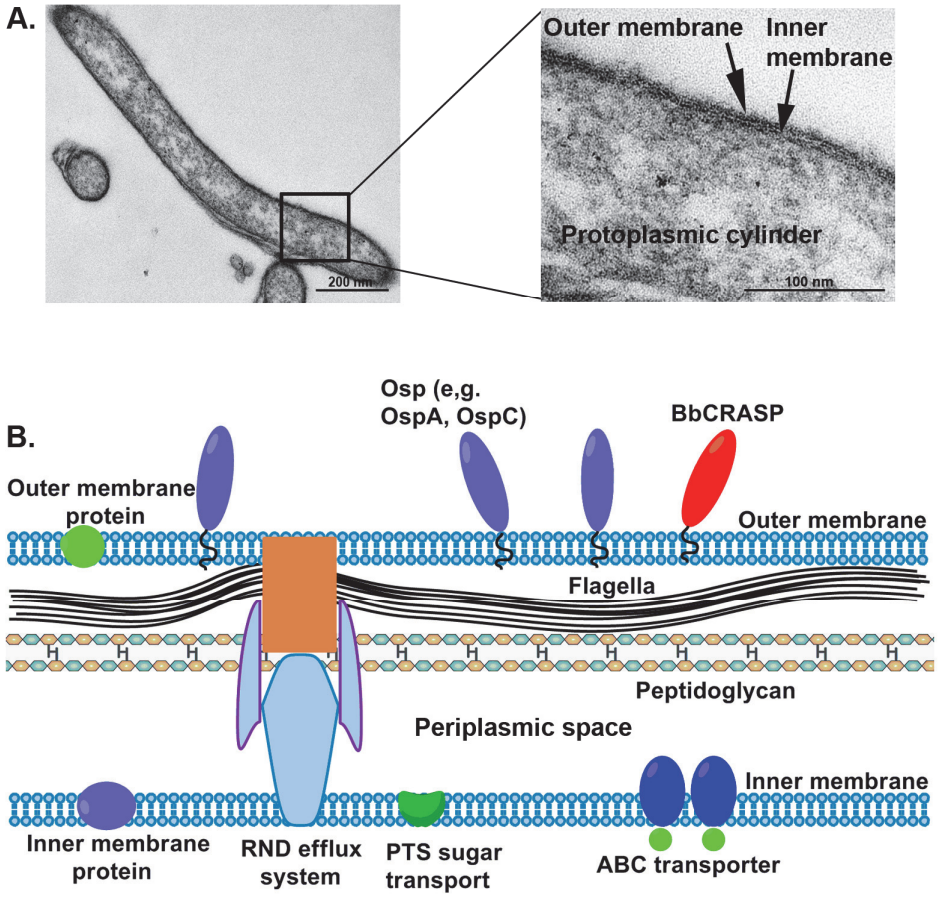

FIGURE 2 *B. burgdorferi* cell envelope. A) TEM images of spirochete (left) and zoomed view of the outer and inner membranes and protoplasmic cylinder of the spirochete (right). B) Simplified schematic illustration of the *B. burgdorferi* cell envelope components. Outer and inner membrane encloses the periplasmic space with flagella and peptidoglycan layer. Outer membrane is rich with outer surface proteins (Osps), complement regulator-acquiring surface proteins (BbCRASPs) and other outer integral membrane proteins. Inner membrane contains membrane proteins, phosphotransferase (PTS) transport system, ATP-binding cassette (ABC) transporters and transmembral resistant-nodulation-division (RND) efflux pump. Modified from Radolf *et al.* 2012.

2.1.3 Pleomorphic forms

B. burgdorferi is pleomorphic and can have other than typical spirochete morphologies during its life cycle when it encounters environmental stress. The Fig. 3 presents the differential interference contrast (DIC) microscopy images of different pleomorphic forms of *B. burgdorferi*. The first publication about pleomorphic bacteria was published in 1899 (Winkler 1899). Since then, pleomorphism has been reported in both Gram-negative and Gram-positive clinically significant bacteria such as *Escherichia coli* and *Listeria monocytogenes* (Domingue and Woody 1997, Dell'Era *et al.* 2009). Most commonly reported atypical variants are called L-forms, cell wall deficient forms (CWD), spheroplasts, or protoplasts. They can form *in vivo* or be induced *in vitro* by lytic enzymes or with antibiotics that inhibit the peptidoglycan biosynthesis (Domingue and Woody 1997, Briers *et al.* 2012). As a result, the complete or partial loss of the cell wall leads to the transformation of the morphology (Glover *et al.* 2009). CWD forms can recover and resynthesize the lost peptidoglycan cell wall without existing peptidoglycan molecules as a template (Kawai *et al.* 2014). In addition to spherical forms, bacteria can have other forms such as biofilms or have filamentous (Justice *et al.* 2004) shapes.

Different forms of *B. burgdorferi* have been induced by changing environmental factors such as pH (Murgia and Cinco 2004), exposure to antibiotics (Barbour *et al.* 1982, Schaller and Neubert 1994, Kersten *et al.* 1995, Mursic *et al.* 1996, Murgia *et al.* 2002, Sapi *et al.* 2011), introduction to distilled H_2O (Brorson and Brorson 1998, Murgia and Cinco 2004, Al-Robaiy *et al.* 2010), culturing without normal serum supplementation in BSK-II culture medium (Brorson and Brorson 1997, Alban *et al.* 2000), or in mammalian cell RPMI medium (Alban *et al.* 2000, Al-Robaiy *et al.* 2010, Dunham-Ems *et al.* 2012). Furthermore, the amount of pleomorphic forms increase when bacteria reach the stationary phase and culture is aging *in vitro* (Feng *et al.* 2015). The nomenclature to name pleomorphic variants of *B. burgdorferi* in the literature has been somewhat inconsistent and has hampered the research in this field. *B. burgdorferi* spherical shapes have been named as round bodies (RBs), CWD forms, L-forms, cysts, spheres or spheroplasts (Mursic *et al.* 1996, Brorson and Brorson 1997, Alban *et al.* 2000, Al-Robaiy *et al.* 2010, Stricker and Johnson 2011, Dunham-Ems *et al.* 2012). Nonetheless, the deficiency of the cell wall or encysted outer membrane typical to cysts has not been previously reported. Here, within this thesis spherical forms of *B. burgdorferi* are called round bodies (RBs) (Fig 2. lower left panel).

In addition, it is reported that *B. burgdorferi* can form blebs (Fig. 2, top right panel) (Kersten *et al.* 1995), granules and pearls detaching from the outer membrane (Barbour and Hayes 1986, Garon *et al.* 1989, Aberer and Duray 1991). The formation of blebs, the partial expansions of the outer membrane in spirochetes, occurs *in vitro* typically as a response to stress such as antibiotics, ageing or complement factors ((Barbour and Hayes 1986). They contain DNA and antigens that stimulate the immune response in patients. The actual function of blebs is still unknown although there are suggestions that they may transfer

genes or associate with disease pathogenesis (Garon *et al.* 1989). Their role in B cell mitogenesis has also been proposed (Whitmire and Garon 1993).

Interestingly, all three most common pathogenic *Borrelia* spp. species have been reported to form biofilm-like colonies (BFL) (Fig 2. lower right panel) *in vitro* on surfaces and in suspension (Barbour and Hayes 1986, Srivastava and de Silva 2009, Sapi *et al.* 2012, Timmaraju *et al.* 2015). Sapi and colleagues, 2012 have shown that *B. burgdorferi sensu stricto* BFLs *in vitro* have similar extracellular polymeric substances than *in vivo* biofilms. For example, Sapi and coworkers, 2012 demonstrated with staining and/or immunolabeling experiments the presence of alginate and extracellular DNA in the *in vitro* BFLs. Both substances are components of the extracellular polymeric substance (EPS) matrix, the main component of the biofilm communities among bacteria (Costerton 1999, Whitchurch *et al.* 2002). Timmaraju and collegues 2015 demonstrated these characteristics further with *B. garinii* and B. *afzelii* subspecies.

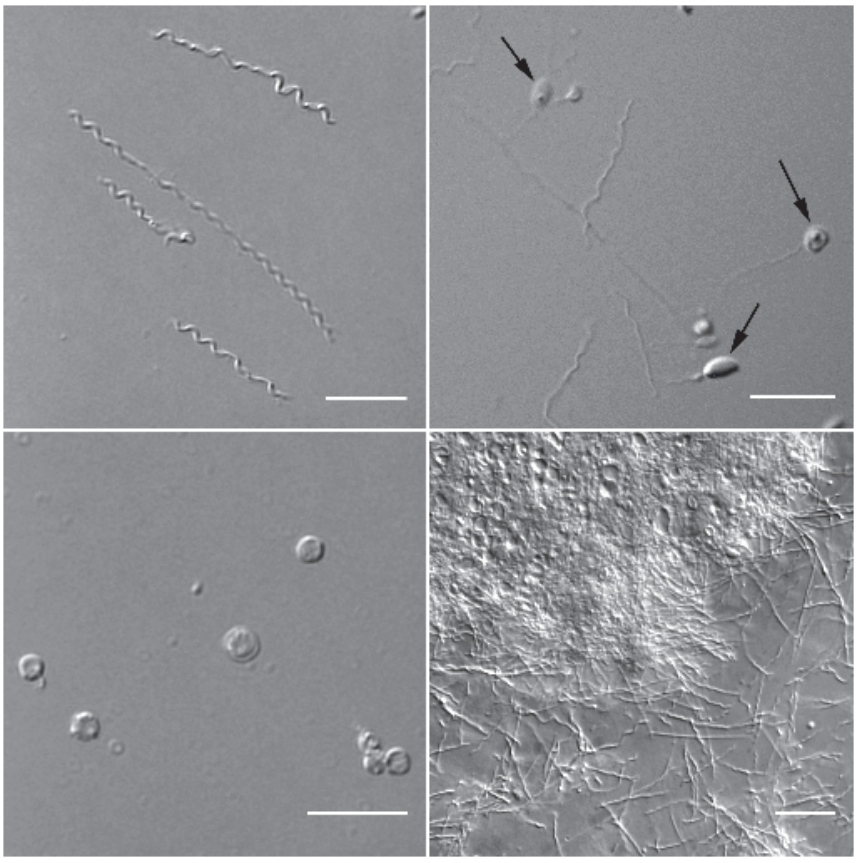

FIGURE 3 DIC microscopy images of different pleomorphic forms of *Borrelia burgdorferi*. The top panel illustrates typical spirochetes (left) and spirochetes with blebs depicted by black arrows (right). Lower panel represents H_2O induced round bodies (left) and a part from a biofilm-like aggregation formed *in vitro* (right). Scale bars 10 μm.

The role of pleomorphic variants is Lyme disease pathogenesis is controversial and extremely debated. There are studies that demonstrate the existence of spherical RBs in patient's tissue samples *in vivo* (MacDonald 1988, Hulinska *et al.* 1994, Aberer *et al.* 1996, Mattman 2001, Miklossy *et al.* 2008). Nonetheless, few recent publications have criticized and challenged the association of pleomorphic form in Lyme and other diseases (Onwuamaegbu *et al.* 2005, Lantos *et al.* 2014, Schnell *et al.* 2014). Due to the lack of clarity, basic knowledge, and standardization in the field, the pathogenicity has been difficult to demonstrate (Glover *et al.* 2009). Little by little, there is more and more evidence to show that the transformation of the morphology to spherical shape could be a survival strategy for bacteria, and aid in antibiotic resistance and immune evasion (Domingue and Woody 1997, Justice *et al.* 2008).

2.2 Lyme disease

2.2.1 Epidemiology

Lyme disease is the most prevalent arthropod-borne infection in Europe and North America, and it is endemic also in Asia (Mead 2011). In 2013, the US Center for Disease Control and Prevention (CDC) in the USA increased the estimate for Lyme disease cases from 30 000 to 300 000 per year (CDC 2013). In Europe around 85 000 cases are reported annually (Lindgren and Jaenson 2006) and in Finland 1679 people were diagnosed with Lyme disease in 2014 (Jaakola *et al.* 2015). The risk of infection correlates with the amount of ticks carrying the bacteria, reservoir hosts and density of ticks in the area. The incidence has increased in 30 years due to the climate change when ticks have spread to the higher latitudes, and because humans have moved to the forested habitats where mammalian reservoirs for *B. burgdorferi* are more present (Lindgren and Jaenson 2006, Radolf *et al.* 2010). However, it is proposed that an actual number of disease cases is three times higher than the number of reported cases in Europe (Hubalek 2009).

B. burgdorferi is transmitted by hard-bodied *Ixodes* ticks: In Europe *Ixodes ricinus* and *Ixodes persulcatus* while in the USA the *Ixodes scapularis* and *Ixodes pacificus* are the main vectors (Smith 2011). Tick life-cycle has four phases (egg, larva, nymph, adult) and after hatching from the egg, they require a blood meal after each life stage. Ticks become infected with *B. burgdorferi* when they feed on infected reservoir animal. The larvae and nymphs feed mainly on small rodents such as rodents or birds, reptiles but sometimes also on larger mammals depending on the regional variation of host community (Smith 2011). Adults feed on medium-sized or large mammals (Eisen and Lane 2002). Nymphs are probably responsible for the majority of infections although adult ticks have higher prevalence of infection. Nymphs are small and difficult to detect on the skin, and they feed during the summer months when people are outdoors while adults feed during the fall (Radolf *et al.* 2010).

2.2.2 *B. burgdorferi* transmission to human and pathogenesis of Lyme disease

B. burgdorferi is located in the mid-gut of the tick. When nymph or adult tick feeds, bacteria start replicating and undergo changes in gene expression that results in the change of lipoprotein expression to enhance colonization and chemotaxis. For example, *B. burgdorferi* express outer surface protein A (OspA) in the tick mid-gut. While tick starts feeding the expression of OspA is downregulated while OspC is upregulated (Schwan *et al.* 1995). OspA promotes bacteria binding in the OspA receptor in the tick mid-gut, while OspC, a potential plasminogen receptor (Onder *et al.* 2012) plays an essential role in colonization to the host tissue. Approximately 36 h after the initial feeding of the tick, bacteria transport to salivary glands and finally to a host via tick saliva (Schwan and Piesman 2002). Both motility and adhesion to the host tissue are important factors for *B. burgdorferi* to disseminate in the host and initiate infection (Finlay and Falkow 1997, Charon and Goldstein 2002). It can penetrate by swimming in the host matrix between the cells and enter the capillaries. Furthermore, *B. burgdorferi* can colonize the large joints, heart, and other tissues in the host (Goldstein *et al.* 2010). In addition to OspC, the increase in the expression of several adhesion proteins facilitate *B. burgdorferi* adhesion to integrins (p66), decorin and glycosaminoglycans (decorin binding protein A and B), laminin (BmpA), and fibronectin (Guo *et al.* 1995, Coburn and Cugini 2003, Brissette *et al.* 2009, Verma *et al.* 2009).

2.2.3 Clinical manifestations

Lyme disease is a multisystem disorder that is divided into acute/early localized infection, early disseminated, and late disseminated infection (Borchers *et al.* 2015). In the early acute phase, the most common manifestation is the bull's eye rash, *erythema migrans* (EM) that forms at the site of the tick bite after 3–32 days from the bite (Steere *et al.* 2004) (Fig. 4). EM is often associated with malaise, arthralgia, fatigue, fever, and headache, yet they may appear without the development of EM. In the early phase neurological manifestations (neuroborreliosis) such as cranial and/or peripheral neuropathies including facial nerve palsy may also occur.

After few days up to several weeks and years bacteria disseminates through blood to tissues and typical manifestations include additional EM lesions, skin rash *acrodermatitis chronicum migrans* (ACA) (mainly in Europe), Lyme arthritis, carditis, migratory musculoskeletal pain, eye manifestations as well as neurological symptoms such as meningitis, radiculoneuropathies and cognitive dysfuntions (Steere *et al.* 2004, Borchers *et al.* 2015). However, the infection does not necessarily develop in steps; some patients may have only localized infection while others suffer only from late stage symptoms (Steere *et al.* 2004). Different genospecies of *Borrelia* spp. are related to specific disease symptoms. In Europe, since three or more genospecies of *B. burgdorferi* are present, different disease manifestations are seen. *B. garinii* infection is linked to neuro-

logical symptoms, *B. afzelii* to cutaneous manifestations and *B. b. sensu stricto* to arthritis. In Europe less than 50% of the patients have EM while in the USA over 75% present EM because of the higher prevalence of *B. b. sensu stricto* in USA (Strle *et al.* 1999, Stanek and Strle 2008, Radolf *et al.* 2010).

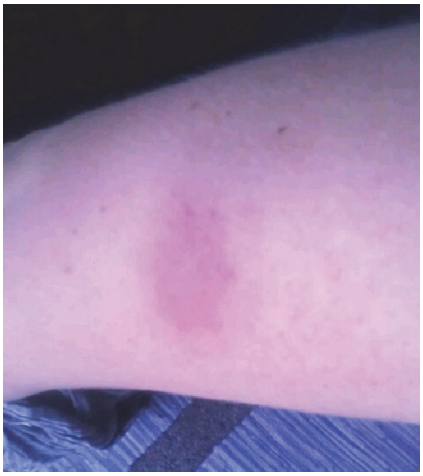

FIGURE 4 *Erythema migrans* skin rash on the right arm after a tick bite. Image by Jonna Kulmuni.

2.2.4 Diagnosis (and treatment)

The diagnosis of Lyme disease is usually a combination of clinical examination, investigation of patient's possible exposure to tick bites and laboratory testing (Wormser *et al.* 2006). PCR is used to detect *B. burgdorferi* from tissues although it is mainly used for research purposes (Borchers *et al.* 2015). The sensitivity varies depending on the methods and biopsies used for analysis: sensitivity in synovial fluid/tissue is between 60–85% (Nocton *et al.* 1996, Cerar *et al.* 2008), whereas in CSF it is 15–30% (Nocton *et al.* 1994). Laboratory testing is most commonly based on IgM and IgG responses. CDC and European guidelines recommend serological two-tier test system for Lyme disease diagnosis. The first step is the sensitive enzyme immunoassay (EIA), usually enzyme-linked immunosorbent assay (ELISA) or in rare cases immunofluorescence assay (IFA) followed by a confirmation of positive or indeterminant results by immunoblotting. CDC has the published criteria how to interpret the immunoblot (WB) results in USA (CDC 1995). According to CDC, IgM WB is considered positive if two of the following three bands are present: 23, 39, and 41 kDa; IgG WB is considered positive if five of the following 10 bands are present: 18, 23, 28, 30, 39, 41, 45, 58, 66, and 93 kDa. However, in Europe, the presence of different *B. burgdorferi* genospecies makes interpretation more complex. It is suggested that species-specific interpretation should be performed to achieve reliable results (Wilske *et al.* 2007).

There are several disadvantages to the two-tier testing system. Antibodies against *Borrelia* species develop slowly: for IgM it takes about two weeks and for IgG 4–6 weeks to be at detectable level. Patients in early disease stage may receive false-negative results since the sensitivity is only 29–40% (Molins *et al.* 2015). Also, antibiotic treatment prior to testing may interfere in the development of seropositivity (Glatz *et al.* 2006). The two-tier test system has been improved throughout the years by the implementation of recombinant antigens instead of using only *in vitro* cultured bacteria lysates. For instance, the incorporation of highly conserved 25-amino acid peptide C6 from the sixth region from commonly used variable surface lipoprotein E (VslE), instead of whole protein, as a diagnostic tool has improved sensitivity and specificity (Liang *et al.* 1999, Bacon *et al.* 2003, Mogilyansky *et al.* 2004, Wormser *et al.* 2008, Wormser *et al.* 2013). In addition to the sensitivity and specificity problems, the two-tier testing is laborious, costly, and sensitive to subjective interpretation (Robertson *et al.* 2000). The development of highly sensitive and specific single-tier test such as ELISA could serve alternative for two-tier test system (Wormser *et al.* 2013).

Lyme disease is treated with antibiotics. In the early phase, if EM is present, laboratory testing is not necessary. Patients are treated with two to three weeks course either with amoxicillin, doxycycline, cefuroxime axetil, or alternatively with microlides (Borchers *et al.* 2015). The treatment recommendations published in USA and Europe by Infectious Diseases Society Of America (IDSA) (Wormser *et al.* 2006) and European Concerted Action On Lyme Borreliosis (EUCALB, www.eucalb.com), respectively, are relatively similar. In disseminated infection, treatment is either oral or intravenous (i.v.) antibiotics such as cetriaxone, penicillin, cefuroxime axetil, amoxicillin or doxycycline for 10–30 days. For Lyme neuroborreliosis treatment recommendation is usually i.v. ceftriaxone, penicillin or cefotaxime also 10–30 days. There is an ongoing debate regarding the appropriate duration of antibiotic treatment. The International Lyme and Associated Diseases Society (ILADS) have proposed the usage of longer antibiotic treatment especially in the treatment of disseminated infections and PTLDS. However, IDSA the main treatment guideline administrator, have not accepted longer antibiotic treatments by stating that there are no scientific support for longer antibiotic courses.

2.3 Immune response to *B. burgdorferi*

2.3.1 Early innate immunity to *B. burgdorferi*

B. burgdorferi induces host's innate and adaptive immunity to fight off infection resulting in severe inflammatory manifestations seen in patients. Unlike many other bacteria, *B. burgdorferi* does not encode toxic compounds (Fraser *et al.* 1997). It is thought that the symptoms seen in patients are due to the tissue damage elicited by the strong immune response to bacteria. The recognition of pathogen and activation of innate immune mechanisms are pivotal for spiro-

chete clearance. When *B. burgdorferi* enters the host, it encounters the complement system and immune cells at the site of infection within the dermis. *B. burgdorferi* can resist complement activation and complement-mediated lysis that emphasize the importance of phagocytic macrophages, dendritic cells and neutrophils in establishing immune response against the organism (Weis and Bockenstedt 2010). Recent studies (Moore *et al.* 2007, Shin *et al.* 2008, Salazar *et al.* 2009) depict that phagocytosis is important in the initiation of innate immune responses against *B. burgdorferi.* Activated phagocytic cells produce cytokines and chemokines and present processed *Borrelia* antigens to naïve T cells to stimulate adaptive immunity.

2.3.2 Macrophages

Macrophages and their precursors, monocytes, are present in almost every tissue in the body. Monocytes are derived from bone marrow myeloid progenitor cell lineage. During infection or tissue injury, monocytes enter the site and differentiate into macrophages. LPS or other microbial products, interferon (IFN) γ and cytokines activate macrophages (Hamilton 2002). The main functions of the macrophages are not only to initiate innate immune responses but also to phagocytose apoptotic cells and cellular debris (Mosser and Edwards 2008). Macrophages have remarkable plasticity; they can change their phenotype in response to environmental signals. Polarization promotes the orientation of the adaptive immunity. Macrophage types have been classified traditionally as M1, M2a, M2b and M2c (Mantovani *et al.* 2004). Differentiation of macrophage populations is based on surface markers and functional properties (Yang *et al.* 2014). For example M1 macrophages produce high levels of IL-12 and IL-23 but low levels of IL-10, whereas M2 phenotype have high IL-10 and low IL-12 expression. In short, M1 macrophages stimulate Th1 response while M2 macrophages promote Th2 response and also have immunoregulatory functions.

2.3.3 Entry into macrophages

Macrophages recognize *B. burgdorferi* mainly via Toll-like- (TLRs) and NOD-like receptors (NLRs). TLRs and NLRs recognize pathogen-associated molecular patterns (PAMPs) on *B. burgdorferi* that are mainly bacterial surface lipoproteins and nucleic acids. TLRs are extracellular and endosomal sensors while NLRs sense intracellular compartments. TLRs are an evolutionary conserved type I transmembrane proteins with extracellular and cytoplasmic domains. The cytoplasmic domain is homologous with the cytoplasmic domain in interleukin (IL)-1 receptor (Wang *et al.* 2014). TLR2/TLR1 heterodimer on the cell surface has been shown to play a major role in the establishment of inflammatory responses to *B. burgdorferi* (Hirschfeld *et al.* 1999). In addition, TLR5 (Shin *et al.* 2008) on the cell surface, endosomal TLR 7/8 and 9 (Shin *et al.* 2008, Petzke *et al.* 2009, Petnicki-Ocwieja *et al.* 2011), and intracellular NOD2 (Petnicki-Ocwieja *et al.* 2011) are involved in *B. burgdorferi* stimulated signaling.

When *B. burgdorferi* binds to a receptor, it leads to a recruitment of adaptor molecule myeloid differentiation primary response protein (MyD88). The formation of this complex leads to signaling cascades that further activate transcription factors NF-κB and interferon regulatory factors (IRFs) and production of pro-inflammatory cytokines TNFα, IL-6, IL-12, IL-1β, and type I IFNs, respectively (Strle *et al.* 2009, Petnicki-Ocwieja and Kern 2014, Wang *et al.* 2014). Nonetheless, there are observations *in vivo* with TLR 2, CD14 and MyD88 in knockout mice that MyD88 independent pathways may contribute the development of Lyme disease as well with increased inflammation (Wooten *et al.* 2002, Bolz *et al.* 2004, Liu *et al.* 2004, Benhnia *et al.* 2005, Behera *et al.* 2006).

B. burgdorferi can be phagocytosed with or without antibody opsonization (Montgomery *et al.* 1994, Montgomery *et al.* 2002, Cruz *et al.* 2008). Internalization of *B. burgdorferi* into macrophage cell begins with attachment to the cell surface by binding to other than TLRs. The integrin receptors $\alpha_v\beta_3$, $\alpha_5\beta_1$ and $\alpha_M\beta_2$ (CD18/CD11, Mac-1, CR3) (Cinco *et al.* 1997, Coburn *et al.* 1998) mainly promote adhesion; however, CR3 mediates MyD88 independent phagocytosis of *B. burgdorferi* into murine macrophages and human monocytes together with TLR2 associated co-receptor CD14 (Hawley *et al.* 2012). There are other phagocytosis mediating receptors such as Macrophage receptor with Collagenous structure (MARCO) that aid in phagocytosis. MARCO is a scavenger receptor that binds promiscuously to the ligand and interacts with TLR2 and CD14 (Bowdish *et al.* 2009, Cervantes *et al.* 2014).

The phagocytosis of *B. burgdorferi* can occur by Fcγ-receptor mediated, by conventional or by coiling phagocytosis. The different phagocytosis mechanisms, simplified signaling routes, and antigen processing are presented in the Fig. 5. Fcγ-receptor mediated internalization requires opsonization of the bacteria with antibodies and involvement of complement factors such as C3b and iC3b. Conventional phagocytosis does not require opsonization and bacteria binds to the cell surface receptors such as integrins and C-lectins (Benach *et al.* 1984, Rittig *et al.* 1992, Montgomery *et al.* 1994, Cervantes *et al.* 2014). Coiling phagocytosis is a unique engulfment mechanism described first in *Legionella pneumophila* (Horwitz 1984). The cell grows F-actin rich unilateral pseudopods to wrap the bacteria and aid in phagocytosis (Linder *et al.* 2001, Naj *et al.* 2013). Approximately 60–70% of the phagocytosis events for *B. burgdorferi* have been reported to occur via coiling phagocytosis (Rittig *et al.* 1992). Phagocytosis and rearrangement of actin filaments for pseudopod formation is complex, fine controlled and have several players involved. GTPases, Wiskott-Aldrich protein (WASP), Arp2/3 complex and formins regulate actin dynamics, reorganize actin filaments and regulate filopodia and formation of coiling pseudopods (Linder *et al.* 2001, Naj *et al.* 2013, Hoffmann *et al.* 2014).

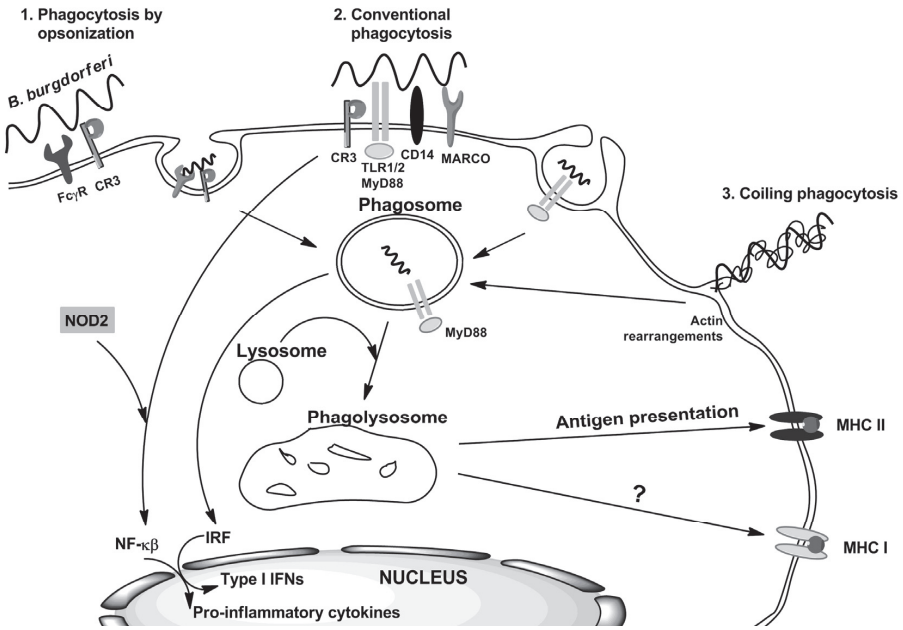

FIGURE 5 Simplified presentation of phagocytosis mechanisms, cytokine production and antigen presentation initiated by *B. burgdorferi* in macrophages. A) Antibody opsonized *B. burgdorferi* binds to Fcγ receptor (FcγC) and phagocytosis mediating complement factors such as CR3 that leads to internalization of the bacterium. B) In conventional phagocytosis, *B. burgdorferi* interacts directly with the surface receptors such as TLR1/2 complex with the cooperation of MyD88. Other receptors such as MARCO and CR3 and co-receptor CD14 mediate phagocytosis. C) During coiling phagocytosis, actin filaments are rearranged to form pseudopods that wrap around spirochete. Binding to TLRs or recognition of *B. burgdorferi* by NOD2 receptor initiate signaling cascades that lead to the activation of transcription factors NF-κβ and IRFs and production of pro-inflammatory cytokines. After phagocytosis bacteria are taken into membrane-bound phagosomes that fuse with lysosomes to form phagolysosomes. In phagolysosomes, bacteria are degraded, and processed antigens are transported finally to the cell surface and presented to T cells by MHC molecules. Phagosomal signaling enhances also the cytokine production.

2.3.4 The role of macrophages in initiation of adaptive immunity

2.3.4.1 Cytokine production

Cytokines are thought to play an important role in Lyme pathogenesis. Cytokines are small proteins that are essential for interaction and communication between the immune cells. Chemokines belong to the family of chemotactic cytokines with a major role in directing the cell migration. Based on the structure, cytokines are divided into interleukins (IL) and tumor necrosis factors (TNF). Chemokines have a group of CC and CXC chemokines. In CC chemokines, the first two cystein residues are located in parallel with each other. CXC chemo-

kines have single amino residue between the first two cysteins (Charo and Ransohoff 2006).

Activated macrophages produce proinflammatory cytokines that are responsible for inflammatory reactions. In *B. burgdorferi* infection the secretion of IL-6, IL-1β, TNFα, IFNγ, IL-8 cytokines and MCP-1 (CCL), MIP-1α (CCL3), MIP-1β (CCL4), CCL9, CXCL9, and CXCL10 chemokines by PBMCs (Giambartolomei *et al.* 1999), peripheral blood mononuclear cells of Lyme patients (Shin *et al.* 2010) and macrophages from EM lesions (Mullegger *et al.* 2000, Salazar *et al.* 2003) as well as from synovial fluid of patients with antibiotic refractory Lyme arthritis (Shin *et al.* 2007) has been observed. In neuroborreliosis also the IL-12, IL-18 and chemokines CXCL12 and CXCL13 have been reported (Grusell *et al.* 2002). CXCL13 has been proposed as a biomarker for Lyme neuroborreliosis since it is present in high concentrations in CSF of European patients (Rupprecht *et al.* 2005, Hytonen *et al.* 2014). Pro-inflammatory IL-6, IL-1β, TNFα are produced by all different cells and they are present in most disease manifestations. Several studies have demonstrated the essential role of anti-inflammatory cytokine IL-10 in regulation of immune response in *B. burgdorferi* infection (Giambartolomei *et al.* 1998, Giambartolomei *et al.* 1999, Murthy *et al.* 2000, Lazarus *et al.* 2008, Gautam *et al.* 2011, Gautam *et al.* 2012). IL-10 downstream the excretion of pro-inflammatory cytokines and decrease phagocytosis of macrophages and dendritic cells (Chung *et al.* 2013).

2.3.4.2 Antigen processing

After phagocytosis, bacteria end up in the phagosomes that are membrane-enclosed endocytic vesicles that subsequently acidify to kill pathogens (Fig. 5). Phagosomes then fuse with early endosomes, late endosomes and finally with lysosomes to form phagolysosomes. In phagolysosomes, bacteria encounter acidic environment and oxidative burst by reactive oxygen species (ROS) such as O_2^- and H_2O_2. In addition, phagolysosomes release granules that are enriched with hydrolytic proteases and other enzymes to degrade bacteria.

Processed bacterial antigens are presented to naïve T cells via major histocompatibility complex (MHC) molecules. There are two classes of MHC molecules: MHC class I and MHC class II. These molecules have different structures and expression patterns in the tissues and cells reflecting distinct effector functions. MHC I molecules present endogenous, cytosol originated, protease degraded peptides commonly from viruses to cytotoxic $CD8^+$ T cells. Peptide fragments from the cytosol are transported to the endoplasmic reticulum where they bind to MHC I and are finally carried to the cell surface via Golgi apparatus. MHC II molecules present antigen from extracellular sources, especially from bacteria that are degraded in the acidic phagolysosomes, to $CD4^+$ T cells. Peptides are loaded onto the MHC II molecules on endosomes prior to transportation to the cell surface where antigen presenting to T cells occurs.

The antigen presentation to T cells is important in the initiation of adaptive immune responses, and it defines the T cell response against the pathogen. Studies with mice have shown that $CD4^+$ cells have a crucial role e.g. in joint

inflammation in *B. burgdorferi* infection (McKisic *et al.* 2000, Sonderegger *et al.* 2012). The presentation of antigens via MHC II molecules together with the cytokine production of macrophages and coordinating transcription factors stimulate $CD4^+$ cells to differentiate to Th1, Th2, Th9, Th17, regulatory T cells (Treg), follicular helper T cells (Tfh) or type I regulatory T cells (Tr1). The detailed description of effector functions, differentiation cytokines, and cellular markers of each $CD4^+$ subsets are presented in the Table 1 (Zhu and Paul 2010, Luckheeram *et al.* 2012, Tan and Gery 2012). Interestingly, studies in human (Busch *et al.* 1996) and mice (Beermann *et al.* 2000) have proposed that *B. burgdorferi* infection could activate $CD8^+$ cells most probably by the cross-presentation of antigens also via MHC I molecules. Furthermore, although there is no scientific evidence yet, it is suggested that coiling phagocytosis could lead to a cross-presentation of *B. burgdorferi* antigens via MHC I (Rittig *et al.* 1994).

TABLE 1 Effector functions, cytokines differentiating specific $CD4^+$ subsets and cytokines produced by the $CD4^+$ subsets. The key cytokines associated with differentiation are bolded.

$CD4^+$ subset	Effector functions	Target pathogens	Differentiation cytokines	Effector cytokines
Th1	Activate macrophages, promote B cell antibody production, organ specific autoimmunity	Intracellular pathogens	**IL-12**, **IFNγ**, IL-2, IL-18	IFNγ, IL-2
Th2	Asthma and allergic responses, B cell activation and IgE switching	Extracellular pathogens, parasites	**IL-4, IL-2**	IL-4, IL-5, IL-9, IL-13, IL-25, TNFα
Th9	Allergy and asthma	Extracellular pathogens	IL-4, TGFβ	IL-9, IL-10
Th17	Generation of autoimmune diseases	Fungi, extracellular pathogens	**IL-23, TGFβ,** IL-6, IL21	IL-1β, IL-17A, IL-17F, IL-21, IL-22
Treg	Maintenance of immune tolerance	-	**TGFβ, IL-2**	IL-10, TGFβ, IL-35
Tfh	Development of antigen-spesific B cells	-	IL-6, IL-21	IL-4, IFNγ, IL-10
Tr1	Maintenance of immune tolerance, prevention of T cell mediated diseases	-	IL-27, IL-10	IL-10, TGFβ, IL-35

2.4 Immune evasion of *B. burgdorferi*

As most pathogenic organisms, *B. burgdorferi* utilize several mechanisms for immune evasion and avoidance of pathogenic killing of the host. Avoidance of host defense is particularly important in pathogens that cause persistent infections. The most significant evasion strategies of *B. burgdorferi* are explained below.

2.4.1 Immune evasion during transmission

Evasion mechanisms are recruited already in the tick before transmission to the host. *B. burgdorferi* binds to Salp15 protein in tick saliva via OspC lipoprotein (Ramamoorthi *et al.* 2005) resulting in protection of bacteria from complement-mediated killing. Salp15 has also been detected to inhibit $CD4^+$ T cell activation (Anguita *et al.* 2002, Juncadella *et al.* 2007) and other innate immune cells (Kubes *et al.* 2002, Montgomery *et al.* 2004). Furthermore, 18 kDa protein in the tick saliva inhibits OspA and OspC stimulated proliferation of B cells (Hannier *et al.* 2004). OspC can also act as a plasminogen receptor. Plasmin is a protease and enzymatically active form of plasminogen. Plasmin degrades fibrin and glycoproteins in extracellular matrix and basement membranes and creates a way for *B. burgdorferi* to enter tissues from circulation and escape immune cells (Onder *et al.* 2012). Furthermore, plasmin activates other extracellular matrix proteases including matrix metalloproteases (MMPs). MMPs are effective degradative agents and participate in the normal host processes, such as wound healing (Norris et al. 2012). Invasion into extracellular matrix may aid in the evasion from the circulating immune cells (Rupprecht *et al.* 2008). In addition to the aid in immune escape, activation of MMPs may be responsible for degradation of synovial cartilage in Lyme arthritis and associate in some of the pathology seen in Lyme disease (Hu *et al.* 2001).

B. burgdorferi has complement regulator-acquiring surface proteins (BbCRASPs) that are surface lipoproteins and bind to complement factor H, factor H-like protein and/or factor H-related protein in the host serum to inhibit alternative complement pathway and cell lysis (Kraiczy *et al.* 2001a, Kraiczy *et al.* 2001b). Currently, five BbCRASPs are known to aid in complement evasion (Radolf *et al.* 2010). The sensitivity to complement-mediated killing varies between the *Borrelia* spp. subspecies; *B. garinii* is sensitive to bactericidal effect, whereas *B. afzelii* is resistant and *B. burgdorferi sensu stricto* is partially sensitive (Breitner-Ruddock *et al.* 1997).

2.4.2 Antigenic variation

Antigenic variation, recombinant shuffling of antigenic epitopes on the antigenic proteins is common mechanism for pathogens to evade immune recognition. *B. burgdorferi* hides immunogenic proteins by antigenic variation to escape tehe host's immune response. For instance, *ospC* gene encoding OspC protein has

molecular polymorphism and antigenic diversity between the subspecies and strains of *B. burgdorferi* (Wilske *et al.* 1993). In addition to the transmission and colonization function, switching from the OspA expression to OspC has a role in initiation of infection and immune evasion for *B. burgdorferi*. OspC expression is diminished after two weeks of infection suggesting the importance in early infection (Liang *et al.* 2002). The evidence for immune evasive role was acquired in the studies where OspC lacking mutants were not able to establish infection (Tilly *et al.* 2006) and they were cleared by the immune system soon after infection, in 48 hours (Tilly *et al.* 2007). In addition OspE has high genetic variability and is known to have multiple polymorphic *ospE* gene alleles (Sung *et al.* 1998). OspE is also known as BbCRASP-3 due to association with inhibition of complement-cascade (Hellwage *et al.* 2001, Alitalo *et al.* 2002, Kraiczy *et al.* 2003) as explained above.

Other important protein associated with persistence and immune evasion in *B. burgdorferi* is 35 kDa surface protein VlsE. *VslE* gene is located in the linear plasmic lp28-1 and it consists of vslE expression site and 15 silent cassettes (Zhang and Norris 1998). Gene conversions in the gene locus result the expression of antigenically diverse VslE proteins (Embers *et al.* 2004). The study with lp28-1 plasmid lacking *B. burgdorferi* mutants in immunodeficient SCID and immunocompetent mice revealed that SCID mice could not resolve the infection while immunocompetent mice cleared the infection (Labandeira-Rey *et al.* 2003). This study demonstrated that the capability to persist in SCID mice was related to the antibody effectiveness against *B. burgdorferi*. Recombination of VslE protein prevents VslE specific antibodies to kill *B. burgdorferi*. Further studies have displayed that VslE is important in establishment of reinfection of *B. burgdorferi* that is also directly associated with evasion from the antibody response. (Rogovskyy and Bankhead 2013).

B. burgdorferi spirochetes and pleomorphic RBs have shown difference in protein expression and antigenicity of the surface proteins (Hulinska *et al.* 1994, Alban *et al.* 2000). Alban et al. 2015 reported about up-regulation of 20 proteins, including OspA, in serum-starved RBs analyzed by two-dimensional gel electrophoresis. However, in other study, Al-Robaiy et al. 2010 did not find difference between spirochetes and 1 d H_2O treated RBs. The discrepancy may be due to the difference in RB induction methods. The different surface protein expression in RBs could allow evasion from the immune system. Although these few studies have shown the antigenicity of RBs there is a lack of knowledge regarding the antigenic properties of RBs.

2.4.3 *B. burgdorferi* persisters

Approximately 10–20% of the patients treated with two to four weeks course of amoxicillin or doxycycline still experience disease manifestations such as musculoskeletal pain, persistent fatigue or memory and concentration difficulties. Symptoms can vary from mild to severe and affect the patient's quality of life. If symptoms are prolonged for six months or longer after antibiotic treatment the state is called as post-treatment Lyme disease syndrome (PTLDS) (Wormser

et al. 2006, Klempner *et al.* 2013, Aucott 2015). There is a controversy in mechanisms behind the development of PTLDS. It is proposed that PTLDS could occur due to these reasons: i) It could be host's inflammatory response to residual bacterial antigens from dead organisms; ii) autoimmune response initiated by molecular mimicry (Bolz and Weis 2004); iii) Persisting spirochetes or other persister forms in tissues that can survive antibiotic therapy. Especially the theory of persister forms has been debated.

B. burgdorferi DNA has been found form tissues after months of antibiotic treatment from dogs (Straubinger *et al.* 1997, Straubinger 2000), mice (Bockenstedt *et al.* 2002, Hodzic *et al.* 2008, Barthold *et al.* 2010, Yrjanainen *et al.* 2010, Bockenstedt *et al.* 2012, Hodzic *et al.* 2014), human primates (Embers *et al.* 2012), and humans (Battafarano *et al.* 1993, Bradley *et al.* 1994, Oksi *et al.* 1999, Picha *et al.* 2008, Yrjanainen *et al.* 2010, Li *et al.* 2011). Some studies have presented the observations of intact spirochetes after antibiotic treatment in mouse or macaque immunolabeled tissues. In addition these studies demonstrated by xenodiagnosis the presence of spirochetes in ticks that fed upon antibiotic-treated infected animals (Bockenstedt *et al.* 2002, Hodzic *et al.* 2008, Embers *et al.* 2012, Hodzic *et al.* 2014). However, these spirochetes have been non-cultivable. Only Embers and colleagues 2012 were able to find small number of spirochetes after nine weeks of culturing from post-mortem mice. The incapability to cultivate these persisters led to suggestion by Wormser and coworkers 2009 that survived spirochetes are attenuated, they do not associate with inflammation, and cannot be the cause of PTLDS. Furthermore, during antibiotic treatment *B. burgdorferi* might loose plasmids such as lp25 and lp28-1 that contain important genes related to infectivity (Bockenstedt *et al.* 2002). Lp-28-1 contains i.e. *vslE* gene that encodes VslE protein, which is important in immune evasion and establishment of infection as explained above.

Despite the critics, there is more recent evidence that PTLDS is caused by the persister forms of *B. burgdorferi* that can survive antibiotic treatment and evade the immune system. Recent study (Feng *et al.* 2015) demonstrated that in the stationary phase of growth more RBs and BFLs are present in the *B. burgdorferi in vitro* culture. This study also found that the susceptibility to antibiotics decreased during aging. Sharma and coworkers 2015 presented more supportive evidence for the increase of persistence in stationary phase. They also demonstrated that after exposure to antibiotics, a small subpopulation of bacteria persisters survived and were antibiotic resistant when regrown. Studies with *in vitro* persister have indicated the different susceptibility to antibiotics and other drugs when compared to parental spirochetes; however there is a discrepancy between the published results. i.e. in the study of Feng *et al.* 2014, the antibiotic candidate daptomycin effectively killed persisters but had poor activity on growing *B. burgdorferi*, whereas Sharma and colleagues 2015 reported opposite results. In their experiments, daptomycin killed replicating cells in stationary phase but not persisters. Furthermore, recent studies with pulse dosing of antibiotics have shown conflicting results (Caskey and Embers 2015, Sharma *et al.* 2015). Pulse dosing is an approach where bacteria are treated with

antibiotics, the level of drug is let to diminish (in this case washed away), and bacteria are allowed to recover before the next antibiotic pulse. Sharma and colleagues 2015 reported that four pulses of ceftriaxone killed all live bacteria including persisters. In contrast, Caskey and Embers 2015 stated that pulse dosing of doxycycline did not eradicate persisters or growing cells. However, the different antibiotics with distinct metabolic action mechanisms used in these studies may explain the discrepancy between the results. Ceftriaxone might be more effective against stationary phase bacteria and persister cells.

RBs and BFLs have also been reported to be more resistant to amoxicillin and doxycycline but more susceptible to tigecycline, metronidazole and tinidazole (Kersten *et al.* 1995, Brorson *et al.* 2009, Sapi *et al.* 2011). The difference in efficacy of the drugs against persisters, RBs, and BFLs may be due to the inability of the drugs to penetrate BFLs, efflux mechanisms and diminished cell wall synthesis (Casjens *et al.* 2000, Brorson *et al.* 2009, Feng *et al.* 2014a). The data from these studies suggest that pleomorphic forms of *B. burgdorferi* could be related to persistent infections. The involvement of pleomorphic forms in immune evasion is definitely worth of further studies.

3 AIMS OF THE STUDY

1. To characterize morphological and biochemical features of pleomorphic *Borrelia burgdorferi* forms.

2. To investigate the processing and immune response of pleomorphic round body forms of *Borrelia burgdorferi* in macrophage cells *in vitro*

3. To examine Lyme disease patient's immune response against pleomorphic round body forms

4 OVERVIEW OF THE METHODS

The materials and methods used in this study are listed in the Table 1. Detailed descriptions of each method can be found in the original publications indicated by Roman numerals.

TABLE 2 Summary of methods used in the original publications included in the thesis.

Method	Publication
B. burgdorferi culture	I, II, III
THP-1 cell culture	II
Induction of RBs	I, II, III
Quantification of pleomorphic forms in different environmental conditions	I
RB reversion experiments	I
ATP determination assay	I
Live cell PH/DIC microscopy	I
Macrophage phagocytosis experiments	II
Immunofluorescence and confocal microscopy	I, II
Electron microscopy	I
Microscopic data processing and analysis	I, II
Two-dimensional gel electrophoresis	II
SDS-PAGE and Western blotting	II
Cytokine and chemokine analysis	II
ELISA	III
Statistical analysis	I, II, III

5 RESULTS AND DISCUSSION

5.1 Induction of pleomorphic forms of *B. burgdorferi in vitro*

As many studies have previously shown, *B. burgdorferi* can change its morphology in unfavorable conditions. The nomenclature to name these different variants has been unclear and inconsistent. Here, we performed comprehensive study where pleomorphic forms of *B. burgdorferi* were induced in several culturing conditions *in vitro* such as in serum-free culture medium, culture medium supplemented with 10% human serum (HS), mammalian cell culture medium RPMI-1640 and in distilled H_2O at 37°C. The different morphologies were determined after different incubation times using live Phase Contrast (PH) microscopy. In normal culturing conditions with BSK-II medium from early exponential growth (day 2) up to late exponential phase (day 4) *B. burgdorferi* was seen mostly as spirochete (92%); however, small amounts of blebs (4%) and biofilm-like aggregations (0.6%) were also observed. In addition, at late exponential phase at day 4, a very small number of spherical RBs were observed (0.4%). The basal level of damaged/dying cells was 0.5% and 3.4% for day 2 and 4, respectively. As a result from microscopic observations, different forms of *B. burgdorferi* were classified to spirochetes, blebs, BFLs and RBs (I, Fig. 1). Blebs have spirochetal morphology with an expanded membrane bleb in the middle or on the tip of the spirochete. RBs are spherical, and their diameter is bigger (2.8 ± 0.46 μm) compared to blebs (1.3 ± 0.43 μm). BFLs are aggregations of spirochetes, blebs and RBs with EPS matrix (I, Table 1).

Culturing in the serum-free conditions has been previously reported to induce RBs in 7–10 d (Al-Robaiy *et al.* 2010) or after three weeks of incubation (Brorson and Brorson 1997). In this study, culturing for 4 d in the serum-free medium did not induce RBs (I, Fig. 2b). The ratio of different forms was similar to controls and bacteria replicated normally. The discrepancy between these results may be due to the very long culturing time in the previous studies that might have affected the morphology instead of actual serum-free culturing.

Feng et al. 2015, have reported that the proportion of RBs increase when the culture ages.

The inoculation of spirochetes into the cerebrospinal fluid (CSF) has been reported to promote RB formation in 24 h (Brorson and Brorson 1998). In this study, the effect of HS to *B. burgdorferi* morphology was demonstrated for the first time. Interestingly, when bacteria were cultured in the presence of 10% HS, the amount of blebs and RBs increased at 4 d to 44% and 22%, respectively (I, Fig. 2c). There were slightly more damaged cells (13%) compared to controls; however, the level was rather low. The transformation to RBs was caused most probably because of the presence of the complement system or antibodies in the serum. Furthermore, when examined with Transmission electron microscopy (TEM) (I, Fig 5a), approximately 30% of the RBs had swollen protoplasmic cylinders representing the lytic effect of the complement system (I, Fig. 5b). *B. burgdorferi sensu stricto*, *B. afzelii*, and some strains of *B. garinii* are complement-resistant and can evade from the complement system by binding to a complement inhibitor factor H with the outer surface protein OspE (van Dam *et al.* 1997, Hellwage *et al.* 2001). Nevertheless, the capability of RBs for complement evasion was not studied. However, clinically it is interesting that HS can induce RBs *in vitro* leading to the question, whether that may also occur *in vivo* and promote immune evasion in general.

Culturing in the RPMI medium did not only increase the transformation of the bacteria to blebs and RBs but also triggered severe cell damage (I, Fig. 2d). In the beginning, the amount of blebs increased to 34% in 2 d but then dropped to 26% after 4 d of culturing. The quantity of RBs increased to 17% while the level of damaged cells reached to 47% in 4 d. Previously, the 2 d exposure to RPMI has been reported to induce 95% of the spirochetes to transform into RBs (Alban *et al.* 2000) that is very different to our observations. In this study, pleomorphic forms were differentiated with relatively high magnification (1000x) of the microscope, while in the previous study only 200x magnification was utilized. To see the damage on the outer cell membrane requires proper microscopy technique. The distinct analysis methods may indeed explain the differences between these two studies.

To execute experiments with RBs, it is necessary to have a technique to induce them fast in high quantities. Here, previously developed method (Brorson and Brorson 1998) with modifications was used, where spirochetes were exposed to distilled H_2O. Bacteria were exposed to H_2O for 10 min, 2h, 4 h, 1 d and 4 d and different forms were counted similarly as with other culturing environments. Exposure times to H_2O were shorter because of the fast transformation of spirochetes to RBs. However, the 4 d time point were included to investigate the long term effects of the exposure to hypotonic environment. As a result, only 0.1% of the bacteria were spirochetes, while 4% and 85% of the cells were present as blebs and RBs after 10 min treatment, respectively (I, Fig. 2e). From 2 h to 4 d time point there were no differences in the proportions of different form: blebs decreased to 1% after 2 h and no other than damaged spirochetes were observed anymore. The level of damaged cells was approximately

10% throughout the experiment. The morphology of the RBs was similar what seen in previous studies (Brorson and Brorson 1998, Murgia and Cinco 2004) where RBs were induced in H_2O at a lower temperature 30–35°C. The hypotonic conditions may cause cells to swell and finally burst. The comparison of HS and H_2O induced RBs by TEM demonstrated that they have similar morphologies (I, Fig 5a) suggesting that the RB formation is not occurring only to a response with osmotic stress.

B. burgdorferi can aggregate into BFLs both in surfaces and in suspension (Barbour and Hayes 1986, Srivastava and de Silva 2009, Sapi *et al.* 2012, Timmaraju *et al.* 2015). Although the presentation of similarity with the *in vivo* biofilms of other bacteria (Sapi et al. 2012) their existence and association with pathogenesis is rather debated. Srivastava and da Silva 2009 have demonstrated the development of BFLs as a result of high cell density in the culture. However, here the development of BFLs was observed already at the early exponential phase of growth (I, Fig 2f). This result suggests that other factors than high cell density also promotes aggregation and biofilm formation of *B. burgdorferi* in suspension cultures.

5.2 Pleomorphic round bodies are viable and have low metabolic activity

Pleomorphism may be a survival strategy for *B. burgdorferi* in inconvenient environment and aid in evasion from the immune system (Lawrence *et al.* 1995, Brorson and Brorson 1998, Murgia and Cinco 2004, Al-Robaiy *et al.* 2010). When environmental conditions become favourable again, H_2O induced RBs revert back to spirochetes (Brorson and Brorson 1998, Murgia and Cinco 2004, Al-Robaiy *et al.* 2010). In this study, to assess the viability of RBs after each time point in H_2O, RBs were placed in normal culture medium and their reversion back to vegetative spirochetes was monitored until the bacteria reached the cell density of $40x10^6$/ml, equal to the mid-log phase of growth. Furthermore, the ATP concentrations of RBs during reversion were analyzed.

When exposure to H_2O was short, 10 min or 2 h, RBs reverted back to spirochetes on average at 6 and 8 d, respectively (I, Fig. 3a). After 4 h treatment, RBs reverted in half of the experiments in 11 d; however, after longer exposures (1 d and 4 d) reversion did not occur at all. The reversion of 1 d, 4 d, 7 d and even 5 week old RBs in 30–34°C have been previously reported (Brorson and Brorson 1998, Murgia and Cinco 2004, Al-Robaiy *et al.* 2010); however, our data did not support the previous findings that RBs could revert back after long exposure to hypotonic conditions. Preferably, these results indicated that *B. burgdorferi* RBs tolerate short exposure to the harsh environment. The different culturing temperatures between our and previous studies could explain these contradictory observations.

Interestingly, 10 min and 2 h RBs did not show ATP production at all (I, Fig 3b). The low metabolic activity of RBs may indeed be a survival mechanism for *B. burgdorferi*, especially from antibiotics. When RBs were placed to BSK-II medium for reversion, ATP activity was not seen even after 24 h. In contrast, the average ATP concentration in spirochetes was 149 nM (I, Fig. 3b). The 10 min RBs achieved the early log phase (10–20x106 cells/ml) in 5 d, while for 2 h RBs it took approximately 6 d (I, Fig. 3b). At that growth phase, the ATP concentrations for 10 min and 2 h RBs were 317 nM and 306 nM, respectively (I, Fig 3b). The 10 min RBs reached the mid log-phase (40–50x106 cells/ml) at day 6 when the ATP concentration was 343 nM. For 2 h RBs, similar growth phase was observed at day 8 with ATP concentration of 480 nM. Alban *et al.* 2000, have suggested that RBs are not degenerative. These results supported the hypothesis and demonstrated that RBs are not degenerative but instead, dormant forms. Nonetheless, RBs can initiate the metabolic activity in favorable conditions and revert back to replicative spirochetes.

5.3 RBs have an intact and elastic cell envelope

Using TEM and previous findings of others (Murgia and Cinco 2004, Al-Robaiy *et al.* 2010), the model for RB formation was developed and illustrated (I, Fig. 4, Movie S1). The transformation from corkscrew shaped spirochete to a RB begins with the expansion of the elastic outer envelope (I, Fig. 4a) that allows the folding of the protoplasmic cylinder within the cell and finally leads to a spherical shape (I, Fig. 4b). The RB formation requires robust flexibility of the outer membrane. It is suggested that the outer and inner membranes of *B. burgdorferi* are anchored together by the export system (Radolf *et al.* 2012). During RB formation structures that connect these two membranes would probably prevent extensive outer envelope flexibility. However, other study (Bunikis *et al.* 2008) have reported that RND transporter system, an efflux pump for toxic compounds, lacks a hairpin domain that leads to a less stable assembly of the pump between the outer and inner membranes. The loose interaction of the pump between the membranes could allow the flexibility of the outer membrane during RB formation without the loss of the pump function.

Furthermore, TEM was utilized to investigate the morphology as well as the cell envelope structure and integrity of spirochetes, blebs, and RBs. Blebs seem to be an intermediate form between the spirochete and RB. The outer envelope have expanded on the other end or on the lateral side of the spirochete followed by a partly folded protoplasmic cylinder inside the expansion (I, Fig. 4a, Fig. 5a). These results provided evidence that H_2O or HS RBs have similar morphologies. Interestingly, neither of them was cell wall deficient, as they have often named (Mattman 2001, Stricker and Johnson 2011) (I, Fig. 5a). When compared to spirochetes, both RBs have identical intact outer and inner membranes (I, Fig. 5a). As a control for membrane damage, spirochetes were treated

with 100 µg/ml doxycycline for 48 h. Doxycycline caused more small holes in the outer membrane when compared to spirochetes and RBs (I, Fig. 5a).

The flagella are located in the periplasmic space of *B. burgdorferi* (Barbour and Hayes 1986) as also seen in the TEM cross-section of the spirochete (I, Fig. 6, top panel). Localization of the flagella in the RBs was studied using TEM, and Confocal microscopy with the bacteria that was immunolabeled using anti-flagellar protein (p41) antibody. Confocal micrographs illustrated that despite the different organization of periplasmic space during outer membrane expansion, RBs have flagella, seen on the outer circle of the RBs (I, Fig. 6). These results provide more evidence that RBs are not CWD forms. The lack of outer membrane would lead to a release of flagellin fibers from the periplasmic space that was not seen in TEM or Confocal images. Furthermore, the presence of flagella indicates that RBs can preserve motility and skeletal components during that life phase and employ them again during reversion to spirochetes.

In summary, these results suggest that RBs have intact outer envelopes with maintained mobility machinery. Since RBs do not lack outer membrane or have encysted thickened cell wall they should not be called as CWD forms, spheroplasts or cysts.

5.4 RBs have different biochemical signatures and protein profiles compared to spirochetes

To further examine the characteristics of the cell envelope in *B. burgdorferi* pleomorphic forms, live bacteria were stained with different dyes, to address DNA, peptidoglycan and lipids. Confocal microscopy was used to illustrate different components in the cells. Furthermore, doxycycline-treated as well as methanol-fixed bacteria were stained with same dyes as controls to demonstrate different staining properties of damaged cell membranes. *B. burgdorferi* have unique and atypical gram-negative cell membrane that differs from many other bacteria (Barbour and Hayes 1986). Propidium iodide (PI) is a DNA stain commonly used to identify disintegrated cell membranes, and it is incorporated in some live/dead cell assays. Several studies have used PI to assess the viability of *B. burgdorferi* spirochetes and RBs (Sapi *et al.* 2011, Feng *et al.* 2014b, Feng *et al.* 2015). Intriguingly, it was shown that PI permeated live mobile spirochetes (I, Fig. 7, Movie S2) indicating that *B. burgdorferi* indeed has a unique cell envelope. In addition, PI stained blebs, RBs, and doxycycline-treated cells. These results suggest that atypical cell envelope characteristic of *B. burgdorferi* should be considered when using these types of dyes to identify cell integrity. PI should not be used to indicate cell death in *B. burgdorferi*.

Wheat germ agglutinin (WGA) conjugated with Alexa 555 was used to address N-acetylglucosamine polysaccharides (GluNAc) in the peptidoglycan cell wall. WGA did not stain GluNAc in the spirochetes or blebs (I, Fig. 7). In contrast, WGA stained GluNAc in RBs very specifically (I, Fig. 7), demonstrat-

ing the difference in the peptidoglycan cell wall components or the architectural structure of the cell envelope between these forms. However, the lipid dye boron-dipyrromethene (BODIPY) stained all the *B. burgdorferi* forms as expected. In *B. burgdorferi* infected Langerhans cells, similar findings have been reported earlier where RBs were labeled positively with WGA (Hulinska *et al.* 1994). Radolf *et al.* 2012, have proposed that the peptidoglycan cell wall of *B. burgdorferi* is located near to the inner membrane. However, Kudryashev *et al.* 2009 had demonstrated using cryo-electron tomography that the cell wall is actually closer to the outer membrane than the cytoplasmic inner membrane. Furthermore, they suggested that peptidoglycan layer is rather elastic than rigid. Elasticity might promote the ability of flagella to modify bacterial shape. The flexibility of the outer membrane and peptidoglycan cell wall together with architectural changes on the membrane components could explain why GluNAc becomes exposed during RB formation.

In contrast, methanol-fixed, permeabilized cells membranes clearly demonstrated more robust internalization of all three dyes compared to live cells, as expected (I, Fig. 7, Fig. S1). For example, BODIPY stained the lipids only on the surface of live RBs while in fixed cells staining pattern was uniform inside the bacteria. Permeabilization of the membranes allowed the dye molecules to leak inside the whole cells. In addition to the TEM images (I, Fig. 5a) that presented the intact outer membrane of RBs, these results confirmed that RBs have complete cell envelope and GluNAc as a cell wall component.

To compare protein profiles of spirochetes and RBs two-dimensional (2D)-electrophoresis was conducted. In total 77 distinguishable proteins were spotted from the gels and 27 of them displayed different expression between spirochetes and RBs (II, Fig. S1 A–B). The proteins with smaller molecular size (15–40 kDa) had higher relative intensities in RBs while mainly larger proteins (97 kDa to ≥ 200 kDa) were expressed more in spirochetes (II, Table 2). However, two proteins with molecular size of 4 and 21 kDa had higher relative intensity in spirochete gels (II, spots 27 and 17, respectively, Fig. S1 A–B). These results correspond to the previous *B. burgdorferi* genome data (Fraser et al. 1993), where proteins ranging between 3.3–254.2 kDa were reported. Altogether, RBs had higher expression of 15 and lower expression of 12 corresponding proteins compared to spirochetes (II, Table 2). Previously, protein profiling have been performed with RPMI serum starved *B. burgdorferi* (Alban *et al.* 2000) and 1 d H_2O induced RBs (Al-Robaiy *et al.* 2010). The three spots with increased intesity in RBs (II, spots 11, 18 and 19, Table 2) corresponded to previously reported results of Alban *et al.* 2000. The other study (Al-Robaiy *et al.* 2010) did not find differences between spirochetes and 1 d H_2O RBs in 6–16 kDa proteins. In contrast, in the present study, two 15 kDa proteins had increased expression in RBs compared to spirochetes (II, spots 24 and 26, Table 2). The decrease in the protein expression observed in earlier studies may be due to long exposure of spirochetes to H_2O.

Conclusively, these results provided more evidence that RBs are not spheroplasts or CWD forms although some structural changes occur in the cell enve-

lope during RB formation. Furthermore, RB formation changes the protein expression in RBs. Different staining properties of spirochetes and RBs, especially the difference in the peptidoglycan cell wall presentation, could be exploited in the diagnosis of Lyme disease and identification of RBs in tissues.

5.5 Spirochetes and RBs are internalized and processed differently in macrophage cells

Macrophages together with the dendritic cells and neutrophils are the first cells to fight off *B. burgdorferi* in the site of infection. The uptake mechanisms of spirochetes are quite well known; however, there are no studies to show how immune cells react when they encounter RBs. To compare internalization of spirochetes and RBs, macrophages, differentiated with phorbol 12-myristate 13-acetate (PMA), were stimulated with either of these two forms for 2 h *in vitro.* Cells were imaged with the confocal microscope, and the phagocytic indexes (PhI) were determined from z-stacks. The higher proportion of cells were found to phagocytose spirochetes (75%) than RBs (62%) (I, Table 1). Furthermore, the PhI value that indicates the number of bacteria per cell was significantly higher with the cells stimulated with spirochetes (I, Table 1). It is proposed that transformation from spirochetes to RBs may help in immune evasion (Miklossy *et al.* 2008). Macrophages internalized more spirochetes than RBs indicating the difference in the uptake and killing of these two bacteria forms.

To further investigate and compare internalization of spirochetes and RBs the colocalization analysis of these forms with F-actin at different time points was performed. The internalization of *B. burgdorferi* into macrophages proceeds either by Fcγ-receptor mediated- (Benach *et al.* 1984, Montgomery *et al.* 1994), conventional CR3-mediated- (Cinco *et al.* 1997, Garcia *et al.* 2005, Hawley *et al.* 2012), or coiling phagocytosis (Rittig *et al.* 1992, Linder *et al.* 2001, Naj *et al.* 2013). Coiling phagocytosis has been reported to be the predominant mechanism for spirochete internalization (Rittig *et al.* 1992), where phagocytic cells grow F-actin rich pseudopods that wrap around spirochetes (Linder *et al.* 2001, Naj *et al.* 2013). However, F-actin polymerization is needed in the monocytic uptake of *B. burgdorferi* in general (Cruz *et al.* 2008). The aim of this study was to compare if spirochetes and RBs utilize the same phagocytic mechanisms.

The F-actin accumulated in the areas where bacteria associated with the cells and finally surrounded them (II, Fig. 1A–F). After 2 h of stimulation, approximately 30% of both spirochetes and RBs colocalized with F-actin (II, Fig. 1G). The colocalization decreased slightly at 8 h and 24 h time points; however, there was no significant difference in colocalization with F-actin between these two bacteria forms (II, Fig. 1G). Phagocytosis inhibition with Cytochalasin D at time point 2 h did not stop phagocytosis totally, but it decreased statistically significantly the colocalization of both forms with F-actin (II, Fig. 1G). These results confirmed that F-actin is essential for phagocytosis of both *B. burgdorferi*

forms. CR3- and Fcγ-receptors mediate the F-actin polymerization during phagocytosis (Linder *et al.* 2001). It is reported that internalization of the unopsonized spirochetes is independent of the Fcγ-receptor (Montgomery *et al.* 1994). Here, we demonstrated that F-actin is important also in the Fcγ independent phagocytosis of unopsonized spirochetes and RBs.

F-actin enriched pseudopodia were occasionally observed to coil around spirochetes that are representative cell structures for coiling phagocytosis (II, Fig 1A). These results support the previous observations of others (Rittig *et al.* 1992) that coiling phagocytosis is one of the uptake mechanisms for *B. burgdorferi* spirochetes. RBs were enclosed by F-actin structures and some coiling around them was detected (Fig. 1B, Fig. 1D). Nonetheless, the similar wrapping of long and thin pseudopodia around RBs was not observed. Yet, it remains indistinguishable, if macrophages use coiling phagocytosis for RB internalization. The difference in spirochete and RB morphology, and the fact that RBs are not mobile as spirochetes may explain why macrophages did not develop similar pseudopods for coiling. It is possible that macrophages prefer coiling phagocytosis to engulf spirochetes and conventional phagocytosis for RBs. These results suggest that there are differences in the internalization of these two *B. burgdorferi* forms.

The adaptive immune response is dependent on how pathogens are processed in phagocytic cells. To compare lysosomal processing of spirochetes and RBs in macrophages, colocalization analysis with lysosome-associated membrane protein 2 (Lamp2) was performed at 2 h, 8 h, and 24 h time points (II, Fig. 2). The colocalization of *B. burgdorferi* spirochetes with immunolabeled lysosomal proteins (Montgomery *et al.* 1993, Montgomery and Malawista 1996, Montgomery *et al.* 2002) as well as LysoTracker stained acidic compartments (Moore *et al.* 2007) have been reported previously. In these studies, colocalization was observed from 10 min time points up to 5 h of stimulation. Nevertheless, the quantification of actual colocalization was performed in only one study (Montgomery *et al.* 1993), where 45% of the spirochetes colocalized with lysosomal endopeptidase enzyme cathepsin L at 10 min time point and 57% after 5 h of incubation. Here, there were no substantial changes in colocalizations between the time points. The maximum colocalization of spirochetes with Lamp2 was 27% (II, Fig 2G) while RBs colocalized less with Lamp2 at all studied time points. Interestingly, at 24 h there were statistically significant difference between spirochetes and RBs. This result indicates that there are differences in spirochete and RB processing in macrophages.

As a control to inhibit microtubules, autophagosome-lysosome fusion and bacteria transport to lysosomes cells were treated with nocodazole at 2 h time point. Nocodazole significantly decreased colocalization of both forms with lysosomes implying that lysosomal pathway indeed is important in *B. burgdorferi* processing (II, Fig. 2G). However, lower colocalization of RBs in general with Lamp2 may be related to utilization of some other than lysosomal pathway in macrophages. Rittig and colleagues 1994 have suggested that coiling phagocytosis may lead to the presentation of processed antigens via MHC I molecules

instead of MHC II. If spirochetes are phagocytosed more with coiling phagocytosis compared to RBs that would also explain the differences seen in processing of these two forms. The previous studies, as explained above, reported higher colocalization percentages of spirochetes with lysosomes compares to this study. These differences may be due to the differences in analysis methods. Previously, kinetic compartmental analysis was used while in this study modern image analysis combined with Costes algorithm for statistical significances was used (Costes *et al.* 2004).

5.6 RBs induce different cytokine and chemokine production in macrophages *in vitro* compared to spirochetes

Cytokines and chemokines, secreted by immune cells, play an important role in Lyme disease pathogenesis. These signaling molecules are important regulators and effectors of the immune response, and they may modulate the different clinical outcomes seen in patients (Widhe *et al.* 2002). To compare the immune-mediator production of macrophages induced by spirochetes and RBs the expression of 36 different cytokines and chemokines were analyzed. As a result, after 24 h stimulation *B. burgdorferi* induced production of 18 different cytokines and chemokines (II, Fig. 3). These results were consistent with the previous studies, where several immune-mediators of CH3 and C57 mouse bone-marrow derived macrophages (Gautam *et al.* 2012) and human macrophages (Strle *et al.* 2009) were analyzed after *B. burgdorferi* stimulation. The cytokines and chemokines similar with this analysis and the previous mouse study (Gautam *et al.* 2012) were G-CSF, GM-CSF, IL-1β, IL-6, CXCL1, CXCL10, MCP-1, MIP-1α, MIP-1β, RANTES and TNF-α. Furthermore, when these results were compared to the earlier study with the human macrophages (Strle *et al.* 2009), the expression of cytokines IL-1β, IL-6, MCP-1 and chemokines MIP-1α, MIP-1β, TNFα, and CXCL10 were observed in both studies. The cytokines IL-10 and IFN-γ are commonly secreted as a response to *B. burgdorferi* phagocytosis (Strle *et al.* 2010). In this study they were not produced at a detectable level. IL-10 has important role in Lyme disease as a regulator of inflammatory responses (Lazarus *et al.* 2006, Gautam *et al.* 2011, Chung *et al.* 2013) while IFN-γ associates with the disease severity (Salazar *et al.* 2003). THP-1 cell line has constitutive IL-8 production (Baqui *et al.* 1999). Both spirochetes and RBs significantly diminished the IL-8 excretion that was not seen when cells were stimulated with *E. coli* (II, Fig. 3H). Decreased IL-8 level indicates most probably a cell-specific response to *B. burgdorferi*.

Spirochetes and RBs induced expression of similar cytokines and chemokines; however, there were statistically significant differences in expression levels of seven specific ones. Spirochetes stimulated significantly elevated production of IL-1β, IL-1ra, IL-6, MIF, MIP-1β and RANTES compared to RBs (II, Fig. 3E–G, 3M, 3O, 3Q, respectively). MIP-1β and RANTES had relatively the high-

est expressions with both bacteria forms (II, Fig 3O and 3Q, respectively). Intriguingly, RBs induced significantly higher expression of chemokine MCP-1 (II, Fig. 3L). Furthermore, RBs stimulated higher IL-23 production; nevertheless, the difference to spirochetes was not statistically significant. The differences in the phagocytosis and processing of spirochetes and RBs may indeed correspond to the different cytokine and chemokine patterns observed in this study.

IL-1β, IL-1ra, IL-6 and IL-23 are all known to differentiate naïve T-cells to helper T cell type 17 (Th17) that associates with many autoimmune diseases (Burchill *et al.* 2003, Zhu and Paul 2010, Chung *et al.* 2013). MCP-1 regulates the migration and infiltration of other immune cells and potentially polarizes naïve T cells to Th2 type (Gu *et al.* 2000). It is suggested that it may facilitate the transmission to host tissue (Kern *et al.* 2015) due to the increase of permeability invascular endothelium cells in dengue fever (Lee *et al.* 2006). Furthermore, MCP-1 is required in the development of experimental Lyme arthritis in mice (Brown et al. 2003). Higher expression of MCP-1 after RB stimulation may suggest RB involvement in Lyme arthritis. Interestingly, the five cytokines secreted significantly less after RB stimulation were either proinflammatory (IL-1β, IL-6, MIF) or chemoattractants (MIP-1β, RANTES). The lower immune-mediator expression may indicate the suppressed immune response against RBs or immune control dysfunction.

5.7 Lyme disease patients react differently against spirochetes and RBs

The role of pleomorphic forms in the pathogenesis of Lyme and other diseases has been criticized in recent past years (Onwuamaegbu *et al.* 2005, Lantos *et al.* 2014, Schnell *et al.* 2014). However, there is a lack of studies to demonstrate the immune response to pleomorphic forms. Only one study has examined the reactivity of two infected monkeys and one Lyme disease patient against serum starved RBs (Alban *et al.* 2000). In addition, there are reports that show the presence of *B. burgdorferi* pleomorphic forms in clinical samples (MacDonald and Miranda 1987, MacDonald 1988, Hulinska *et al.* 1994, Aberer *et al.* 1996, Mattman 2001, Miklossy *et al.* 2008). Here, the aim was to compare antigenic properties of spirochetes and RBs and investigate the immune response of Lyme disease patients against RBs.

The comparison of antigenicity of spirochetes and RBs was performed with WB analysis using seven Lyme positive and three negative sera. As a result, all the positive sera were reactive against both forms. However, there was variation between the patient's IgG responses against different antigens: for instance, only five patients out of seven were reactive against 58 kDa protein (II, Table 3). Interestingly, patients were more immunoreactive against 39, 60 and 66 kDa antigens in RBs than in spirochetes (II, Table 3, Fig S1 C). In other words, the intensities of bands with these specific antigens were stronger, and patients

reacted against these antigens more often on the RB WBs as compared to spirochete WBs. These three antigens correspond to a laminin binding protein BmpA (Simpson *et al.* 1990), heat shock protein GroEl (Carreiro *et al.* 1990) and p66 (Bunikis *et al.* 1995). These proteins have been previously reported in *B. burgdorferi* B31 Western blots (Ma *et al.* 1992) and they are included in the diagnosis criteria of CDC (CSC 1995). Nonetheless, this was the first study to show their antigenicity in RBs.

In the previous study (Alban *et al.* 2000), sera from two monkeys and one Lyme patient were less reactive against 41 kDa and 46 kDa proteins in RBs than spirochetes. Here, all the tested sera were reactive against 41 kDa and 45 kDa proteins. These two antigens correspond to well known immunogenic antigens flagellar protein B (FlaB) and variable surface lipoprotein E (VslE) (Aguero-Rosenfeld *et al.* 2005). With respect to 41 kDa protein, there was no difference in reactivity between spirochetes and RBs. The 45 kDa protein was less reactive in RBs with four sera as also seen in the previous study. Nevertheless, three of the examined sera had equal reactivity between these two forms. The difference in reactivity with the 41 kDa protein between these two studies may relate to the different immune responses of patients against antigens or distinct RB induction methods used between these studies.

To extensively investigate the Lyme disease patient's immune response against RBs, and test if the RBs are a suitable candidate as an antigen to implement in the Lyme disease diagnostic tests, the multiplex ELISA was executed. RBs haven't been previously included in the diagnostic test tools. In total 54 Lyme positive and 15 negative serum samples were tested. All the patients were clinically examined and tested with the two-tier test system where positive ELISA tests were confirmed by the immunoblotting. Patients were divided in the following three groups based on their disease symptoms and test results: acute infection, PTLDS, and PTLDS with co-infections (III, Table S1). As a result, 18 and 27% of the Lyme disease patients had IgM and IgG response against RBs, respectively (III, Fig 1.). Interestingly, patients had IgM response against RBs more frequently than against spirochetes (III, Fig. 1).

When the specific patient groups were analyzed, all the patients with acute infection (100%) had IgG response against RBs. However, the PTLD patients and PTLD patients with co-infections demonstrated relatively high IgG responses against RBs as well (44% and 40%, respectively) (III, Table 1). When IgG responses of the acute group were compared to other groups, the difference was statistically significant (III, Table 1). Furthermore, the Cohen's Kappa analysis was performed to assess the agreement between each antigen pair in the ELISA test. The calculated kappa coefficient (κ) explains the reliability and agreement level between the antigens in the diagnostic test (Viera and Garrett 2005). The Cohen's kappa analysis provides information about how closely two antigens are related to each other. Intriguingly, RBs were found independent of other antigens. There was only a slight dependency to a peptide C6 and *B. burgdorferi* B31 spirochetes (κ = 0.226–0.410). These results support the data from the serological analysis where some patients were reactive only against

RBs or against some other antigens (III, Table S2). These results suggest that patients may receive false negative results in conventional tests although they possibly react to RBs and actually be positive.

In conclusion, these results provided evidence that patients have serological response against RBs as previously suggested (Alban *et al.* 2000). Furthermore, some patients are even more reactive to specific antigens in RBs than spirochetes. Based on the serological response in patients, RBs were found to be a good antigen candidate for Lyme disease diagnosis. These results suggest that RBs associate with the pathogenesis of Lyme disease and they should be included in new diagnostic tools.

6 CONCLUSIONS

The main conclusions of this thesis are:

1. The pleomorphic RBs of *B. burgdorferi* can be easily induced *it vitro,* and they can revert back to parent spirochete form although they have low metabolic activity. RBs have a flexible and intact cell envelope. However, the architectural structure of components in the cell envelope changes during RB formation leading to different biochemical characteristics compared to spirochetes.

2. Macrophages phagocytose RBs less than spirochetes, and the phagocytic cells may utilize a different mechanism for uptake of RBs than for uptake of spirochetes. Furthermore, RB processing partly occurs via some other than the lysosomal pathway. Spirochetes and RBs induce distinct cytokine and chemokine patterns in macrophage cells.

3. RBs have different antigenic properties compared to spirochetes. Some patients have more intense serological response against RBs than spirochetes. Furthermore, the immunological response to RBs may be independent of spirochetes or other antigens. RBs have a role in Lyme disease pathogenesis and they are a good antigen candidate for Lyme disease diagnostics.

ACKNOWLEDGEMENTS

This work was carried out during 2010–2015 at the University of Jyväskylä, at the Department of Biological and Environmental Sciences and NanoScience Center, in the Division of Cell and Molecular Biology. The thesis was supported by University of Jyväskylä Doctoral Programme, the National Doctoral Programme in NanoSciences (NGS-NANO), Antti and Jenny Wihuri Foundation, and Schwarz Foundation.

I express my warmest gratitude to my supervisor Docent Leona Gilbert for her endless support and encouragement throughout all these years. She provided me not only supervision in this extremely interesting research field but also helped me to develop as an independent scientist. The enthusiasm for building a team spirit in the research group promoted both good scientific as well as the social atmosphere in our group.

I also would like to thank my thesis reviewers, PhD Jyotsna Shah and PhD, MD Horst Maxeiner for their constructive and valuable comments. I am grateful and honoured for Associate Professor Monica Embers for kind acceptance of serving as an opponent in the public examination of my dissertation. My thesis committee members Professor Seppo Meri and MD Armin Schwarzbach are greatly acknowledged for all the advice, guidance and great humor. Special thank for Seppo for taking care of me in the huge Immunology Conference in Nice where I did not know anybody!

I am extremely grateful for my AWESOME current and previous Lee's group members: "Kai" Kanoktip, Laura, Kunal, Heidi, Bettina, Petri, Martin, Jonna, "Book" Nitipon and of course all the Kiddies and Minions. You provided unforgettable and fun working environment through all these years. I thank you for the scientific and non-scientific conversations but especially I enjoyed all the jokes, craziness after 16.30 in the afternoon (especially this thank goes to Kunal!) and sometimes even before that, coffee breaks, parties and social events that gave good balance for all the hard work in the lab. Kai and Laura get special thanks for keeping up my energy levels by cooking great Thai food and baking excellent cakes! I also want to acknowledge my (absolutely) fabulous colleagues in the SMB corridors: Ritika, Maria, Moona, Elina, Jori, Visa, Mari, Mira, and Marie. Thanks for all the discussions about work and life in the corridors, lab and dark microscope rooms. Thank you also for all the laughter and fun at work and outside work from the gym to karonkka and other parties.

Next I want to thank my dear friends (in alphabetical order): Barbara a.k.a. Oode, Ezme, Hälly-Hälinen, Kastike-Kulmuni, Paananen (please, don't be mad about this ;), Tatjaana, Tinni and Vipe. I have known you all for a long time, and I cannot express how much I love you all and how much I appreciate your friendship. We all have lived in different places during these years, but you have always been there for me, no matter how rough the life has sometimes been. Warm thank also goes to my mother, father and my brother Juho for all their support. Whether I want to admit it or not, my father obviously had a great influence in why I ended up to study Biology by telling me constantly that

girls can be good in Science too! A big thanks goes also to my “second family”, the whole family of Leskinen. You have always made me feel like that I am part of your family and supported me.

Last but not least I express my deepest gratitude to Mikko, my rock who has always stood by me. We shared the life of a Ph.D. student and were able to discuss and support each other through all the good and bad that came on the way. Being a Ph.D. student is not always easy as we both experienced. Without your endless love and support, I would not have been able to do all of this.

YHTEENVETO (RÉSUMÉ IN FINNISH)

Lymen tauti eli Borrelioosi on yleisin *Ixodes*-sukuun kuuluvien puutiaisten levittämä infektiotauti, jonka aiheuttavat *Borrelia burgdorferi sensu lato*-ryhmään kuuluvat korkkiruuvinmuotoiset spirokeettabakteerit. *Borrelia burgdorferi sensu lato*-ryhmään kuuluu useita bakteerin eri alalajeja, joista *Borrelia garinii*, *Borrelia afzelii* ja *Borrelia bugdorferi sensu stricto* aiheuttavat tautia yleisimmin. Borrelioosia tavataan lähes koko Euroopassa, Pohjois-Amerikassa ja Aasiassa metsäisillä alueilla ja se on yleistynyt huomattavasti viimeisen kahden vuosikymmenen aikana. Borrelioosin tyypillisiä oireita ovat pian puutiaisen pureman jälkeen iholle ilmestyvä vaeltava ihottumarengas *Erythema migrans*, kuume, väsymys, nivel- ja lihaskivut, sekä erilaiset hermostolliset oireet. Taudin oikea diagnoosi ja hoito varhaisessa vaiheessa on tärkeää, koska infektion pitkittyessä bakteeri leviää iholta muualle elimistöön ja eri elimiin. Bakteerin levittyessä elimistöön, potilaiden oireet usein pahenevat ja infektio on hankalampi hoitaa.

B. burgdorferi on pleomorfinen eli se pystyy muuttamaan muotoaan ympäristöolosuhteiden muuttuessa sille epäsuotuisiksi. *B. burgdorferin* tiedetään muuntuvan esimerkiksi pyöreiksi pallomaisiksi muodoiksi, se voi muodostaa spirokeettojen keskivaiheille ja päihin granulaarisia solukalvon laajennoksia ja bakteerit pystyvät liittymään yhteen biofilmeiksi, joissa on mukana ekstrasellulaarisia komponentteja. *B. burgdorferin* pyöreät muodot eroavat spirokeetoista morfologisten erojen lisäksi esimerkiksi biokemiallisten ominaisuuksien ja antigeenisyyden suhteen. Pleomorfisuus auttaa bakteeria todennäköisesti välttelemään ja suojautumaan isäntäeliön immuunipuolustusreaktioilta ja levittäytymään elimistössä. Tiedetään, että monet kliinisesti merkittävät bakteerit, kuten *Escherichia coli,* ovat pleomorfisia mutta näiden epätyypillisten muotojen rooli taudin patogeneesissä on ollut epäselvä. Havainnot siitä, että bakteereilla voisi olla useita eri muotoja elinkierron aikana on horjuttanut monomorfista paradigmaa ja aiheuttanut keskustelua ja ristiriitoja. Tämän tutkimustyön tarkoituksena oli karakterisoida *B. burgdorferin* pyöreiden muotojen ominaisuuksia kuten soluseinän morfologiaa ja biokemiallista koostumusta, muodon bioaktiivisuutta, antigeenisyyttä ja vertailla spirokeettojen ja pyöreiden muotojen aikaansaamia immuunireaktioita. Lisäksi testattiin pyöreiden muotojen mahdollista sopivuutta antigeeniksi diagnostiseen testiin.

Ensimmäisessä osatyössä pleomorfisia muotoja indusoitiin eri kasvatusolosuhteissa *in vitro* ja niiden suhteelliset osuudet kvantifioitiin. Tutkimuksissa havaittiin, että ihmisen seerumi saa aikaan spirokeettojen muuntautumisen pyöreiksi muodoiksi. Lisäksi havaittiin, että pyöreät muodot ovat metabolisesti inaktiivisia mutta niillä on kyky palautua takaisin lisääntymiskykyisiksi spirokeetoiksi. Tulokset osoittivat, että pyöreät muodot eivät ole soluseinättömiä kuten usein on ajateltu. Niillä on myös hieman erilaiset biokemialliset ominaisuudet ja eroja proteiinisynteesissä verrattuna spirokeettoihin.

Toisessa osatyössä keskityttiin tarkastelemaan ja vertailemaan spirokeettojen ja pyöreiden muotojen fagosytoosia makrofagisoluihin, niiden prosessointia soluissa ja niiden stimuloimaa sytokiinien eritystä *in vitro*. Makrofagit fagosytoivat enemmän spirokeettoja kuin pyöreitä muotoja ja näiden kahden muodon välillä löydettiin myös eroja niiden käsittelystä soluissa. Pyöreitä muotoja prosessoidaan mahdollisesti myös muulla tavoin kuin tyypillisen lysosomaalisen hajotuksen kautta mutta tämän varmistaminen vaatii lisätutkimuksia. Lisäksi havaittiin, että spirokeettojen ja pyöreiden muotojen stimuloimassa sytokiinien erityksessä oli eroja. Pyöreitä muotoja fagosytoineet makrofagit erittivät enemmän MCP-1:tä kuin spirokeettoja sisäänsä ottaneet solut mutta vastaavasti sytokiineja IL-1, IL-1ra, IL-6, MIF, MIP-1β ja RANTES erittyi merkittävästi vähemmän. Kun borrelioosipotilaiden immuunireaktiota spirokeettoja ja pyöreitä muotoja vastaan verrattiin, havaittiin ensimmäistä kertaa, että potilaat tuottavat vasta-aineita myös pyöreitä muotoja vastaan. Joissakin tapauksissa potilaiden vasta-ainereaktio näitä muotoja vastaan oli voimakkaampi.

Kolmannessa osatyössä testattiin uudenlaista antigeeniyhdistelmää Elisa-borrelioositestiä varten. Erilaisten antigeenien kuten rekombinantti-proteiinien, eri borrelian alalajien ja muiden puutiaisvälitteisten patogeenien sisällyttämisellä oli tarkoitus parantaa Elisa-testin luotettavuutta. Lisäksi pyöreiden muotojen sopivuutta mahdolliseksi uudeksi antigeeniksi Elisa-testiin tutkittiin ensimmäistä kertaa. Tulokset osoittivat, että potilaat kaikissa taudin eri vaiheissa tuottivat vasta-aineita, erityisesti IgG:tä pyöreitä muotoja vastaan. Cohenin kappa-analyysi osoitti, että pyöreät muodot ovat riippumattomia muista antigeeneistä eli mahdollinen positiivinen tai negatiivinen tulos jollekin muulle antigeenille ei ennusta vasta-ainereaktiota pyöreille muodoille. Kaiken kaikkiaan pyöreät muodot lisäsivät Elisa-testin sensitiivisyyttä ja spesifisyyttä. Tulosten perusteella niiden sisällyttäminen serodiagnostisiin testeihin parantaisi testien luotettavuutta.

B. burgdorferi-bakteerin pleomorfiset muodot saattavat osittain selittää, miksi potilaiden taudinoireet ja immuunireaktiot bakteeria vastaan vaihtelevat yksilöiden välillä huomattavan paljon. Erilainen immuunivaste pleomorfisia muotoja vastaan voi liittyä immuunipuolustukselta piiloutumiseen ja edistää bakteerin kykyä selviytyä elimistössä pitkiäkin aikoja. Huolimatta tutkijoiden välisistä mielipide-eroista pleomorfisten muotojen roolista borrelioosin patogeneesissä, niiden tutkimus on ensiarvoisen tärkeää, jotta bakteerin elinkierto ja sen merkitys voidaan kokonaisvaltaisesti ymmärtää. Myös parantamalla diagnostisten testien luotettavuutta edistetään potilaiden varhaista diagnoosia ja hoitoa.

REFERENCES

Aberer E. & Duray P.H. 1991. Morphology of *Borrelia burgdorferi:* structural patterns of cultured borreliae in relation to staining methods. *J Clin Microbiol* 29(4): 764-772.

Aberer E., Kersten A., Klade H., Poitschek C. & Jurecka W. 1996. Heterogeneity of *Borrelia burgdorferi* in the skin. *Am J Dermatopathol* 18(6): 571-579.

Afzelius A. 1910. Verhandlungen der dermatologischen gesellschaft zu Stockholm. *Arch. Dermatol. Syph.* 10: 404.

Aguero-Rosenfeld M.E., Wang G., Schwartz I. & Wormser G.P. 2005. Diagnosis of lyme borreliosis. *Clin Microbiol Rev* 18(3): 484-509.

Al-Robaiy S., Dihazi H., Kacza J., Seeger J., Schiller J., Huster D., Knauer J. & Straubinger R.K. 2010. Metamorphosis of *Borrelia burgdorferi* organisms--RNA, lipid and protein composition in context with the spirochetes' shape. *J Basic Microbiol* 50 Suppl 1: S5-17.

Alban P.S., Johnson P.W. & Nelson D.R. 2000. Serum-starvation-induced changes in protein synthesis and morphology of *Borrelia burgdorferi*. *Microbiology* 146 (Pt 1): 119-127.

Alitalo A., Meri T., Lankinen H., Seppala I., Lahdenne P., Hefty P.S., Akins D. & Meri S. 2002. Complement inhibitor factor H binding to Lyme disease spirochetes is mediated by inducible expression of multiple plasmid-encoded outer surface protein E paralogs. *J Immunol* 169(7): 3847-3853.

Anguita J., Ramamoorthi N., Hovius J.W., Das S., Thomas V., Persinski R., Conze D., Askenase P.W., Rincon M., Kantor F.S. & Fikrig E. 2002. Salp15, an ixodes scapularis salivary protein, inhibits $CD4^+$ T cell activation. *Immunity* 16(6): 849-859.

Aucott J.N. 2015. Posttreatment Lyme disease syndrome. *Infect Dis Clin North Am* 29(2): 309-323.

Bacon R.M., Biggerstaff B.J., Schriefer M.E., Gilmore R.D., Jr., Philipp M.T., Steere A.C., Wormser G.P., Marques A.R. & Johnson B.J. 2003. Serodiagnosis of Lyme disease by kinetic enzyme-linked immunosorbent assay using recombinant VlsE1 or peptide antigens of *Borrelia burgdorferi* compared with 2-tiered testing using whole-cell lysates. *J Infect Dis* 187(8): 1187-1199.

Baqui A.A., Meiller T.F. & Falkler W.A. 1999. Enhanced interleukin-8 production in THP-1 human monocytic cells by lipopolysaccharide from oral microorganisms and granulocyte-macrophage colony-stimulating factor. *Oral microbiology and immunology* 14(5): 275-280.

Barbour A.G., Todd W.J. & Stoenner H.G. 1982. Action of penicillin on *Borrelia hermsii*. *Antimicrob Agents Chemother* 21(5): 823-829.

Barbour A.G. & Hayes S.F. 1986. Biology of Borrelia species. *Microbiol Rev* 50(4): 381-400.

Barthold S.W., Hodzic E., Imai D.M., Feng S., Yang X. & Luft B.J. 2010. Ineffectiveness of tigecycline against persistent *Borrelia burgdorferi*. *Antimicrob Agents Chemother* 54(2): 643-651.

Battafarano D.F., Combs J.A., Enzenauer R.J. & Fitzpatrick J.E. 1993. Chronic septic arthritis caused by *Borrelia burgdorferi*. *Clin Orthop Relat Res*(297): 238-241.

Beermann C., Wunderli-Allenspach H., Groscurth P. & Filgueira L. 2000. Lipoproteins from *Borrelia burgdorferi* applied in liposomes and presented by dendritic cells induce $CD8^+$ T-lymphocytes *in vitro*. *Cell Immunol* 201(2): 124-131.

Behera A.K., Hildebrand E., Bronson R.T., Perides G., Uematsu S., Akira S. & Hu L.T. 2006. MyD88 deficiency results in tissue-specific changes in cytokine induction and inflammation in interleukin-18-independent mice infected with *Borrelia burgdorferi*. *Infect Immun* 74(3): 1462-1470.

Ben-Menachem G., Kubler-Kielb J., Coxon B., Yergey A. & Schneerson R. 2003. A newly discovered cholesteryl galactoside from *Borrelia burgdorferi*. *Proc Natl Acad Sci U S A* 100(13): 7913-7918.

Benach J.L., Fleit H.B., Habicht G.S., Coleman J.L., Bosler E.M. & Lane B.P. 1984. Interactions of phagocytes with the Lyme disease spirochete: role of the Fc receptor. *J Infect Dis* 150(4): 497-507.

Benhnia M.R., Wroblewski D., Akhtar M.N., Patel R.A., Lavezzi W., Gangloff S.C., Goyert S.M., Caimano M.J., Radolf J.D. & Sellati T.J. 2005. Signaling through CD14 attenuates the inflammatory response to *Borrelia burgdorferi*, the agent of Lyme disease. *J Immunol* 174(3): 1539-1548.

Bergström S. & Zückert W.R. 2010. Structure, Function, and Biogenesis of the Borrelia Cell Envelope. In: Samuels D.S. and Radolf J.D. (eds.), Borrelia: Molecular Biology, Host Interaction and Pathogenesis, Caister Academic Press, Norfolk, UK, pp. 139–166.

Bockenstedt L.K., Mao J., Hodzic E., Barthold S.W. & Fish D. 2002. Detection of attenuated, noninfectious spirochetes in *Borrelia burgdorferi*-infected mice after antibiotic treatment. *J Infect Dis* 186(10): 1430-1437.

Bockenstedt L.K., Gonzalez D.G., Haberman A.M. & Belperron A.A. 2012. Spirochete antigens persist near cartilage after murine Lyme borreliosis therapy. *J Clin Invest* 122(7): 2652-2660.

Bolz D.D., Sundsbak R.S., Ma Y., Akira S., Kirschning C.J., Zachary J.F., Weis J.H. & Weis J.J. 2004. MyD88 plays a unique role in host defense but not arthritis development in Lyme disease. *J Immunol* 173(3): 2003-2010.

Bolz D.D. & Weis J.J. 2004. Molecular mimicry to *Borrelia burgdorferi*: pathway to autoimmunity? *Autoimmunity* 37(5): 387-392.

Borchers A.T., Keen C.L., Huntley A.C. & Gershwin M.E. 2015. Lyme disease: a rigorous review of diagnostic criteria and treatment. *J Autoimmun* 57: 82-115.

Bowdish D.M., Sakamoto K., Kim M.J., Kroos M., Mukhopadhyay S., Leifer C.A., Tryggvason K., Gordon S. & Russell D.G. 2009. MARCO, TLR2, and CD14 are required for macrophage cytokine responses to mycobacterial

trehalose dimycolate and Mycobacterium tuberculosis. *PLoS Pathog* 5(6): e1000474.

Bradley J.F., Johnson R.C. & Goodman J.L. 1994. The persistence of spirochetal nucleic acids in active Lyme arthritis. *Ann Intern Med* 120(6): 487-489.

Brandt M.E., Riley B.S., Radolf J.D. & Norgard M.V. 1990. Immunogenic integral membrane proteins of *Borrelia burgdorferi* are lipoproteins. *Infect Immun* 58(4): 983-991.

Breitner-Ruddock S., Wurzner R., Schulze J. & Brade V. 1997. Heterogeneity in the complement-dependent bacteriolysis within the species of *Borrelia burgdorferi*. *Med Microbiol Immunol* 185(4): 253-260.

Briers Y., Staubli T., Schmid M.C., Wagner M., Schuppler M. & Loessner M.J. 2012. Intracellular vesicles as reproduction elements in cell wall-deficient L-form bacteria. *PLoS One* 7(6): e38514.

Brissette C.A., Bykowski T., Cooley A.E., Bowman A. & Stevenson B. 2009. *Borrelia burgdorferi* RevA antigen binds host fibronectin. *Infect Immun* 77(7): 2802-2812.

Brorson O. & Brorson S.H. 1997. Transformation of cystic forms of *Borrelia burgdorferi* to normal, mobile spirochetes. *Infection* 25(4): 240-246.

Brorson O. & Brorson S.H. 1998. A rapid method for generating cystic forms of *Borrelia burgdorferi*, and their reversal to mobile spirochetes. *APMIS* 106(12): 1131-1141.

Brorson O., Brorson S.H., Scythes J., MacAllister J., Wier A. & Margulis L. 2009. Destruction of spirochete *Borrelia burgdorferi* round-body propagules (RBs) by the antibiotic tigecycline. *Proc Natl Acad Sci U S A* 106(44): 18656-18661.

Buchwald A. 1883. Ein fall von diffuser idiopathischer Haunt-Atrofie. *Arch. Dermatol. Syph.* 10: 553-556.

Bunikis I., Denker K., Ostberg Y., Andersen C., Benz R. & Bergstrom S. 2008. An RND-type efflux system in *Borrelia burgdorferi* is involved in virulence and resistance to antimicrobial compounds. *PLoS Pathog* 4(2): e1000009.

Bunikis J., Noppa L. & Bergstrom S. 1995. Molecular analysis of a 66-kDa protein associated with the outer membrane of Lyme disease Borrelia. *FEMS Microbiol Lett* 131(2): 139-145.

Burchill M.A., Nardelli D.T., England D.M., DeCoster D.J., Christopherson J.A., Callister S.M. & Schell R.F. 2003. Inhibition of interleukin-17 prevents the development of arthritis in vaccinated mice challenged with *Borrelia burgdorferi*. *Infect Immun* 71(6): 3437-3442.

Busch D.H., Jassoy C., Brinckmann U., Girschick H. & Huppertz H.I. 1996. Detection of *Borrelia burgdorferi*-specific CD8+ cytotoxic T cells in patients with Lyme arthritis. *J Immunol* 157(8): 3534-3541.

Carreiro M.M., Laux D.C. & Nelson D.R. 1990. Characterization of the heat shock response and identification of heat shock protein antigens of *Borrelia burgdorferi*. *Infect Immun* 58(7): 2186-2191.

Casjens S., Palmer N., van Vugt R., Huang W.M., Stevenson B., Rosa P., Lathigra R., Sutton G., Peterson J., Dodson R.J., Haft D., Hickey E., Gwinn M., White O. & Fraser C.M. 2000. A bacterial genome in flux: the twelve

linear and nine circular extrachromosomal DNAs in an infectious isolate of the Lyme disease spirochete *Borrelia burgdorferi*. *Mol Microbiol* 35(3): 490-516.

Casjens S.R., Eggers C.H. & Schwartz I. 2010. Borrelia Genomics: Chromosome, Plasmids, Bacteriophages and Genetics. In: Samuels D.S. and Radolf J.D. (eds.), Borrelia: Molecular Biology, Host Interaction and Pathogenesis, Caster Academic Press, Norfolk, UK, pp. 27–53.

Caskey J.R. & Embers M.E. 2015. Persister Development by *B. burgdorferi* Populations *In Vitro*. *Antimicrob Agents Chemother*.

Centers for Disease Control and Prevention (CDC) 1995. Recommendations for test performance and interpretation from the Second National Conference on Serologic Diagnosis of Lyme Disease. *MMWR Morb Mortal Wkly Rep* 44: 590–591.

Centers for Disease Control and Prevention (CDC) 2013. CDC provides an estimate of Americans diagnosed with Lyme disease each year. <URL:http://www.cdc.gov/media/releases/2013/p0819-lyme-disease.html> [Cited 28.72015].

Cerar T., Ogrinc K., Cimperman J., Lotric-Furlan S., Strle F. & Ruzic-Sabljic E. 2008. Validation of cultivation and PCR methods for diagnosis of Lyme neuroborreliosis. *J Clin Microbiol* 46(10): 3375-3379.

Cervantes J.L., Hawley K.L., Benjamin S.J., Weinerman B., Luu S.M. & Salazar J.C. 2014. Phagosomal TLR signaling upon *Borrelia burgdorferi* infection. *Frontiers in cellular and infection microbiology* 4: 55.

Charo I.F. & Ransohoff R.M. 2006. The many roles of chemokines and chemokine receptors in inflammation. *N Engl J Med* 354(6): 610-621.

Charon N.W. & Goldstein S.F. 2002. Genetics of motility and chemotaxis of a fascinating group of bacteria: the spirochetes. *Annual review of genetics* 36: 47-73.

Charon N.W., Goldstein S.F., Marko M., Hsieh C., Gebhardt L.L., Motaleb M.A., Wolgemuth C.W., Limberger R.J. & Rowe N. 2009. The flat-ribbon configuration of the periplasmic flagella of *Borrelia burgdorferi* and its relationship to motility and morphology. *J Bacteriol* 191(2): 600-607.

Chung Y., Zhang N. & Wooten R.M. 2013. *Borrelia burgdorferi* elicited-IL-10 suppresses the production of inflammatory mediators, phagocytosis, and expression of co-stimulatory receptors by murine macrophages and/or dendritic cells. *PLoS One* 8(12): e84980.

Cinco M., Murgia R., Presani G. & Perticarari S. 1997. Integrin CR3 mediates the binding of nonspecifically opsonized *Borrelia burgdorferi* to human phagocytes and mammalian cells. *Infect Immun* 65(11): 4784-4789.

Coburn J., Magoun L., Bodary S.C. & Leong J.M. 1998. Integrins alpha(v)beta3 and alpha5beta1 mediate attachment of lyme disease spirochetes to human cells. *Infect Immun* 66(5): 1946-1952.

Coburn J. & Cugini C. 2003. Targeted mutation of the outer membrane protein P66 disrupts attachment of the Lyme disease agent, *Borrelia burgdorferi*, to integrin alphavbeta3. *Proc Natl Acad Sci U S A* 100(12): 7301-7306.

Costerton J.W. 1999. Introduction to biofilm. *Int J Antimicrob Agents* 11(3-4): 217-221; discussion 237-219.

Costes S.V., Daelemans D., Cho E.H., Dobbin Z., Pavlakis G. & Lockett S. 2004. Automatic and quantitative measurement of protein-protein colocalization in live cells. *Biophys J* 86(6): 3993-4003.

Cruz A.R., Moore M.W., La Vake C.J., Eggers C.H., Salazar J.C. & Radolf J.D. 2008. Phagocytosis of *Borrelia burgdorferi*, the Lyme disease spirochete, potentiates innate immune activation and induces apoptosis in human monocytes. *Infect Immun* 76(1): 56-70.

Dell'Era S., Buchrieser C., Couve E., Schnell B., Briers Y., Schuppler M. & Loessner M.J. 2009. Listeria monocytogenes L-forms respond to cell wall deficiency by modifying gene expression and the mode of division. *Mol Microbiol* 73(2): 306-322.

Domingue G.J., Sr. & Woody H.B. 1997. Bacterial persistence and expression of disease. *Clin Microbiol Rev* 10(2): 320-344.

Dunham-Ems S.M., Caimano M.J., Eggers C.H. & Radolf J.D. 2012. *Borrelia burgdorferi* Requires the Alternative Sigma Factor RpoS for Dissemination within the Vector during Tick-to-Mammal Transmission. *PLoS Pathog* 8(2): e1002532.

Eisen L. & Lane R.S. 2002. Vectors of *Borrelia burgdorferi sensu lato*. In: Gray J.S., Kahl O., Lane R.S. and Stanek G. (eds.), Lyme Borreliosis, CABI Publishing, New York, pp. 91–115.

Embers M.E., Ramamoorthy R. & Philipp M.T. 2004. Survival strategies of *Borrelia burgdorferi*, the etiologic agent of Lyme disease. *Microbes Infect* 6(3): 312-318.

Embers M.E., Barthold S.W., Borda J.T., Bowers L., Doyle L., Hodzic E., Jacobs M.B., Hasenkampf N.R., Martin D.S., Narasimhan S., Phillippi-Falkenstein K.M., Purcell J.E., Ratterree M.S. & Philipp M.T. 2012. Persistence of *Borrelia burgdorferi* in rhesus macaques following antibiotic treatment of disseminated infection. *PLoS One* 7(1): e29914.

European Concerted Action on Lyme Disease. <URL:http://eucalb.com/> [Cited 21.08.2015].

Feng J., Wang T., Shi W., Zhang S., Sullivan D., Auwaerter P.G. & Zhang Y. 2014a. Identification of novel activity against *Borrelia burgdorferi* persisters using an FDA approved drug library. *Emerging microbes & infections* 3(7): e49.

Feng J., Wang T., Zhang S., Shi W. & Zhang Y. 2014b. An optimized SYBR Green I/PI assay for rapid viability assessment and antibiotic susceptibility testing for *Borrelia burgdorferi*. *PLoS One* 9(11): e111809.

Feng J., Auwaerter P.G. & Zhang Y. 2015. Drug combinations against *Borrelia burgdorferi* persisters *in vitro*: eradication achieved by using daptomycin, cefoperazone and doxycycline. *PLoS One* 10(3): e0117207.

Finlay B.B. & Falkow S. 1997. Common themes in microbial pathogenicity revisited. *Microbiology and molecular biology reviews : MMBR* 61(2): 136-169.

Fraser C.M., Casjens S., Huang W.M., Sutton G.G., Clayton R., Lathigra R., White O., Ketchum K.A., Dodson R., Hickey E.K., Gwinn M., Dougherty B., Tomb J.F., Fleischmann R.D., Richardson D., Peterson J., Kerlavage A.R., Quackenbush J., Salzberg S., Hanson M., van Vugt R., Palmer N., Adams M.D., Gocayne J., Weidman J., Utterback T., Watthey L., McDonald L., Artiach P., Bowman C., Garland S., Fuji C., Cotton M.D., Horst K., Roberts K., Hatch B., Smith H.O. & Venter J.C. 1997. Genomic sequence of a Lyme disease spirochaete, *Borrelia burgdorferi*. *Nature* 390(6660): 580-586.

Garcia R.C., Murgia R. & Cinco M. 2005. Complement receptor 3 binds the *Borrelia burgdorferi* outer surface proteins OspA and OspB in an iC3b-independent manner. *Infect Immun* 73(9): 6138-6142.

Garon C.F., Dorward D.W. & Corwin M.D. 1989. Structural features of *Borrelia burgdorferi*--the Lyme disease spirochete: silver staining for nucleic acids. *Scanning Microsc Suppl* 3: 109-115.

Gautam A., Dixit S., Philipp M.T., Singh S.R., Morici L.A., Kaushal D. & Dennis V.A. 2011. Interleukin-10 alters effector functions of multiple genes induced by *Borrelia burgdorferi* in macrophages to regulate Lyme disease inflammation. *Infect Immun* 79(12): 4876-4892.

Gautam A., Dixit S., Embers M., Gautam R., Philipp M.T., Singh S.R., Morici L. & Dennis V.A. 2012. Different patterns of expression and of IL-10 modulation of inflammatory mediators from macrophages of Lyme disease-resistant and -susceptible mice. *PLoS One* 7(9): e43860.

Giambartolomei G.H., Dennis V.A. & Philipp M.T. 1998. *Borrelia burgdorferi* stimulates the production of interleukin-10 in peripheral blood mononuclear cells from uninfected humans and rhesus monkeys. *Infect Immun* 66(6): 2691-2697.

Giambartolomei G.H., Dennis V.A., Lasater B.L. & Philipp M.T. 1999. Induction of pro- and anti-inflammatory cytokines by *Borrelia burgdorferi* lipoproteins in monocytes is mediated by CD14. *Infect Immun* 67(1): 140-147.

Glatz M., Golestani M., Kerl H. & Mullegger R.R. 2006. Clinical relevance of different IgG and IgM serum antibody responses to *Borrelia burgdorferi* after antibiotic therapy for erythema migrans: long-term follow-up study of 113 patients. *Arch Dermatol* 142(7): 862-868.

Glover W.A., Yang Y. & Zhang Y. 2009. Insights into the molecular basis of L-form formation and survival in *Escherichia coli*. *PLoS One* 4(10): e7316.

Goldstein S.F., Charon N.W. & Kreiling J.A. 1994. *Borrelia burgdorferi* swims with a planar waveform similar to that of eukaryotic flagella. *Proc Natl Acad Sci U S A* 91(8): 3433-3437.

Goldstein S.F., Li C., Liu J., Miller M., Motaleb A., Norris S.J., Silversmith C.W., Wolgemuth C.W. & Charon N.W. 2010. The Chic Motility and Chemotaxis of Borrelia burgdorferi. In: Samuels D.S. and Radolf J.D. (eds.), Borrelia: Molecular Biology, Host Interaction and Pathogenesis, Caister Academic Press, Norfolk, UK, pp. 167–187.

Grusell M., Widhe M. & Ekerfelt C. 2002. Increased expression of the Th1-inducing cytokines interleukin-12 and interleukin-18 in cerebrospinal fluid but not in sera from patients with Lyme neuroborreliosis. *J Neuroimmunol* 131(1-2): 173-178.

Gu L., Tseng S., Horner R.M., Tam C., Loda M. & Rollins B.J. 2000. Control of TH2 polarization by the chemokine monocyte chemoattractant protein-1. *Nature* 404(6776): 407-411.

Guo B.P., Norris S.J., Rosenberg L.C. & Hook M. 1995. Adherence of Borrelia burgdorferi to the proteoglycan decorin. *Infect Immun* 63(9): 3467-3472.

Hamilton T.A. 2002. Molecular basis of macrophage activation: from gene expression to phenotypic diversity. In: Bourke B. and Lewis C. (eds.), The Macrophage, Oxford University Press, Oxford, UK, pp. 73–102.

Hannier S., Liversidge J., Sternberg J.M. & Bowman A.S. 2004. Characterization of the B-cell inhibitory protein factor in Ixodes ricinus tick saliva: a potential role in enhanced Borrelia burgdoferi transmission. *Immunology* 113(3): 401-408.

Hawley K.L., Olson C.M., Jr., Iglesias-Pedraz J.M., Navasa N., Cervantes J.L., Caimano M.J., Izadi H., Ingalls R.R., Pal U., Salazar J.C., Radolf J.D. & Anguita J. 2012. CD14 cooperates with complement receptor 3 to mediate MyD88-independent phagocytosis of *Borrelia burgdorferi*. *Proc Natl Acad Sci U S A* 109(4): 1228-1232.

Hellwage J., Meri T., Heikkila T., Alitalo A., Panelius J., Lahdenne P., Seppala I.J. & Meri S. 2001. The complement regulator factor H binds to the surface protein OspE of *Borrelia burgdorferi*. *J Biol Chem* 276(11): 8427-8435.

Hirschfeld M., Kirschning C.J., Schwandner R., Wesche H., Weis J.H., Wooten R.M. & Weis J.J. 1999. Cutting edge: inflammatory signaling by *Borrelia burgdorferi* lipoproteins is mediated by toll-like receptor 2. *J Immunol* 163(5): 2382-2386.

Hodzic E., Feng S., Holden K., Freet K.J. & Barthold S.W. 2008. Persistence of *Borrelia burgdorferi* following antibiotic treatment in mice. *Antimicrob Agents Chemother* 52(5): 1728-1736.

Hodzic E., Imai D., Feng S. & Barthold S.W. 2014. Resurgence of persisting non-cultivable *Borrelia burgdorferi* following antibiotic treatment in mice. *PLoS One* 9(1): e86907.

Hoffmann A.K., Naj X. & Linder S. 2014. Daam1 is a regulator of filopodia formation and phagocytic uptake of *Borrelia burgdorferi* by primary human macrophages. *FASEB J* 28(7): 3075-3089.

Horwitz M.A. 1984. Phagocytosis of the Legionnaires' disease bacterium (Legionella pneumophila) occurs by a novel mechanism: engulfment within a pseudopod coil. *Cell* 36(1): 27-33.

Hu L.T., Eskildsen M.A., Masgala C., Steere A.C., Arner E.C., Pratta M.A., Grodzinsky A.J., Loening A. & Perides G. 2001. Host metalloproteinases in Lyme arthritis. *Arthritis Rheum* 44(6): 1401-1410.

Hubalek Z. 2009. Epidemiology of lyme borreliosis. *Curr Probl Dermatol* 37: 31-50.

Hulinska D., Bartak P., Hercogova J., Hancil J., Basta J. & Schramlova J. 1994. Electron microscopy of Langerhans cells and *Borrelia burgdorferi* in Lyme disease patients. *Zentralbl Bakteriol* 280(3): 348-359.

Hytonen J., Kortela E., Waris M., Puustinen J., Salo J. & Oksi J. 2014. CXCL13 and neopterin concentrations in cerebrospinal fluid of patients with Lyme neuroborreliosis and other diseases that cause neuroinflammation. *J Neuroinflammation* 11: 103.

Izard J., Renken C., Hsieh C.E., Desrosiers D.C., Dunham-Ems S., La Vake C., Gebhardt L.L., Limberger R.J., Cox D.L., Marko M. & Radolf J.D. 2009. Cryo-electron tomography elucidates the molecular architecture of Treponema pallidum, the syphilis spirochete. *J Bacteriol* 191(24): 7566-7580.

Jaakola S., Lyytikäinen O., Huusko S., Salmenlinna S., Pirhonen J., Savolainen-Kopra C., Liitsola K., Jalava J., Toropainen M., Nohynek H., Virtanen M., Löflund J.-E., Kuusi M. & Salminen M. (2015). Tartuntataudit Suomessa 2014. M. S. Helsinki, Terveyden ja hyvinvoinnin laitos (THL). 11/2015.

Juncadella I.J., Garg R., Ananthnarayanan S.K., Yengo C.M. & Anguita J. 2007. T-cell signaling pathways inhibited by the tick saliva immunosuppressor, Salp15. *FEMS Immunol Med Microbiol* 49(3): 433-438.

Justice S.S., Hung C., Theriot J.A., Fletcher D.A., Anderson G.G., Footer M.J. & Hultgren S.J. 2004. Differentiation and developmental pathways of uropathogenic Escherichia coli in urinary tract pathogenesis. *Proc Natl Acad Sci U S A* 101(5): 1333-1338.

Justice S.S., Hunstad D.A., Cegelski L. & Hultgren S.J. 2008. Morphological plasticity as a bacterial survival strategy. *Nat Rev Microbiol* 6(2): 162-168.

Kawai Y., Mercier R. & Errington J. 2014. Bacterial cell morphogenesis does not require a preexisting template structure. *Curr Biol* 24(8): 863-867.

Kern A., Schnell G., Bernard Q., Boeuf A., Jaulhac B., Collin E., Barthel C., Ehret-Sabatier L. & Boulanger N. 2015. Heterogeneity of *Borrelia burgdorferi* Sensu Stricto Population and Its Involvement in Borrelia Pathogenicity: Study on Murine Model with Specific Emphasis on the Skin Interface. *PLoS One* 10(7): e0133195.

Kersten A., Poitschek C., Rauch S. & Aberer E. 1995. Effects of penicillin, ceftriaxone, and doxycycline on morphology of *Borrelia burgdorferi*. *Antimicrob Agents Chemother* 39(5): 1127-1133.

Klempner M.S., Baker P.J., Shapiro E.D., Marques A., Dattwyler R.J., Halperin J.J. & Wormser G.P. 2013. Treatment trials for post-Lyme disease symptoms revisited. *Am J Med* 126(8): 665-669.

Kraiczy P., Skerka C., Brade V. & Zipfel P.F. 2001a. Further characterization of complement regulator-acquiring surface proteins of *Borrelia burgdorferi*. *Infect Immun* 69(12): 7800-7809.

Kraiczy P., Skerka C., Kirschfink M., Brade V. & Zipfel P.F. 2001b. Immune evasion of *Borrelia burgdorferi* by acquisition of human complement regulators FHL-1/reconectin and Factor H. *Eur J Immunol* 31(6): 1674-1684.

Kraiczy P., Hellwage J., Skerka C., Kirschfink M., Brade V., Zipfel P.F. & Wallich R. 2003. Immune evasion of *Borrelia burgdorferi*: mapping of a

complement-inhibitor factor H-binding site of BbCRASP-3, a novel member of the Erp protein family. *Eur J Immunol* 33(3): 697-707.

Kubes M., Kocakova P., Slovak M., Slavikova M., Fuchsberger N. & Nuttall P.A. 2002. Heterogeneity in the effect of different ixodid tick species on human natural killer cell activity. *Parasite Immunol* 24(1): 23-28.

Kudryashev M., Cyrklaff M., Wallich R., Baumeister W. & Frischknecht F. 2009. Distinct in situ structures of the Borrelia flagellar motor. *J Struct Biol* 169(1): 54-61.

Labandeira-Rey M., Seshu J. & Skare J.T. 2003. The absence of linear plasmid 25 or 28-1 of *Borrelia burgdorferi* dramatically alters the kinetics of experimental infection via distinct mechanisms. *Infect Immun* 71(8): 4608-4613.

Lantos P.M., Auwaerter P.G. & Wormser G.P. 2014. A systematic review of *Borrelia burgdorferi* morphologic variants does not support a role in chronic Lyme disease. *Clin Infect Dis* 58(5): 663-671.

Lawrence C., Lipton R.B., Lowy F.D. & Coyle P.K. 1995. Seronegative chronic relapsing neuroborreliosis. *Eur Neurol* 35(2): 113-117.

Lazarus J.J., Meadows M.J., Lintner R.E. & Wooten R.M. 2006. IL-10 deficiency promotes increased *Borrelia burgdorferi* clearance predominantly through enhanced innate immune responses. *J Immunol* 177(10): 7076-7085.

Lazarus J.J., Kay M.A., McCarter A.L. & Wooten R.M. 2008. Viable *Borrelia burgdorferi* enhances interleukin-10 production and suppresses activation of murine macrophages. *Infect Immun* 76(3): 1153-1162.

Lee Y.R., Liu M.T., Lei H.Y., Liu C.C., Wu J.M., Tung Y.C., Lin Y.S., Yeh T.M., Chen S.H. & Liu H.S. 2006. MCP-1, a highly expressed chemokine in dengue haemorrhagic fever/dengue shock syndrome patients, may cause permeability change, possibly through reduced tight junctions of vascular endothelium cells. *J Gen Virol* 87(Pt 12): 3623-3630.

Li X., McHugh G.A., Damle N., Sikand V.K., Glickstein L. & Steere A.C. 2011. Burden and viability of *Borrelia burgdorferi* in skin and joints of patients with erythema migrans or lyme arthritis. *Arthritis Rheum* 63(8): 2238-2247.

Liang F.T., Alvarez A.L., Gu Y., Nowling J.M., Ramamoorthy R. & Philipp M.T. 1999. An immunodominant conserved region within the variable domain of VlsE, the variable surface antigen of *Borrelia burgdorferi*. *J Immunol* 163(10): 5566-5573.

Liang F.T., Jacobs M.B., Bowers L.C. & Philipp M.T. 2002. An immune evasion mechanism for spirochetal persistence in Lyme borreliosis. *J Exp Med* 195(4): 415-422.

Linder S., Heimerl C., Fingerle V., Aepfelbacher M. & Wilske B. 2001. Coiling phagocytosis of *Borrelia burgdorferi* by primary human macrophages is controlled by CDC42Hs and Rac1 and involves recruitment of Wiskott-Aldrich syndrome protein and Arp2/3 complex. *Infect Immun* 69(3): 1739-1746.

Lindgren E. & Jaenson T.G.T. 2006. Lyme borreliosis in Europe: influences of climate and climate change, epidemiology, ecology and adaptation measures. *World Health Organization*.

Liu N., Montgomery R.R., Barthold S.W. & Bockenstedt L.K. 2004. Myeloid differentiation antigen 88 deficiency impairs pathogen clearance but does not alter inflammation in *Borrelia burgdorferi*-infected mice. *Infect Immun* 72(6): 3195-3203.

Luckheeram R.V., Zhou R., Verma A.D. & Xia B. 2012. CD4(+)T cells: differentiation and functions. *Clin Dev Immunol* 2012: 925135.

Ma B., Christen B., Leung D. & Vigo-Pelfrey C. 1992. Serodiagnosis of Lyme borreliosis by western immunoblot: reactivity of various significant antibodies against *Borrelia burgdorferi*. *J Clin Microbiol* 30(2): 370-376.

MacDonald A.B. & Miranda J.M. 1987. Concurrent neocortical borreliosis and Alzheimer's disease. *Hum Pathol* 18(7): 759-761.

MacDonald A.B. 1988. Concurrent Neocortical Borreliosis and Alzheimer's Disease Demonstration of a Spirochetal Cyst Form. *Ann NY Acad Sci* 539: 468–470.

Mantovani A., Sica A., Sozzani S., Allavena P., Vecchi A. & Locati M. 2004. The chemokine system in diverse forms of macrophage activation and polarization. *Trends in immunology* 25(12): 677-686.

Mattman L.H. (2001). Cell Wall Deficient Forms - Stealth Pathogens. Boca Raton, Florida, CRC Press LLC.

McKisic M.D., Redmond W.L. & Barthold S.W. 2000. Cutting edge: T cell-mediated pathology in murine Lyme borreliosis. *J Immunol* 164(12): 6096-6099.

Mead P.S. 2011. Global Epidemiology of *Borrelia burgdorferi* Infections. In: Halperin J.J. (eds.), Lyme Disease: An Evidence-based Approach – Advances in Molecular and Cellular Microbiology 20, CAB International, Oxfordshire, pp. 110–114.

Miklossy J., Kasas S., Zurn A.D., McCall S., Yu S. & McGeer P.L. 2008. Persisting atypical and cystic forms of *Borrelia burgdorferi* and local inflammation in Lyme neuroborreliosis. *J Neuroinflammation* 5: 40.

Mogilyansky E., Loa C.C., Adelson M.E., Mordechai E. & Tilton R.C. 2004. Comparison of Western immunoblotting and the C6 Lyme antibody test for laboratory detection of Lyme disease. *Clin Diagn Lab Immunol* 11(5): 924-929.

Molins C.R., Ashton L.V., Wormser G.P., Hess A.M., Delorey M.J., Mahapatra S., Schriefer M.E. & Belisle J.T. 2015. Development of a metabolic biosignature for detection of early Lyme disease. *Clin Infect Dis* 60(12): 1767-1775.

Montgomery R.R., Nathanson M.H. & Malawista S.E. 1993. The fate of *Borrelia burgdorferi*, the agent for Lyme disease, in mouse macrophages. Destruction, survival, recovery. *J Immunol* 150(3): 909-915.

Montgomery R.R., Nathanson M.H. & Malawista S.E. 1994. Fc- and non-Fc-mediated phagocytosis of *Borrelia burgdorferi* by macrophages. *J Infect Dis* 170(4): 890-893.

Montgomery R.R. & Malawista S.E. 1996. Entry of *Borrelia burgdorferi* into macrophages is end-on and leads to degradation in lysosomes. *Infect Immun* 64(7): 2867-2872.

Montgomery R.R., Lusitani D., de Boisfleury Chevance A. & Malawista S.E. 2002. Human phagocytic cells in the early innate immune response to *Borrelia burgdorferi*. *J Infect Dis* 185(12): 1773-1779.

Montgomery R.R., Lusitani D., De Boisfleury Chevance A. & Malawista S.E. 2004. Tick saliva reduces adherence and area of human neutrophils. *Infect Immun* 72(5): 2989-2994.

Moore M.W., Cruz A.R., LaVake C.J., Marzo A.L., Eggers C.H., Salazar J.C. & Radolf J.D. 2007. Phagocytosis of *Borrelia burgdorferi* and Treponema pallidum potentiates innate immune activation and induces gamma interferon production. *Infect Immun* 75(4): 2046-2062.

Mosser D.M. & Edwards J.P. 2008. Exploring the full spectrum of macrophage activation. *Nat Rev Immunol* 8(12): 958-969.

Motaleb M.A., Corum L., Bono J.L., Elias A.F., Rosa P., Samuels D.S. & Charon N.W. 2000. *Borrelia burgdorferi* periplasmic flagella have both skeletal and motility functions. *Proc Natl Acad Sci U S A* 97(20): 10899-10904.

Mullegger R.R., McHugh G., Ruthazer R., Binder B., Kerl H. & Steere A.C. 2000. Differential expression of cytokine mRNA in skin specimens from patients with erythema migrans or acrodermatitis chronica atrophicans. *J Invest Dermatol* 115(6): 1115-1123.

Murgia R., Piazzetta C. & Cinco M. 2002. Cystic forms of *Borrelia burgdorferi sensu lato*: induction, development, and the role of RpoS. *Wien Klin Wochenschr* 114(13-14): 574-579.

Murgia R. & Cinco M. 2004. Induction of cystic forms by different stress conditions in *Borrelia burgdorferi*. *APMIS* 112(1): 57-62.

Mursic V.P., Wanner G., Reinhardt S., Wilske B., Busch U. & Marget W. 1996. Formation and cultivation of *Borrelia burgdorferi* spheroplast-L-form variants. *Infection* 24(3): 218-226.

Murthy P.K., Dennis V.A., Lasater B.L. & Philipp M.T. 2000. Interleukin-10 modulates proinflammatory cytokines in the human monocytic cell line THP-1 stimulated with *Borrelia burgdorferi* lipoproteins. *Infect Immun* 68(12): 6663-6669.

Naj X., Hoffmann A.K., Himmel M. & Linder S. 2013. The formins FMNL1 and mDia1 regulate coiling phagocytosis of *Borrelia burgdorferi* by primary human macrophages. *Infect Immun* 81(5): 1683-1695.

Nocton J.J., Dressler F., Rutledge B.J., Rys P.N., Persing D.H. & Steere A.C. 1994. Detection of *Borrelia burgdorferi* DNA by polymerase chain reaction in synovial fluid from patients with Lyme arthritis. *N Engl J Med* 330(4): 229-234.

Nocton J.J., Bloom B.J., Rutledge B.J., Persing D.H., Logigian E.L., Schmid C.H. & Steere A.C. 1996. Detection of *Borrelia burgdorferi* DNA by polymerase chain reaction in cerebrospinal fluid in Lyme neuroborreliosis. *J Infect Dis* 174(3): 623-627.

Oksi J., Marjamaki M., Nikoskelainen J. & Viljanen M.K. 1999. *Borrelia burgdorferi* detected by culture and PCR in clinical relapse of disseminated Lyme borreliosis. *Ann Med* 31(3): 225-232.

Onder O., Humphrey P.T., McOmber B., Korobova F., Francella N., Greenbaum D.C. & Brisson D. 2012. OspC is potent plasminogen receptor on surface of *Borrelia burgdorferi*. *J Biol Chem* 287(20): 16860-16868.

Onwuamaegbu M.E., Belcher R.A. & Soare C. 2005. Cell wall-deficient bacteria as a cause of infections: a review of the clinical significance. *J Int Med Res* 33(1): 1-20.

Paster B.J., Dewhirst F.E., Weisburg W.G., Tordoff L.A., Fraser G.J., Hespell R.B., Stanton T.B., Zablen L., Mandelco L. & Woese C.R. 1991. Phylogenetic analysis of the spirochetes. *J Bacteriol* 173(19): 6101-6109.

Petnicki-Ocwieja T., DeFrancesco A.S., Chung E., Darcy C.T., Bronson R.T., Kobayashi K.S. & Hu L.T. 2011. Nod2 suppresses *Borrelia burgdorferi* mediated murine Lyme arthritis and carditis through the induction of tolerance. *PLoS One* 6(2): e17414.

Petnicki-Ocwieja T. & Kern A. 2014. Mechanisms of *Borrelia burgdorferi* internalization and intracellular innate immune signaling. *Frontiers in cellular and infection microbiology* 4: 175.

Petzke M.M., Brooks A., Krupna M.A., Mordue D. & Schwartz I. 2009. Recognition of *Borrelia burgdorferi*, the Lyme disease spirochete, by TLR7 and TLR9 induces a type I IFN response by human immune cells. *J Immunol* 183(8): 5279-5292.

Picha D., Moravcova L., Holeckova D., Zd'arsky E., Valesova M., Maresova V., Hercogova J. & Vanousova D. 2008. Examination of specific DNA by PCR in patients with different forms of Lyme borreliosis. *Int J Dermatol* 47(10): 1004-1010.

Radolf J.D., Salazar J.C. & Dattwyler R.J. 2010. Lyme Disease in Humans. In: Samuels D.S. and Radolf J.D. (eds.), Borrelia: Molecular Biology, Host Interaction and Pathogenesis, Caister Academic Press, Norfolk, UK, pp. 487–533.

Radolf J.D., Caimano M.J., Stevenson B. & Hu L.T. 2012. Of ticks, mice and men: understanding the dual-host lifestyle of Lyme disease spirochaetes. *Nat Rev Microbiol* 10(2): 87-99.

Ramamoorthi N., Narasimhan S., Pal U., Bao F., Yang X.F., Fish D., Anguita J., Norgard M.V., Kantor F.S., Anderson J.F., Koski R.A. & Fikrig E. 2005. The Lyme disease agent exploits a tick protein to infect the mammalian host. *Nature* 436(7050): 573-577.

Rittig M.G., Krause A., Haupl T., Schaible U.E., Modolell M., Kramer M.D., Lutjen-Drecoll E., Simon M.M. & Burmester G.R. 1992. Coiling phagocytosis is the preferential phagocytic mechanism for*Borrelia burgdorferi*. *Infect Immun* 60(10): 4205-4212.

Rittig M.G., Haupl T., Krause A., Kressel M., Groscurth P. & Burmester G.R. 1994. *Borrelia burgdorferi*-induced ultrastructural alterations in human phagocytes: a clue to pathogenicity? *J Pathol* 173(3): 269-282.

Robertson J., Guy E., Andrews N., Wilske B., Anda P., Granstrom M., Hauser U., Moosmann Y., Sambri V., Schellekens J., Stanek G. & Gray J. 2000. A European multicenter study of immunoblotting in serodiagnosis of lyme borreliosis. *J Clin Microbiol* 38(6): 2097-2102.

Rogovskyy A.S. & Bankhead T. 2013. Variable VlsE is critical for host reinfection by the Lyme disease spirochete. *PLoS One* 8(4): e61226.

Rudenko N., Golovchenko M., Grubhoffer L. & Oliver J.H., Jr. 2011. Updates on *Borrelia burgdorferi sensu lato* complex with respect to public health. *Ticks Tick Borne Dis* 2(3): 123-128.

Rupprecht T.A., Pfister H.W., Angele B., Kastenbauer S., Wilske B. & Koedel U. 2005. The chemokine CXCL13 (BLC): a putative diagnostic marker for neuroborreliosis. *Neurology* 65(3): 448-450.

Rupprecht T.A., Koedel U., Fingerle V. & Pfister H.W. 2008. The pathogenesis of lyme neuroborreliosis: from infection to inflammation. *Mol Med* 14(3-4): 205-212.

Salazar J.C., Pope C.D., Sellati T.J., Feder H.M., Jr., Kiely T.G., Dardick K.R., Buckman R.L., Moore M.W., Caimano M.J., Pope J.G., Krause P.J., Radolf J.D. & Lyme Disease N. 2003. Coevolution of markers of innate and adaptive immunity in skin and peripheral blood of patients with erythema migrans. *J Immunol* 171(5): 2660-2670.

Salazar J.C., Duhnam-Ems S., La Vake C., Cruz A.R., Moore M.W., Caimano M.J., Velez-Climent L., Shupe J., Krueger W. & Radolf J.D. 2009. Activation of human monocytes by live *Borrelia burgdorferi* generates TLR2-dependent and -independent responses which include induction of IFN-beta. *PLoS Pathog* 5(5): e1000444.

Sapi E., Kaur N., Anyanwu S., Luecke D.F., Datar A., Patel S., Rossi M. & Stricker R.B. 2011. Evaluation of in-vitro antibiotic susceptibility of different morphological forms of *Borrelia burgdorferi*. *Infect Drug Resist* 4: 97-113.

Sapi E., Bastian S.L., Mpoy C.M., Scott S., Rattelle A., Pabbati N., Poruri A., Burugu D., Theophilus P.A.S., Pham T.V., Datar A., Dhaliwal N.K., MacDonald A., Rossi M.J., Sinha S.K. & Luecke D.F. 2012. Characterization of Biofilm Formation by *Borrelia burgdorferi In Vitro*. *PLoS One* 7(10): e48277.

Schaller M. & Neubert U. 1994. Ultrastructure of *Borrelia burgdorferi* after exposure to benzylpenicillin. *Infection* 22(6): 401-406.

Schleifer K.H. & Kandler O. 1972. Peptidoglycan types of bacterial cell walls and their taxonomic implications. *Bacteriological reviews* 36(4): 407-477.

Schnell B., Staubli T., Harris N.L., Rogler G., Kopf M., Loessner M.J. & Schuppler M. 2014. Cell-wall deficient L. monocytogenes L-forms feature abrogated pathogenicity. *Frontiers in cellular and infection microbiology* 4: 60.

Schwan T.G., Piesman J., Golde W.T., Dolan M.C. & Rosa P.A. 1995. Induction of an outer surface protein on *Borrelia burgdorferi* during tick feeding. *Proc Natl Acad Sci U S A* 92(7): 2909-2913.

Schwan T.G. & Piesman J. 2002. Vector interactions and molecular adaptations of lyme disease and relapsing fever spirochetes associated with transmission by ticks. *Emerg Infect Dis* 8(2): 115-121.

Sharma B., Brown A.V., Matluck N.E., Hu L.T. & Lewis K. 2015. *Borrelia burgdorferi*, the Causative Agent of Lyme Disease, Forms Drug-Tolerant Persister Cells. *Antimicrob Agents Chemother* 59(8): 4616-4624.

Shin J.J., Glickstein L.J. & Steere A.C. 2007. High levels of inflammatory chemokines and cytokines in joint fluid and synovial tissue throughout the course of antibiotic-refractory lyme arthritis. *Arthritis Rheum* 56(4): 1325-1335.

Shin J.J., Strle K., Glickstein L.J., Luster A.D. & Steere A.C. 2010. *Borrelia burgdorferi* stimulation of chemokine secretion by cells of monocyte lineage in patients with Lyme arthritis. *Arthritis Res Ther* 12(5): R168.

Shin O.S., Isberg R.R., Akira S., Uematsu S., Behera A.K. & Hu L.T. 2008. Distinct roles for MyD88 and Toll-like receptors 2, 5, and 9 in phagocytosis of *Borrelia burgdorferi* and cytokine induction. *Infect Immun* 76(6): 2341-2351.

Simpson W.J., Schrumpf M.E. & Schwan T.G. 1990. Reactivity of human Lyme borreliosis sera with a 39-kilodalton antigen specific to *Borrelia burgdorferi*. *J Clin Microbiol* 28(6): 1329-1337.

Smith R.P. 2011. Ticks: the Vectors of Lyme Disease. In: Halperin J.J. (eds.), Lyme Disease, An Evidence-Based Approach, Cambridge University Press, Oxfordshire, UK, pp. 1–28.

Sonderegger F.L., Ma Y., Maylor-Hagan H., Brewster J., Huang X., Spangrude G.J., Zachary J.F., Weis J.H. & Weis J.J. 2012. Localized production of IL-10 suppresses early inflammatory cell infiltration and subsequent development of IFN-gamma-mediated Lyme arthritis. *J Immunol* 188(3): 1381-1393.

Srivastava S.Y. & de Silva A.M. 2009. Characterization of *Borrelia burgdorferi* aggregates. *Vector Borne Zoonotic Dis* 9(3): 323-329.

Stanek G. & Strle F. 2008. Lyme disease: European perspective. *Infect Dis Clin North Am* 22(2): 327-339, vii.

Steere A.C., Coburn J. & Glickstein L. 2004. The emergence of Lyme disease. *J Clin Invest* 113(8): 1093-1101.

Straubinger R.K., Summers B.A., Chang Y.F. & Appel M.J. 1997. Persistence of *Borrelia burgdorferi* in experimentally infected dogs after antibiotic treatment. *J Clin Microbiol* 35(1): 111-116.

Straubinger R.K. 2000. PCR-Based quantification of *Borrelia burgdorferi* organisms in canine tissues over a 500-Day postinfection period. *J Clin Microbiol* 38(6): 2191-2199.

Stricker R.B. & Johnson L. 2011. Lyme disease: the next decade. *Infect Drug Resist* 4: 1-9.

Strle F., Nadelman R.B., Cimperman J., Nowakowski J., Picken R.N., Schwartz I., Maraspin V., Aguero-Rosenfeld M.E., Varde S., Lotric-Furlan S. & Wormser G.P. 1999. Comparison of culture-confirmed erythema migrans

caused by *Borrelia burgdorferi sensu stricto* in New York State and by *Borrelia afzelii* in Slovenia. *Ann Intern Med* 130(1): 32-36.

Strle K., Drouin E.E., Shen S., Khoury J.E., McHugh G., Ruzic-Sabljic E., Strle F. & Steere A.C. 2009. *Borrelia burgdorferi* stimulates macrophages to secrete higher levels of cytokines and chemokines than *Borrelia afzelii* or *Borrelia garinii*. *J Infect Dis* 200(12): 1936-1943.

Sung S.Y., Lavoie C.P., Carlyon J.A. & Marconi R.T. 1998. Genetic divergence and evolutionary instability in ospE-related members of the upstream homology box gene family in *Borrelia burgdorferi sensu lato* complex isolates. *Infect Immun* 66(10): 4656-4668.

Takayama K., Rothenberg R.J. & Barbour A.G. 1987. Absence of lipopolysaccharide in the Lyme disease spirochete, *Borrelia burgdorferi*. *Infect Immun* 55(9): 2311-2313.

Tan C. & Gery I. 2012. The unique features of Th9 cells and their products. *Critical reviews in immunology* 32(1): 1-10.

Tilly K., Krum J.G., Bestor A., Jewett M.W., Grimm D., Bueschel D., Byram R., Dorward D., Vanraden M.J., Stewart P. & Rosa P. 2006. *Borrelia burgdorferi* OspC protein required exclusively in a crucial early stage of mammalian infection. *Infect Immun* 74(6): 3554-3564.

Tilly K., Bestor A., Jewett M.W. & Rosa P. 2007. Rapid clearance of Lyme disease spirochetes lacking OspC from skin. *Infect Immun* 75(3): 1517-1519.

Timmaraju A., Theophilus P.A., Balasubramanian K., Shakih S., Leucke D.F. & Sapi E. 2015. Biofilm formation by Borrelia sensu lato. *FEMS Microbiol Lett*.

Toledo A.B., J.L 2011. Borrelia: Biology of the Organism. In: Halperin J.J. (eds.), Lyme Disease: An Evidence-based Approach – Advances in Molecular and Cellular Microbiology 20, CAB International, Oxfordshire, pp.

van Dam A.P., Oei A., Jaspars R., Fijen C., Wilske B., Spanjaard L. & Dankert J. 1997. Complement-mediated serum sensitivity among spirochetes that cause Lyme disease. *Infect Immun* 65(4): 1228-1236.

Verma A., Brissette C.A., Bowman A. & Stevenson B. 2009. *Borrelia burgdorferi* BmpA is a laminin-binding protein. *Infect Immun* 77(11): 4940-4946.

Viera A.J. & Garrett J.M. 2005. Understanding interobserver agreement: the kappa statistic. *Family medicine* 37(5): 360-363.

Vollmer W., Blanot D. & de Pedro M.A. 2008. Peptidoglycan structure and architecture. *FEMS Microbiol Rev* 32(2): 149-167.

Wang G., Liveris D., Mukherjee P., Jungnick S., Margos G. & Schwartz I. 2014. Molecular Typing of *Borrelia burgdorferi*. *Curr Protoc Microbiol* 34: 12C 15 11-12C 15 31.

Weis J.J. & Bockenstedt L.K. 2010. Host response. In: Samuels D.S. and Radolf J.D. (eds.), Borrelia: Molecular Biology, Host Interaction and Pathogenesis, Caister Academic Press, Norfolk, UK, pp. 413–441.

Whitchurch C.B., Tolker-Nielsen T., Ragas P.C. & Mattick J.S. 2002. Extracellular DNA required for bacterial biofilm formation. *Science* 295(5559): 1487.

Whitmire W.M. & Garon C.F. 1993. Specific and nonspecific responses of murine B cells to membrane blebs of *Borrelia burgdorferi*. *Infect Immun* 61(4): 1460-1467.

Widhe M., Grusell M., Ekerfelt C., Vrethem M., Forsberg P. & Ernerudh J. 2002. Cytokines in Lyme borreliosis: lack of early tumour necrosis factor-alpha and transforming growth factor-beta1 responses are associated with chronic neuroborreliosis. *Immunology* 107(1): 46-55.

Wilske B., Preac-Mursic V., Jauris S., Hofmann A., Pradel I., Soutschek E., Schwab E., Will G. and Wanner G. 1993. Immunological and molecular polymorphisms of OspC, an immunodominant major outer surface protein of *Borrelia burgdorferi*. *Infect Immun* 61(5): 2182-2191.

Wilske B., Fingerle V. & Schulte-Spechtel U. 2007. Microbiological and serological diagnosis of Lyme borreliosis. *FEMS Immunol Med Microbiol* 49(1): 13-21.

Winkler W. 1899. Untersuchungen über das Wessen der Bakterien und deren einordnung im pilzsystem. *Zbl. Bakt.II Abt. Orig*. 5: 569–579.

Wolgemuth C.W., Charon N.W., Goldstein S.F. & Goldstein R.E. 2006. The flagellar cytoskeleton of the spirochetes. *J Mol Microbiol Biotechnol* 11(3-5): 221-227.

Wooten R.M., Ma Y., Yoder R.A., Brown J.P., Weis J.H., Zachary J.F., Kirschning C.J. & Weis J.J. 2002. Toll-like receptor 2 is required for innate, but not acquired, host defense to *Borrelia burgdorferi*. *J Immunol* 168(1): 348-355.

Wormser G.P., Dattwyler R.J., Shapiro E.D., Halperin J.J., Steere A.C., Klempner M.S., Krause P.J., Bakken J.S., Strle F., Stanek G., Bockenstedt L., Fish D., Dumler J.S. & Nadelman R.B. 2006. The clinical assessment, treatment, and prevention of lyme disease, human granulocytic anaplasmosis, and babesiosis: clinical practice guidelines by the Infectious Diseases Society of America. *Clin Infect Dis* 43(9): 1089-1134.

Wormser G.P., Liveris D., Hanincova K., Brisson D., Ludin S., Stracuzzi V.J., Embers M.E., Philipp M.T., Levin A., Aguero-Rosenfeld M. & Schwartz I. 2008. Effect of *Borrelia burgdorferi* genotype on the sensitivity of C6 and 2-tier testing in North American patients with culture-confirmed Lyme disease. *Clin Infect Dis* 47(7): 910-914.

Wormser G.P., Schwartz I. 2009. Antibiotic treatment of animals infected with Borrelia burgdorferi. *Clin Microbiol Rev* 22(3):387-395.

Wormser G.P., Schriefer M., Aguero-Rosenfeld M.E., Levin A., Steere A.C., Nadelman R.B., Nowakowski J., Marques A., Johnson B.J. & Dumler J.S. 2013. Single-tier testing with the C6 peptide ELISA kit compared with two-tier testing for Lyme disease. *Diagn Microbiol Infect Dis* 75(1): 9-15.

Yang J., Zhang L., Yu C., Yang X.F. & Wang H. 2014. Monocyte and macrophage differentiation: circulation inflammatory monocyte as biomarker for inflammatory diseases. *Biomarker research* 2(1): 1.

Yrjanainen H., Hytonen J., Hartiala P., Oksi J. & Viljanen M.K. 2010. Persistence of borrelial DNA in the joints of *Borrelia burgdorferi*-infected mice after ceftriaxone treatment. *APMIS* 118(9): 665-673.

Zhang J.R. & Norris S.J. 1998. Genetic variation of the *Borrelia burgdorferi* gene vlsE involves cassette-specific, segmental gene conversion. *Infect Immun* 66(8): 3698-3704.

Zhu J. & Paul W.E. 2010. Peripheral CD4+ T-cell differentiation regulated by networks of cytokines and transcription factors. *Immunol Rev* 238(1): 247-262.

ORIGINAL PAPERS

I

MORPHOLOGICAL AND BIOCHEMICAL FEATURES OF *BORRELIA BURGDORFERI* PLEOMORPHIC FORMS

by

Leena Meriläinen, Anni Herranen, Armin Schwarzbach and Leona Gilbert, 2015

Microbiology 151: 516-527.

Microbiology (2015), **161**, 516–527 **DOI** 10.1099/mic.0.000027

Morphological and biochemical features of *Borrelia burgdorferi* pleomorphic forms

Leena Meriläinen,[1] Anni Herranen,[1] Armin Schwarzbach[2] and Leona Gilbert[1]

[1]Department of Biological and Environmental Sciences and NanoScience Center, University of Jyväskylä, Jyväskylä, Finland

[2]Borreliose Centrum Augsburg, Augsburg, Germany

Correspondence
Leena Meriläinen
leena.m.merilainen@jyu.fi

Received 11 November 2014
Accepted 27 December 2014

The spirochaete bacterium *Borrelia burgdorferi sensu lato* is the causative agent of Lyme disease, the most common tick-borne infection in the northern hemisphere. There is a long-standing debate regarding the role of pleomorphic forms in Lyme disease pathogenesis, while very little is known about the characteristics of these morphological variants. Here, we present a comprehensive analysis of *B. burgdorferi* pleomorphic formation in different culturing conditions at physiological temperature. Interestingly, human serum induced the bacterium to change its morphology to round bodies (RBs). In addition, biofilm-like colonies in suspension were found to be part of *B. burgdorferi*'s normal *in vitro* growth. Further studies provided evidence that spherical RBs had an intact and flexible cell envelope, demonstrating that they are not cell wall deficient, or degenerative as previously implied. However, the RBs displayed lower metabolic activity compared with spirochaetes. Furthermore, our results indicated that the different pleomorphic variants were distinguishable by having unique biochemical signatures. Consequently, pleomorphic *B. burgdorferi* should be taken into consideration as being clinically relevant and influence the development of novel diagnostics and treatment protocols.

INTRODUCTION

Lyme disease is the most commonly reported tick-borne infection in Europe and North America, and is also endemic in many areas in Asia (Mead, 2011; Radolf *et al.*, 2012). The disease is caused by the different genospecies of the spirochaete bacterium *Borrelia burgdorferi sensu lato* group (Radolf *et al.*, 2012). The cell envelope of *B. burgdorferi* consists of a protoplasmic cylinder covered by two lipid membranes (Barbour & Hayes, 1986). Between the outer and inner membrane is the periplasmic space that comprises the peptidoglycan layer and flagellar filaments (Kudryashev *et al.*, 2009). The general structure of *B. burgdorferi*'s cell envelope is exceptional and differs significantly from the typical Gram-negative bacteria. LPSs are usually outer membrane components of Gram-negative bacteria; however, *B. burgdorferi* lacks LPS (Takayama *et al.*, 1987), and has immunoreactive glycolipids instead (Ben-Menachem *et al.*, 2003). Flagella are located in the periplasmic space, while other bacteria commonly have them outside the cell (Harman *et al.*, 2013). Furthermore, the flagella not only provide the motility function, but also confine the cell shape in *B. burgdorferi* (Motaleb *et al.*, 2000).

B. burgdorferi sensu lato is pleomorphic, being able to change its morphology as a response to environmental conditions. The existence of pleomorphism among many bacterial species *in vitro* has been known for over a century (Mattman, 2001; Winkler, 1899). At the beginning of the 19th century, researchers proposed that spirochaete species had multiple morphologies (Berndtson, 2013). Today it is well known that many Gram-negative and Gram-positive bacteria can spontaneously or by stimulation change their morphology both *in vitro* and *in vivo* (Domingue & Woody, 1997).

Pleomorphism is commonly induced *in vitro* using compounds that either lyse the cell wall (lytic enzymes), or interfere with the cell wall synthesis, such as antibiotics (Briers *et al.*, 2012). This treatment usually leads to a complete or partial loss of peptidoglycan cell wall and the resulting cells have been called cell wall deficient (CWD), L-forms or spheroplasts (Glover *et al.*, 2009; Ranjit & Young, 2013). In addition to CWD forms, various bacteria

Abbreviations: BFL, biofilm-like; BODIPY, boron-dipyrromethene; CWD, cell wall deficient; DIC, differential interference contrast (microscopy); EPS, extracellular polymeric substance matrix; GluNAc, *N*-acetylglucosamine polysaccharides; HS, human serum; PH, phase-contrast; PI, propidium iodide; RB, round body; TEM, transmission electron microscopy; WGA, wheatgerm agglutinin.

One supplementary figure and two supplementary movies are available with the online Supplementary Material.

can aggregate into biofilms (Flemming & Wingender, 2010). Furthermore, filamentous bacteria shapes of many clinically important bacteria, such as *Escherichia coli*, have been reported (Justice *et al.*, 2004). In addition to the typical spirochaete, *B. burgdorferi* is seen also as small spherical shapes (Al-Robaiy *et al.*, 2010; Alban *et al.*, 2000; Dunham-Ems *et al.*, 2012; Miklossy *et al.*, 2008), blebs (Kersten *et al.*, 1995), detaching granules or pearls (Aberer & Duray, 1991; Barbour & Hayes, 1986; Garon *et al.*, 1989), and agglomerations of spirochaetes into biofilm-like (BFL) colonies (Sapi *et al.*, 2012; Srivastava & de Silva, 2009).

Previously, the round bodies (RBs) of *B. burgdorferi* have been ambiguously named in various ways. These terms include CWD and L-forms, spheroplasts, protoplasts, propagules and even cysts (Domingue & Woody, 1997; Stricker & Johnson, 2011). Nonetheless, all of these labels describe the same spherical structures. This terminology is confusing and makes presumptions about the biochemical and morphological characteristics of *B. burgdorferi* RBs, such as a lack of cell wall (CWD, spheroplasts and protoplasts), or that these forms are encysted with a capsulated outer membrane (cysts). However, the cell envelope components and morphology of *B. burgdorferi* RBs have not been clearly studied before.

Although RBs of *B. burgdorferi* have been observed from limited *in vivo* clinical samples (Aberer *et al.*, 1996; Hulínská *et al.*, 1994; Mattman, 2001; Miklossy *et al.*, 2008), the role of pleomorphism in pathogenesis of Lyme disease and other diseases has been hugely debatable and recently criticized (Lantos *et al.*, 2014; Onwuamaegbu *et al.*, 2005; Schnell *et al.*, 2014). However, there is more and more plausible evidence that pleomorphism in general may help the bacteria to evade the immune system or decrease antibiotic susceptibility, as well as change its pathogenic mechanisms (Domingue & Woody, 1997; Justice *et al.*, 2008). This study provides a systematic in-depth compilation of *B. burgdorferi* pleomorphic variant characterization. The analysis of induction in different conditions, morphology, cell envelope architecture and metabolic activity as well as biochemical features of pleomorphic forms provides new insight into the morphological variants of *B. burgdorferi*. In order to fully understand the complex life cycle of *B. burgdorferi* and mechanisms of how pleomorphism is associated with diseases, it is crucial to understand what will induce different forms and what the basic features are that they convey.

METHODS

Bacterial strain and growth conditions. Infectious *B. burgdorferi* strain B31 was obtained from ATCC (ATCC 35210). Cultures were grown in Barbour–Stoenner–Kelly medium (BSK-II) without gelatin (Barbour, 1984), supplemented with 6 % rabbit serum at recommended temperature 37 °C (ATCC). The optimum growth temperature for *B. burgdorferi* B31 is reported to be 33 °C (Hubálek *et al.*, 1998); however, bacteria were cultured at physiologically relevant 37 °C. Low-passage number of bacteria, normally 1–2, was used in all experiments and utilized before cell density reached the late-exponential phase.

Imaging of live pleomorphic forms. From bacterial cultures in the mid-exponential phase, 4 µl was mounted on a microscope slide to view spirochaetes, blebs and BFL aggregates. Spirochaetes were transformed to RBs by exposure to distilled H_2O for 10 min. Samples were visualized using a Leica DM5500 fluorescence microscope with differential interference contrast microscopy (DIC) set-up and ×100 objective.

Induction of pleomorphic forms in different culturing environments. Induction of pleomorphic forms was studied using complete BSK-II medium without 6 % rabbit serum, BSK-II medium supplements of with 10 % human serum (HS) or RPMI 1640 medium without the supplements of serum and BSA. To prevent complement-mediated cell lysis, the HS was heat-inactivated (see technical specifications; Sigma). Normal BSK-II medium with 6 % rabbit serum was used as a control. A total of 80×10^6 cells were centrifuged at 5000 ***g*** for 10 min, resuspended in 4 ml appropriate medium and incubated at 37 °C for 4 days in order to reach the very-late-exponential phase of growth. Samples were prepared as triplicates. A moderately high initial density of bacteria was used to enable the counting with high magnification. After 2 and 4 days, 4 µl sample from each tube was prepared on the microscope slide and spirochaetes, blebs, RBs, BFL aggregates and cells with outer membrane damage were counted using a Leica DM5500 fluorescence microscope with phase-contrast (PH) set-up and ×100 objective.

Induction of pleomorphic forms of *B. burgdorferi* with distilled H_2O. Bacteria at mid-exponential phase were exposed to H_2O for 10 min, 2 h, 4 h, 1 day and 4 days. Samples and controls were prepared and pleomorphic forms were counted at each exposure time as described above. To determine the mean diameter of RBs and blebs, 2 h H_2O-induced RBs and spirochaetes with membrane blebs from control cultures in normal BSK-II medium were imaged with a Leica fluorescence microscope using PH and ×100 objective. The diameters of 100 RBs and blebs (approximately 33 per experiment) were measured from images using ImageJ software (NIH).

***B. burgdorferi* growth curve and BFL development.** Bacterial growth and development of BFL aggregates was examined by counting cell concentration and BFL colonies daily for 10 days from the stationary until the late-exponential phase. *B. burgdorferi* cultures with 2×10^4 cells ml^{-1} were prepared as triplicates. Cells and biofilms were counted each day using a C-Chip DHC-N01 Disposable Haemocytometer (System Neubauer Improved; Digital Bio) and Leica fluorescence microscope with DIC and ×20 objective. Aggregates of more than ten cells were counted as BFL.

Reversion of RB forms to spirochaetes. RBs were induced by H_2O as described above and 60×10^6 treated cells were centrifuged at 5000 ***g*** for 10 min, resuspended to a final concentration of 10×10^6 cells ml^{-1} and incubated at 37 °C. Reversion cultures were viewed regularly every 2–4 days with DIC or PH microscopy to observe the transformation of RBs to normal spirochaetes. When there were signs of reversion, corresponding to a small amount of single motile spirochaetes, cultures were viewed more often until the growth reached exponential phase and concentration of approximately 40×10^6 ml^{-1}. Cultures that showed no reversion after 21 days were kept in the incubator for up to 3 months and were regularly checked for growth. In parallel, to address if bystander spirochaetes from H_2O- induced RB cultures were able to replicate and interfere in the reversion experiments, 30×10^6 treated cells were filtered using a Filtropur S 0.45 µm filter to remove RBs. The filtered suspension with possible bystander spirochaetes was centrifuged at 5000 ***g*** for 10 min, resuspended to 3 ml in BSK-II medium and incubated at 37 °C. The growth and morphology were observed as described above.

ATP determination assay. ATP activity of parental spirochaetes, and 10 min and 2 h H_2O-induced RBs were analysed using an ATP

determination kit (Molecular Probes). To determine the increase in ATP metabolism during reversion, ATP activity of RBs reintroduced to normal medium with initial concentrations of 10×10^6 ml^{-1} for 1 h, 24 h and even up to early- and mid-exponential phase of growth was assayed. The growth in reversion cultures was defined to be in early- and mid-exponential phase when the spirochaete counts were approximately $10–20 \times 10^6$ and $40–50 \times 10^6$, respectively. Spirochaetes treated with 100 µg doxycycline ml^{-1} for 24 h and methanol-killed spirochaetes were used as negative controls. The luminescence of all samples was measured in white opaque 96-well plates with 1×10^7 cells per well using a Victor X Multilabel Plate Reader. The ATP concentrations were determined from a standard curve prepared with known ATP concentration standards provided by the kit.

Modelling of RB transformation. RB formation was animated and rendered with Blender 2.69 (http://www.blender.org). The expanding outer membrane was modelled with a transparent sphere and made to grow in every step. The spirochaete outer membrane and protoplasmic cylinder were modelled with 3D Bézier curves. The shape of the internal Bézier curve was set manually for each time point, after which it was duplicated, cut on the edge of the sphere and enlarged to form an external spirochaete tail. The protoplasmic cylinder was set to green and opaque while outer membrane was set as transparent.

Morphological analysis with transmission electron microscopy (TEM). The morphologies of spirochaetes, blebs and 2 h H_2O and 4 days HS RBs, as well as the localization of the flagella, were studied using TEM. In addition, the different steps of RB formation, especially the folding of the protoplasmic cylinder, were examined and modelled. To obtain a high quantity of blebs, 25 ml of 2 h H_2O RBs with a concentration of 40×10^6 ml^{-1} were introduced to 25 ml normal culture medium for 1 h to induce RB unfolding to blebs. In addition, spirochaetes treated with 100 µg doxycycline ml^{-1} for 24 h were used as a control to demonstrate the damage at the outer membrane. All samples were prepared as duplicates with 1×10^9 cells using a recently published protocol (Huttunen *et al.*, 2014), embedded in embedding resin medium, cut and finally visualized with a JEOL JEM1400 transmission electron microscope. The swollen RBs were counted in H_2O and HS RB images to compare the amounts in these treatments. Protoplasmic cylinders with a diameter of approximately 200 nm were considered normal size. Where the diameter was >200 nm, they were counted as swollen. The total numbers of measured H_2O and HS RBs were 171 and 212, respectively.

Immunolabelling of flagella. Approximately 20×10^6 spirochaetes, 2 h H_2O RBs, and 4 days HS RBs were centrifuged at 9300 ***g*** for 5 min, fixed with ice-cold methanol for 20 min at −20 °C and washed with PBS. Cells were immunolabelled using a previously described protocol (Thammasri *et al.*, 2013). Here, primary anti-flagellin p41 antibody (Acris) (1 : 50) and secondary goat anti-mouse IgG conjugated with Alexa 488 (1 : 200) were used. Cells were mounted with Prolong Gold antifade reagent with DAPI (Molecular Probes) and visualized with an Olympus microscope IX81 with a FluoView-1000 confocal set-up with ×60 objective using 488 nm laser and DIC.

Composition analysis of pleomorphic forms with fluorescence microscopy. Bacterial cultures (100 µl) were stained with 50 µg propidium iodide (PI) ml^{-1}, or 10 µg wheatgerm agglutinin (WGA) ml^{-1} conjugated with Alexa 488 for 1 h at room temperature, or 50 µg boron-dipyrromethene (BODIPY 493/503) ml^{-1} for 1 h at 37 °C (followed by a wash with medium), or 1 % (w/v) acid fuchsin for 1 h at room temperature to indicate DNA, polysaccharides, lipids and collagen, respectively. Live cells with PI were imaged immediately. To address the specificity of the stains in live cells, cells were fixed with ice-cold methanol for 20 min and labelled with similar dyes for 10 min, washed with PBS and mounted with Prolong Gold with DAPI. BFL aggregates from late phase bacterial cultures were purified with MACS 30 µm pre-separation filters (Miltenyi Biotec) and washed with BSK-II medium to remove individual spirochaetes. Samples were visualized using an Olympus confocal IX81 microscope, ×60 objective, 488 or 546 nm laser and DIC. The Supplementary Movie S2, available in the online Supplementary Material, was acquired using a Nikon A1R confocal microscope with resonant scanning, ×60 objective and 561 nm laser.

Microscopy data analysis. All microscopy data were processed and analysed using open source ImageJ software. The brightness and contrast settings of images were adjusted and applied to all parts of the image. The noise from green and red fluorescent images was suppressed using Gaussian blur filter with sigma (radius) 1–2. If needed, the uneven illumination was corrected in the DIC images using pseudocorrection.

RESULTS

Various *in vitro* culturing environments can induce pleomorphism of *B. burgdorferi*

In this study, the induction of different pleomorphic forms in various culturing environments including HS was extensively examined. In addition, cells with outer membrane damage were quantified; however, these were not defined as pleomorphic. Here, we compiled the descriptions of different morphological variants based on our findings at a physiologically relevant culturing temperature of 37 °C (Table 1). It is notable that the mean size of RBs (2.8 µm) was greater when compared with the blebs (1.3 µm) on spirochaetes (Table 1). When in physiologically relevant *in vitro* culturing environment, *B. burgdorferi* is most commonly seen as a spirochaete (Fig. 1a), but other forms such as membrane blebs (Fig. 1b) and BFL aggregates (Fig. 1d) are also present in low levels (Fig. 2). Fig. 1(c) displays the spirochaetes converted to the smaller RBs when exposed to H_2O for 10 min; however, these forms also exist in small numbers in normal culturing conditions (Fig. 2a).

In the standard culturing environment, BSK-II medium at 37 °C, the mean number of different pleomorphic forms remained the same during the whole culturing period from early-exponential phase until the late phase of growth up to day 4 (Fig. 2a). At 4 days, 92 % of the bacteria were parental spirochaetes, 4 % were blebs and 0.6 % were BFL aggregates. After 2 days RBs were not observed; however, after 4 days, 0.4 % of the bacteria were observed in this form. There is a basal level of damaged cells in cultures that increases with time. Here, the damaged cells in control cultures increased from 0.5 % to 3.4 % from day 2 to day 4. When bacteria were exposed to BSK-II medium without rabbit serum, there was little effect on bacteria when compared to controls (Fig. 2b). At day 2, bacteria had a stress reaction seen as an elevated number of blebs (24 %), but after 4 days the level was normalized back to 6 %. After 4 days there was exactly the same amount of spirochaetes (93 %) as in controls, and only 1.3 % of the cells were damaged. In addition, bacteria in BSK-II medium without rabbit serum replicated normally and maintained motility.

Table 1. Description of different pleomorphic forms of *B. burgdorferi*

Form	Description of morphology	Size
Spirochaete	Long, corkscrew-shaped	Mean length, 20 μm
Bleb	Spirochaete with membrane bleb	Diameter of bleb, 1.3 ± 0.43 μm*
RB	Spherical	Diameter, 2.8 ± 0.46 μm*
BFL	Colony of mostly spirochaetes; however, blebs and RBs are commonly present. Contains EPS	Consists of more than 10 spirochaetes/blebs/RBs

*Mean ± SD

To simulate the physiological conditions in humans, *B. burgdorferi* was grown in BSK-II medium without supplement of BSA or rabbit serum, but instead with 10 % HS. Interestingly, the amount of spirochaetes decreased from 93 % to 24 % in 4 days, while blebs and RBs as well as the quantity of damaged cells increased to 40 %, 22 % and 13 %, respectively (Fig. 2c). The level of cell damage remained the same throughout the experiment. In addition, bacteria were exposed to the mammalian cell culture medium RPMI 1640 without supplement of FBS or antibiotics. RPMI medium clearly induced RBs and blebs, but also caused severe cell damage (Fig. 2d). After 4 days, only 10 % of the cells were spirochaetes. The level of RBs increased to 17 % during the 4 day experiment. Furthermore, the amount of blebs decreased from day 2 (34 %) to day 4 (26 %), whereas the amount of damaged cells increased from 28 % to as much as 47 %.

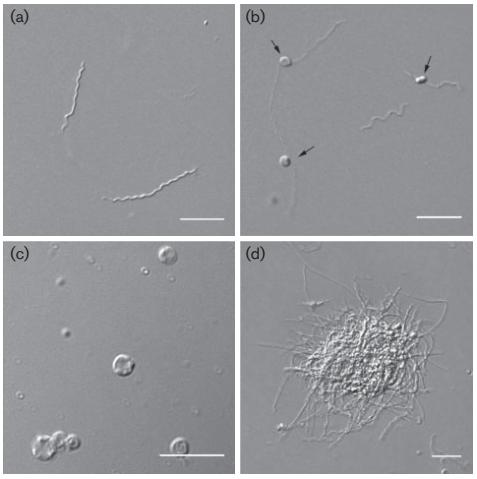

Fig. 1. Typical pleomorphic forms of *B. burgdorferi* B31. Live cell DIC images of *B. burgdorferi* cultures representing (a) spirochaetes, (b) blebs on spirochaetes (black arrows), (c) 10 min H_2O-induced RBs and (d) BFL aggregates. Bars, 10 μm.

In order to study pleomorphic forms *in vitro*, it is important to develop methods to induce them easily in high quantities. Here, we followed a previously published method (Brorson & Brorson, 1998) with modifications to induce RBs with distilled H_2O. The incubation times were shorter (10 min, 2 h, 4 h and 1 day) compared to the other culturing experiments, because RB formation in H_2O was very rapid. The longer 4 day time point was included to examine the long-term effects in H_2O. After 10 min 85 % of the cells were perceived as RBs (Fig. 2e). Only 0.1 % of the cells were seen as parental spirochaetes and 4 % as blebs. As expected, H_2O caused cell damage, observed in 10 % of the cells throughout the experiment. From 2 h to 4 days of incubation, normal spirochaetes did not exist in the cultures. All the spirochaetes observed had damaged outer cell membranes, and blebs decreased to 1 % or less.

Suspended BFL aggregates were consistently present in all culture conditions, although at low levels of 2 % or less (Fig. 2a–c, e), except at day 4 in RPMI medium when aggregates were not observed (Fig. 2d). BFL colonies were detected early, even before cells reached the exponential phase of growth (Fig. 2f). Even at day 4 from the initial growth, when cell density was 3.7×10^6 ml^{-1}, the first aggregates were measured as having a concentration of 170 aggregates ml^{-1} (Fig. 2f). Along with the proliferation of the cells, the amount of biofilm also increased to 57 000 ml^{-1} in late-exponential phase at 9 days.

RBs have the ability to become viable spirochaetes

To test viability, and to see if RBs were able to revert to their parent vegetative spirochaetes, RBs induced with H_2O were transferred to normal culturing conditions. The mean reversion time was determined when the newly formed spirochaetes were in mid-exponential phase of growth with a cell density of 40×10^6 ml^{-1}. H_2O-induced 10 min and 2 h RBs reverted to motile spirochaetes each time, and reached a density of 40×10^6 ml^{-1} at 6 and 8 days, respectively (Fig. 3a). The 4 h RBs reverted in half of the cases, and the mean reversion time was 11 days. After 1 day or 4 days exposure to H_2O, RBs did not revert even after 3 months of culturing. To confirm that bystander spirochaetes are not replicating and interfering with the reversion assay, the growth of filtered spirochaetes was

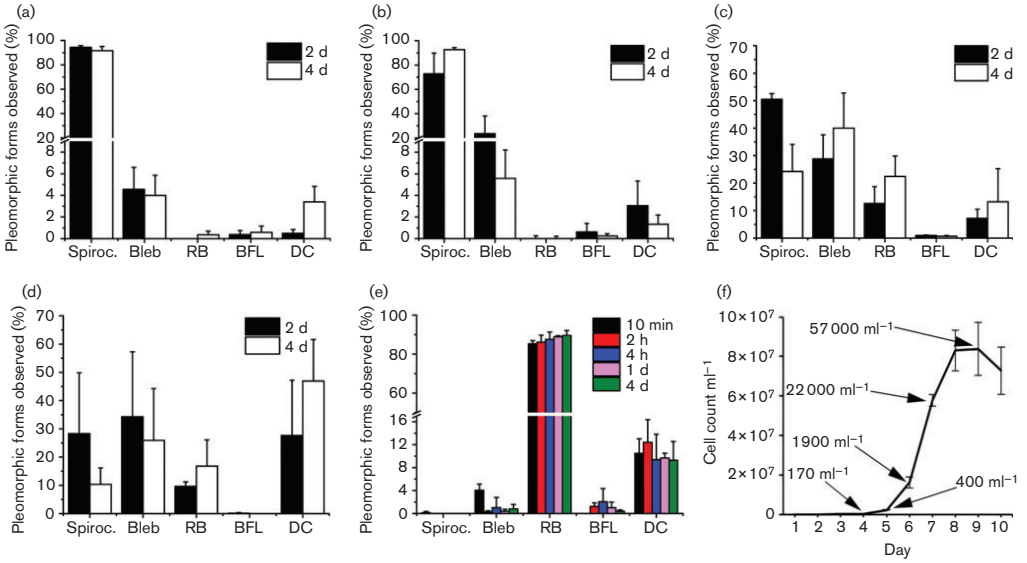

Fig. 2. Unfavourable culturing conditions induced pleomorphic forms. The percentages of observed spirochaetes, blebs, RBs, BFL aggregates and cells with damaged outer membrane (DC) in (a) normal BSK-II, (b) serum-free, (c) HS, (d) mammalian culture medium and (e) distilled H_2O culture conditions. Cells were viewed with PH microscopy using a ×100 objective and different forms were counted from each sample at 2 days and 4 days. The H_2O RBs were counted at time points 10 min, 2 h, 4 h, 1 day and 4 days. Collective observations are provided from three independent experiments. In total, approximately 800 cells per treatment were counted. (f) Growth curve of 80 000 cells in a total volume of 4 ml was recorded. Arrows depict development of BFL colonies at days 4, 5, 6, 7 and 9 with colony count ml^{-1}. Error bars illustrate SD from three experiments.

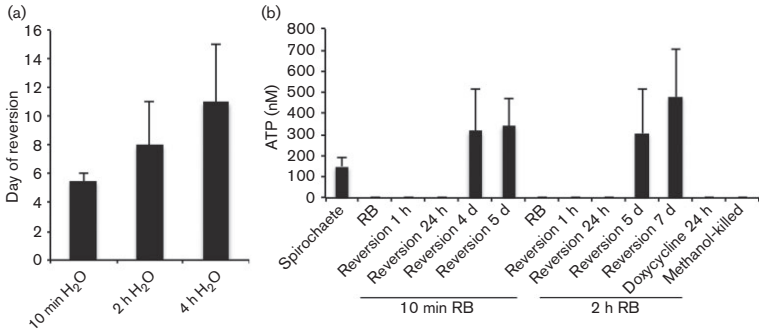

Fig. 3. RBs do not have ATP activity but have the ability to revert to viable spirochaetes. (a) Mean reversion times of 10 min, 2 h and 4 h H_2O RBs. RBs from each time point were reintroduced to a normal BSK-II medium and incubated at 37 °C until the spirochaete density reached 40×10^6 ml^{-1}. Error bars indicate SD from three different experiments. (b) ATP concentrations of spirochaetes, 10 min and 2 h H_2O RBs, RBs reverted in BSK-II medium for 1 h, 24 h, as well as until early- and mid-exponential phase of growth ($10–20\times10^6$ ml^{-1} and 50×10^6 ml^{-1}, respectively). RBs exposed to H_2O for 10 min reached the early growth phase in approximately 5 days whereas 2 h RBs achieved it at day 6. Mid-exponential phase growth was reached in approximately 6 days with 10 min RBs and in 8 days with 2 h RBs. Cells treated with 100 μg doxycycline ml^{-1} for 24 h and methanol-fixed cells were used as negative controls. Error bars indicate SD from three experiments.

monitored in parallel. Eventually, bystander spirochaete cultures did not show growth (data not shown).

RBs display lower metabolic activity

ATP determination experiments indicated that 10 min and 2 h RBs do not have ATP production (Fig. 3b), while control spirochaetes in mid- or late-exponential phase of growth had a mean ATP concentration of 149 nM. Furthermore, when RBs were placed in normal culture medium to revert to spirochaete form, ATP activity was not detected after 1 h or 24 h. However, RBs were able to revert and become metabolically active spirochaetes. At approximately 5 days of culturing, 10 min RBs reached the early-exponential phase ($10–20 \times 10^6$ cells ml^{-1}) with an ATP concentration of 317 nM (Fig. 3b). When cells were in mid-exponential phase ($40–50 \times 10^6$ cells ml^{-1}) at approximately day 6, ATP production was almost the same, 343 nM. The 2 h RBs achieved the early-exponential phase at approximately day 6 and mid-exponential phase at day 8, demonstrating ATP production of 306 and 480 nM, respectively (Fig. 3b).

Model for RB formation

The development of *B. burgdorferi* RBs proceeded in steps that are presented on TEM illustrations (Fig. 4a). *B. burgdorferi* has an elastic outer envelope that expands and allows folding of the protoplasmic cylinder within the cell. This leads to the transformation of spirochaetal corkscrew morphology to a spherical shape. The completed RB with folded protoplasmic cylinder is presented in three different cross sections in Fig. 4(b). In addition, an animation (Movie S1) that is based on observations from TEM and DIC/PH imaging is provided to demonstrate this folding.

Pleomorphic forms have a cell wall

To further investigate the morphology and the cell wall characteristics of different *B. burgdorferi* forms, spirochaetes, RBs and blebs were analysed using TEM. Doxycycline-treated cells were used as a control for outer cell envelope damage. Fig. 5 presents morphologies of spirochaete, bleb, H_2O RB, HS RB and doxycycline-treated spirochaete, respectively (top panels). Insets depict magnified areas (lower panels). Arrows highlight the outer and inner membranes as well as the protoplasmic cylinder. Blebs were revealed to be an intermediate stage between the spirochaete and the RB, with an expanded outer envelope usually on the other end or on the lateral part of the spirochaete with a partly folded protoplasmic cylinder inside (Figs 4a and 5a). TEM images clearly indicated that both H_2O and HS RBs have intact double outer and inner membranes around the protoplasmic cylinder, similar to the spirochaete (Fig. 5a). Doxycycline-treated cells displayed more damage seen as small holes on the outer membrane when compared to the other forms (Fig. 5a). Interestingly, TEM also unveiled that 28 % of the HS RBs displayed swollen protoplasmic cylinders, while only 4 % of the H_2O RBs were swollen (Fig. 5b).

Flagella are present in RBs

The localization of flagella in RBs was examined using TEM and fluorescence microscopy. In spirochaetes, the flagella are localized in the periplasmic space between the outer and inner membrane, as seen in Fig. 6. Fluorescence

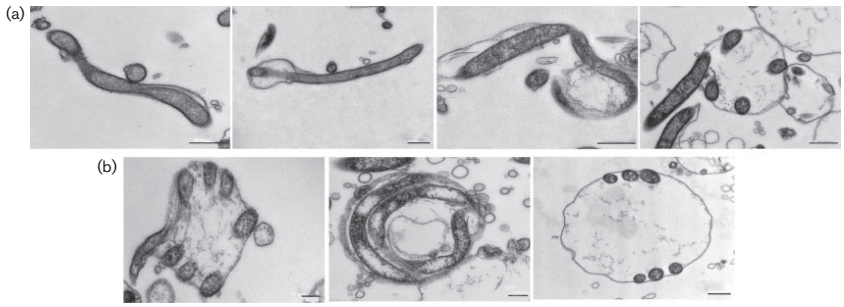

Fig. 4. RB formation evolved through the expansion of the outer membrane and folding of the protoplasmic cylinder. (a) Stepwise demonstration of RB development using TEM images of H_2O and HS RBs. Presented from left to right: parental spirochaete; spirochaete with initial membrane expansion; bleb where folding of the protoplasmic cylinder inside the outer membrane is initiated; bleb transitioning to the RB formation with folded protoplasmic cylinder under the expanded outer membrane. Bars, 500 nm. (b) Cross-sections of completed RBs and the organization of folded protoplasmic cylinder are visualized with TEM micrographs. RB is displayed from the side, from the front and from the top, respectively, from left to right. Bars, 200 nm, 200 nm and 500 nm, respectively.

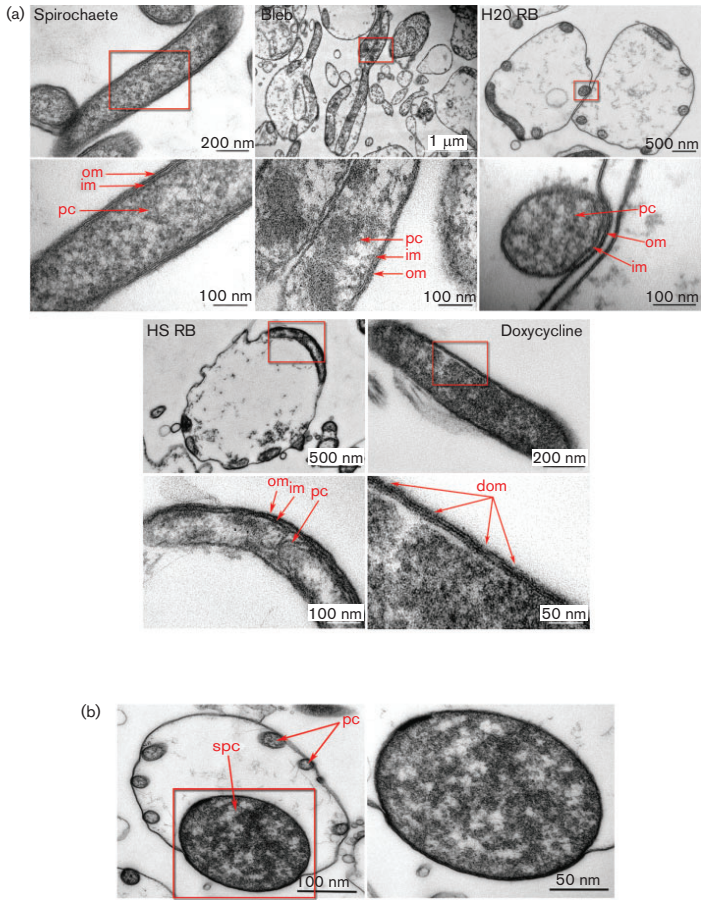

Fig. 5. Pleomorphic forms of *B. burgdorferi* are not CWD. (a) TEM micrographs of Epon-embedded spirochaetes, blebs, 2 h H_2O RBs, 4 days HS RBs and cells with outer membrane damage induced by treatment with 100 µg doxycycline ml^{-1} for 24 h. Blebs were prepared by induction of 2 h H_2O RBs and were then reintroduced to normal culture medium and incubated for 1 h at 37 °C. The upper panels represent the overall view of the whole cell, and expanded insets in the lower panels indicate the zoomed morphology of the outer envelope. The outer membrane (om), inner membrane (im) and protoplasmic cylinder (pc) are easily discernible in zoomed images. The lower panel of the doxycycline-treated spirochaete illustrates the damaged outer membrane (dom). (b) TEM images of swollen 4 days HS RB with swollen protoplasmic cylinder. Left panel illustrates the RB with normal size protoplasmic cylinders (pc) and one swollen protoplasmic cylinder (spc). Right panel displays the zoomed view of the swollen protoplasmic cylinder.

images of cells immunolabelled with p41 antibody indicated that the flagella extend through the whole spirochaete. In RBs, the expanded periplasmic space is presented quite differently compared to the spirochaete (Figs 4a, b and 5a); nonetheless, the flagella are visualized inside the RBs (Fig. 6).

B. burgdorferi pleomorphic forms have atypical cell wall characteristics

Live pleomorphic variants of *B. burgdorferi* were stained with several dyes and imaged with laser scanning confocal microscopy to address different cell envelope components (Fig. 7). As a control, the same dyes were used on

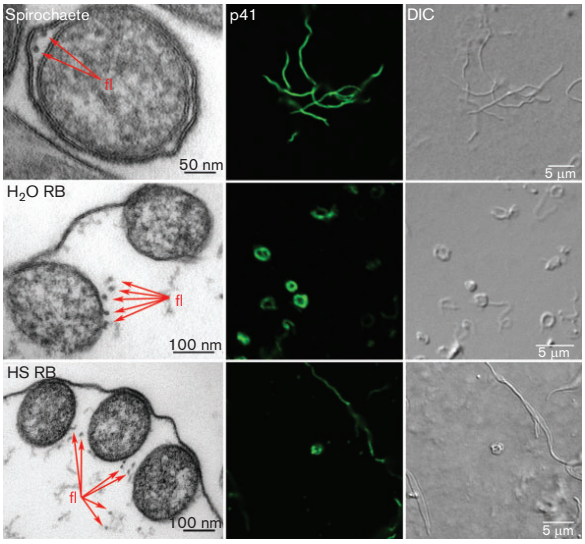

Fig. 6. Flagella are present in RBs. TEM and confocal micrographs of flagella localization in spirochaetes, 2 h H_2O RBs and 4 days HS RBs. TEM images (left panels) demonstrate the cross-section of the cell, where flagella (fl) are indicated by arrows. Middle panels display confocal images of cells immunolabelled with p41 flagellin protein antibody and Alexa 488 (green). Right panels illustrate the DIC image.

doxycycline-treated (Fig. 7) and methanol-fixed cells (Fig. S1). This demonstrates the difference in the capability of the dyes to penetrate intact and damaged cell membranes. PI is a DNA stain that is thought to be unable to permeate intact cell membranes. However, here we demonstrated that PI stained live motile spirochaetes (Fig. 7, Movie S2), demonstrating the unique, atypical Gram-negative outer envelope of *B. burgdorferi*. In addition PI penetrated all different live forms (blebs, RBs, BFL aggregates) and doxycycline-treated cells. WGA 555 was used to label *N*-acetylglucosamine polysaccharides (GluNAc), the structural component of the bacterial peptidoglycan cell wall. Intriguingly, WGA stained the cell wall of the RBs very specifically. Spirochaetes, blebs and BFL aggregates did not have labelled GluNAc while doxycycline-treated and methanol-fixed cells displayed staining (Figs 7 and S1), presumably because of the leakage through the damaged outer membrane. As expected, the lipid-binding BODIPY stained all the *B. burgdorferi* variants. Because acid fuchsin is suitable only on fixed cells, live cell imaging could not be performed with this particular dye. Nevertheless, we used fixed cells to indicate staining of collagen on the bacteria. As a result, only BFL colonies were stained, indicating that the suspension biofilms observed in normal cultures have proteins, especially collagen, on their extracellular polymeric substance (EPS) matrix (Fig. 7). This provides more evidence that these cultured BFL aggregates of *B. burgdorferi* share characteristics with surface-bound biofilms (Flemming & Wingender, 2010). Furthermore, fixed cells with permeabilized cell envelopes clearly had a more robust internal staining pattern, indicating that all pleomorphic variants have an intact cell envelope.

DISCUSSION

In addition to typical spirochaetes, *B. burgdorferi* has pleomorphic forms present in normal culturing conditions although in low quantities (Figs 1 and 2a), raising the question of whether these forms are part of the *B. burgdorferi* normal life cycle and how that may affect pathogenesis of the disease. Blebs, similar to those seen within this study (Figs 1b and 2a), have been detected earlier during standard *in vivo* and *in vitro* culturing at 34 °C (Garon *et al.*, 1989; Miklossy *et al.*, 2008; Radolf *et al.*, 1994). It is known that different disturbances, such as antibiotics, ageing and complement factors (Barbour & Hayes, 1986), can cause bleb development in *B. burgdorferi*, and this supports our findings that the formation of blebs increases under environmental stress. Blebs contain tightly packed DNA and it is suggested that they may be involved in transfer of genetic material and have certain protectoral functions (Garon *et al.*, 1989). Their role in the initiation of autoimmune disease processes is also proposed (Whitmire & Garon, 1993). Nevertheless, the function of these blebs is still relatively unknown.

Interestingly, transformation of spirochaetes to RBs increased remarkably when growth conditions changed to medium with HS, nutrient-poor mammalian RPMI culture medium or H_2O (Fig. 2). The effect of HS on the morphology of *B. burgdorferi* has not been examined before, and growth in this environmental circumstance remarkably increased the quantity of blebs and RBs without causing extensive cellular damage (Fig. 2c). Growth in hypotonic conditions with distilled H_2O at 37 °C (Figs 1c and 2e) induced similar morphologies, as previously described at

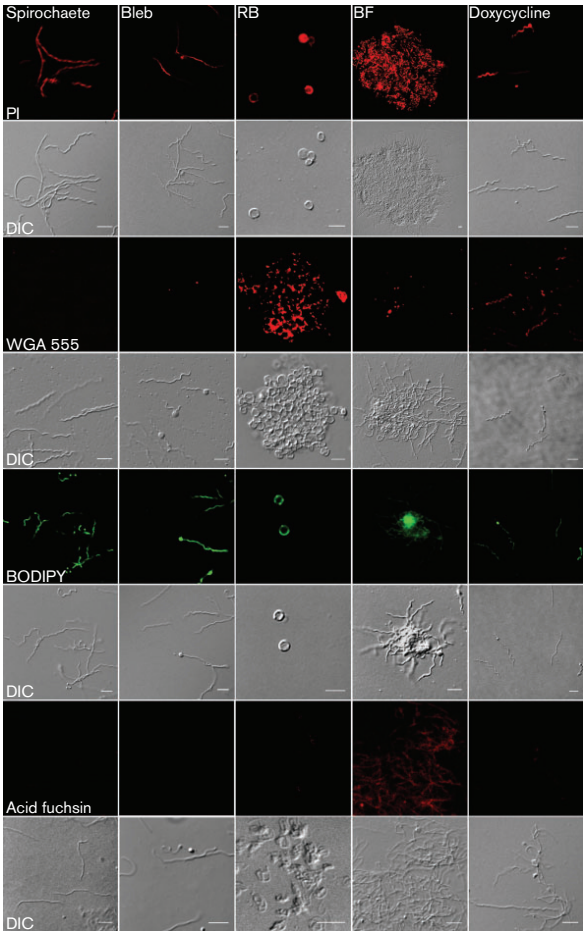

Fig. 7. Composition analysis of *B. burgdorferi* indicates the distinction between the different pleomorphic forms and presents atypical cell wall characteristics. Live spirochaetes, blebs observed in normal culture conditions, 2 h H_2O RBs and BFL aggregates in suspension as well as 24 h doxycycline-treated damaged cells were stained with PI, WGA conjugated with Alexa 555 (WGA 555) and BODIPY to indicate DNA, polysaccharides and lipids. Acid fuchsin was used for methanol-fixed cells to stain collagen. Upper panel visualizes the cells imaged with confocal laser scanning microscopy. Lower panel represents the morphology of the cells with DIC. Bars, 5 μm.

30–35 °C (Brorson & Brorson, 1998; Murgia & Cinco, 2004). The treatment with HS and distilled H_2O induced morphologically similar RBs, indicating that the transformation does not occur only because of the osmotic stress. Rabbit serum normally supplementing the *B. burgdorferi* culture medium has the same osmolarity as the HS. Most probably, the complement system or antibodies in the serum are responsible for the changes in the morphology, which is clinically interesting and worthy of further studies. An antibody–complement system in HS has been found to be lethal for some L-forms (McGee *et al.*, 1972). Here, the bacteriolytic effect of the serum components was also seen in one-third of the RBs (Fig. 5b) as protoplasmic cylinder swelling.

RPMI medium induced RBs and blebs; however, it also triggered severe cell damage (Fig. 2d). This is distinctly different from the 95 % RBs that were reported after 2 days culture in similar media (Alban *et al.*, 2000). With respect to culturing in rabbit serum-free BSK-II medium, RB formation did not occur in growth at 37 °C up to 4 days (Fig. 2b). Others have documented RBs in cultures at 33–34 °C after 7–10 days (Al-Robaiy *et al.*, 2010) or six weeks (Brorson & Brorson, 1997). The dissimilarity in these observations may be due to the different growth temperatures, where 37 °C actually provides culturing conditions that better suit the maintenance of the bacterial growth. Long-term cultures of up to six weeks in rabbit serum-free medium may have indeed induced RBs, although this was not mentioned by other authors. In addition, these studies used relatively low magnification (approximately ×200) for counting the different morphologies, but here we used ×1000 magnification to enhance the actual

distinction between different pleomorphic forms and damaged cells.

In vitro growth of *B. burgdorferi* biofilm colonies both on surfaces and in suspension at 33 °C or at 35 °C has been displayed in several studies (Barbour, 1984; Sapi *et al.*, 2012; Srivastava & de Silva, 2009). High cell density promotes BFL formation of *B. burgdorferi in vitro* (Srivastava & de Silva, 2009). Here, there is evidence that BFL colonies are established even at early-exponential phase of growth (Fig. 2f), suggesting that high density is not the only factor enhancing biofilm formation in suspension. Suspended *B. burgdorferi* biofilms share common characteristics with surface-attached biofilms such as alginate polysaccharide and extracellular DNA on the matrix of EPS (Sapi *et al.*, 2012). We demonstrated here that collagen is present on EPS of *B. burgdorferi* BFL colonies in suspension (Fig. 7), supporting the previous findings that suspended biofilms are biofilms, not just cell aggregates. Furthermore, DIC images (Figs. 1d and 7) provide visual evidence that these biofilms have cellular architecture similar to surface biofilms (Serra *et al.*, 2013). There is a lack of literature that correlates *B. burgdorferi* biofilms with clinical consequences; however, it is speculated (Barbour, 1984) that bacterial aggregation may enhance the binding of bacteria to host tissue with the avoidance of phagocytosis. The presence of collagen-like protein in EPS may indeed encourage *B. burgdorferi* suspension biofilm binding to host tissue.

It has been suggested that transformation of *B. burgdorferi* from spirochaetes to RBs may enhance survival in inconvenient environmental conditions (Murgia & Cinco, 2004) and evasion from the immune system (Al-Robaiy *et al.*, 2010; Brorson & Brorson, 1998; Lawrence *et al.*, 1995). Remarkably, we found that RBs have lower metabolic activity (Fig. 3b); however, they have the ability to revert to spirochaete form and regain their ATP activity. Low metabolic rate may indeed enhance the survival of bacteria during antibiotic treatment. It remains unknown whether the RBs can utilize something other than the ATP metabolic pathway. Within this study, when H_2O-induced RBs were grown in normal culturing medium at 37 °C, they were able to revert to viable spirochaetes only if the exposure to H_2O was not more than 4 h. Previous studies (Al-Robaiy *et al.*, 2010; Brorson & Brorson, 1998; Murgia & Cinco, 2004) have presented the reversion of 1 day, 4 days, 7 days or 5 weeks in 30–34 °C H_2O-exposed RBs, but we did not see reversion of 1 day and 4 days H_2O-exposed RBs. Again, the difference in these observations could be due to the different culturing temperatures. However, it seemed that *B. burgdorferi* RBs could tolerate short exposure to harsh environment but not long-term exposures.

We provide a step-by-step model, which is in harmony with the findings of others (Al-Robaiy *et al.*, 2010; Murgia & Cinco, 2004), that the outer membrane of *B. burgdorferi* is flexible, allowing it to expand during RB transformation when the protoplasmic cylinder is folding within the envelope (Figs 4 and 5a, Movie S1). Furthermore, the flagella, located in the periplasmic space in spirochaetes (Barbour & Hayes, 1986; Zhao *et al.*, 2013), were present in RBs, indicating that these forms can maintain the motility and skeletal components and then recruit them again during reversion to spirochaetes (Fig. 6). It is suggested that the export system is anchored between the outer and inner membrane (Radolf *et al.*, 2012). However, our model indicates that the protoplasmic cylinder is flexible and not tightly anchored to the outer and inner membrane, allowing it to fold within the confinements of the RB outer envelope (Movie S1). *B. burgdorferi* is known to utilize the RND transporter system, an efflux pump for toxic compounds, situated on the outer and inner membranes in Gram-negative bacteria. They are thought to be associated with antibiotic resistance in *B. burgdorferi* (Bunikis *et al.*, 2008; Li & Nikaido, 2004). The adaptor protein in the RND transporter efflux pump in *B. burgdorferi* lacks a hairpin domain, which results in a smaller interaction with the outer and inner membrane components, leading to a less stable assembly of the pump (Bunikis *et al.*, 2008). This supports our observations about the flexibility of the *B. burgdorferi* outer membrane. The loose assembly of the efflux pump components could allow pump function even during RB formation.

B. burgdorferi is known to have an atypical Gram-negative cell membrane (Barbour & Hayes, 1986). However, this phenomenon of the unique cell wall properties and the consequences of it have not been widely discussed. Here we demonstrated the unique nature of the *B. burgdorferi* cell envelope by showing that exclusion stains, such as PI tested here, are able to enter living cells (Movie S2). PI is commonly used to identify dead cells or cells with compromised membranes, and caution is needed when interpreting PI staining results, especially to indicate cell death of *B. burgdorferi*. Intriguingly, RBs were seen to have a very specific binding of WGA to GluNac, indicating the differences in polysaccharide composition from other forms. This is in harmony with a previous study (Hulínská *et al.*, 1994), where RBs, but not spirochaetes, were found to be positive for WGA in *B. burgdorferi*-infected Langerhans cells. The advantage of having adaptable *in vivo* conformations could allow the bacteria to evade the immune system, leading to a persistent stage while still having efflux capabilities seen in the parent form. The peptidoglycan layer of *B. burgdorferi* is thought to be located close to the inner membrane (Radolf *et al.*, 2012); however, others (Kudryashev *et al.*, 2009) have presented that the layer is actually located in the periplasmic space near the outer membrane. Elasticity of the outer membrane and reorganization of the membrane components during RB formation could explain why GluNAc is being exposed.

Here we confirmed for the first time that RBs actually have an intact cell envelope with a peptidoglycan layer (Figs 5 and 7), indicating that they do not fulfil clearly the definitions of spheroplasts, CWD or encysted forms although there are some modifications in the cell envelope

and cell wall architecture. Furthermore, the intact cell envelope of RBs (Fig. 5), similar to the spirochaete, provides evidence for the previous suggestion (Alban *et al.*, 2000) that RBs are not degrading cells. To avoid confusing terminology, we suggest that *B. burgdorferi* spherical shapes are termed 'round bodies' to describe these forms better.

Taken together, these results implied that pleomorphic forms of *B. burgdorferi* can be easily induced in different culturing environments with the presence of serum components, nutrient starvation or osmotic stress; however, low levels of the observed variants are present in normal culturing conditions at 37 °C. Our findings reassert the unique features of *B. burgdorferi* spirochaetes and their morphological variants: RBs have cell wll and flagella within the intact outer membranes. Furthermore, RBs and BFL colonies in suspension displayed specific staining properties when compared to other forms. Reorganization or modification of the cell envelope components that leads to exposure of the peptidoglycan layer in RBs could be exploited in diagnostics and recognition of RBs in tissue samples.

ACKNOWLEDGEMENTS

We thank Lassi Paavolainen for RB modelling, and Laura Pitkänen for technical assistance. This work was supported by the Schwartz Foundation and the Jenny and Antti Wihuri Foundation.

REFERENCES

Aberer, E. D. P. H. & Duray, P. H. (1991). Morphology of *Borrelia burgdorferi*: structural patterns of cultured borreliae in relation to staining methods. *J Clin Microbiol* **29**, 764–772.

Aberer, E., Kersten, A., Klade, H., Poitschek, C. & Jurecka, W. (1996). Heterogeneity of *Borrelia burgdorferi* in the skin. *Am J Dermatopathol* **18**, 571–579.

Al-Robaiy, S., Dihazi, H., Kacza, J., Seeger, J., Schiller, J., Huster, D., Knauer, J. & Straubinger, R. K. (2010). Metamorphosis of *Borrelia burgdorferi* organisms RNA, lipid and protein composition in context with the spirochetes' shape. *J Basic Microbiol* **50** (Suppl. 1), S5–S17.

Alban, P. S., Johnson, P. W. & Nelson, D. R. (2000). Serum-starvation-induced changes in protein synthesis and morphology of *Borrelia burgdorferi*. *Microbiology* **146**, 119–127.

Barbour, A. G. (1984). Isolation and cultivation of Lyme disease spirochetes. *Yale J Biol Med* **57**, 521–525.

Barbour, A. G. & Hayes, S. F. (1986). Biology of *Borrelia* species. *Microbiol Rev* **50**, 381–400.

Ben-Menachem, G., Kubler-Kielb, J., Coxon, B., Yergey, A. & Schneerson, R. (2003). A newly discovered cholesteryl galactoside from *Borrelia burgdorferi*. *Proc Natl Acad Sci U S A* **100**, 7913–7918.

Berndtson, K. (2013). Review of evidence or immune evasion and persistent infection in Lyme disease. *Int J Gen Med* **6**, 291–306.

Briers, Y., Staubli, T., Schmid, M. C., Wagner, M., Schuppler, M. & Loessner, M. J. (2012). Intracellular vesicles as reproduction elements in cell wall-deficient L-form bacteria. *PLoS ONE* **7**, e38514.

Brorson, O. & Brorson, S. H. (1997). Transformation of cystic forms of *Borrelia burgdorferi* to normal, mobile spirochetes. *Infection* **25**, 240–246.

Brorson, O. & Brorson, S. H. (1998). A rapid method for generating cystic forms of *Borrelia burgdorferi*, and their reversal to mobile spirochetes. *APMIS* **106**, 1131–1141.

Bunikis, I., Denker, K., Ostberg, Y., Andersen, C., Benz, R. & Bergström, S. (2008). An RND-type efflux system in *Borrelia burgdorferi* is involved in virulence and resistance to antimicrobial compounds. *PLoS Pathog* **4**, e1000009.

Domingue, G. J., Sr & Woody, H. B. (1997). Bacterial persistence and expression of disease. *Clin Microbiol Rev* **10**, 320–344.

Dunham-Ems, S. M., Caimano, M. J., Eggers, C. H. & Radolf, J. D. (2012). *Borrelia burgdorferi* requires the alternative sigma factor RpoS for dissemination within the vector during tick-to-mammal transmission. *PLoS Pathog* **8**, e1002532.

Flemming, H. C. & Wingender, J. (2010). The biofilm matrix. *Nat Rev Microbiol* **8**, 623–633.

Garon, C. F., Dorward, D. W. & Corwin, M. D. (1989). Structural features of *Borrelia burgdorferi* the Lyme disease spirochete: silver staining for nucleic acids. *Scanning Microsc Suppl* **3**, 109–115.

Glover, W. A., Yang, Y. & Zhang, Y. (2009). Insights into the molecular basis of L-form formation and survival in *Escherichia coli*. *PLoS ONE* **4**, e7316.

Harman, M., Vig, D. K., Radolf, J. D. & Wolgemuth, C. W. (2013). Viscous dynamics of Lyme disease and syphilis spirochetes reveal flagellar torque and drag. *Biophys J* **105**, 2273–2280.

Hubálek, Z., Halouzka, J. & Heroldová, M. (1998). Growth temperature ranges of *Borrelia burgdorferi sensu lato* strains. *J Med Microbiol* **47**, 929–932.

Hulínská, D., Barták, P., Hercogová, J., Hancil, J., Basta, J. & Schramlová, J. (1994). Electron microscopy of Langerhans cells and *Borrelia burgdorferi* in Lyme disease patients. *Zentralbl Bakteriol* **280**, 348–359.

Huttunen, M., Waris, M., Kajander, R., Hyypiä, T. & Marjomäki, V. (2014). Coxsackievirus A9 infects cells via nonacidic multivesicular bodies. *J Virol* **88**, 5138–5151.

Justice, S. S., Hung, C., Theriot, J. A., Fletcher, D. A., Anderson, G. G., Footer, M. J. & Hultgren, S. J. (2004). Differentiation and developmental pathways of uropathogenic *Escherichia coli* in urinary tract pathogenesis. *Proc Natl Acad Sci U S A* **101**, 1333–1338.

Justice, S. S., Hunstad, D. A., Cegelski, L. & Hultgren, S. J. (2008). Morphological plasticity as a bacterial survival strategy. *Nat Rev Microbiol* **6**, 162–168.

Kersten, A., Poitschek, C., Rauch, S. & Aberer, E. (1995). Effects of penicillin, ceftriaxone, and doxycycline on morphology of *Borrelia burgdorferi*. *Antimicrob Agents Chemother* **39**, 1127–1133.

Kudryashev, M., Cyrklaff, M., Baumeister, W., Simon, M. M., Wallich, R. & Frischknecht, F. (2009). Comparative cryo-electron tomography of pathogenic Lyme disease spirochetes. *Mol Microbiol* **71**, 1415–1434.

Lantos, P. M., Auwaerter, P. G. & Wormser, G. P. (2014). A systematic review of *Borrelia burgdorferi* morphologic variants does not support a role in chronic Lyme disease. *Clin Infect Dis* **58**, 663–671.

Lawrence, C., Lipton, R. B., Lowy, F. D. & Coyle, P. K. (1995). Seronegative chronic relapsing neuroborreliosis. *Eur Neurol* **35**, 113–117.

Li, X. Z. & Nikaido, H. (2004). Efflux-mediated drug resistance in bacteria. *Drugs* **64**, 159–204.

Mattman, L. H. (2001). *Cell Wall Deficient Forms – Stealth Pathogens*, 3rd edn. Boca Raton, FL: CRC Press.

McGee, Z. A., Ratner, H. B., Bryant, R. E., Rosenthal, A. S. & Koenig, M. G. (1972). An antibody-complement system in human serum lethal to L-phase variants of bacteria. *J Infect Dis* **125**, 231–242.

Mead, P. S. (2011). Global epidemiology of *Borrelia burgdorferi* infections. In *Lyme Disease: an Evidence-based Approach*, pp. 110–114. Edited by J. J. Halperin. Wallingford: CAB International.

Miklossy, J., Kasas, S., Zurn, A. D., McCall, S., Yu, S. & McGeer, P. L. (2008). Persisting atypical and cystic forms of *Borrelia burgdorferi* and local inflammation in Lyme neuroborreliosis. *J Neuroinflammation* **5**, 40.

Motaleb, M. A., Corum, L., Bono, J. L., Elias, A. F., Rosa, P., Samuels, D. S. & Charon, N. W. (2000). *Borrelia burgdorferi* periplasmic flagella have both skeletal and motility functions. *Proc Natl Acad Sci U S A* **97**, 10899–10904.

Murgia, R. & Cinco, M. (2004). Induction of cystic forms by different stress conditions in *Borrelia burgdorferi*. *APMIS* **112**, 57–62.

Onwuamaegbu, M. E., Belcher, R. A. & Soare, C. (2005). Cell wall-deficient bacteria as a cause of infections: a review of the clinical significance. *J Int Med Res* **33**, 1–20.

Radolf, J. D., Bourell, K. W., Akins, D. R., Brusca, J. S. & Norgard, M. V. (1994). Analysis of *Borrelia burgdorferi* membrane architecture by freeze-fracture electron microscopy. *J Bacteriol* **176**, 21–31.

Radolf, J. D., Caimano, M. J., Stevenson, B. & Hu, L. T. (2012). Of ticks, mice and men: understanding the dual-host lifestyle of Lyme disease spirochaetes. *Nat Rev Microbiol* **10**, 87–99.

Ranjit, D. K. & Young, K. D. (2013). The Rcs stress response and accessory envelope proteins are required for de novo generation of cell shape in *Escherichia coli*. *J Bacteriol* **195**, 2452–2462.

Sapi, E., Bastian, S. L., Mpoy, C. M., Scott, S., Rattelle, A., Pabbati, N., Poruri, A., Burugu, D., Theophilus, P. A. S. & other authors (2012). Characterization of biofilm formation by *Borrelia burgdorferi in vitro*. *PLoS ONE* **7**, e48277.

Schnell, B., Staubli, T., Harris, N. L., Rogler, G., Kopf, M., Loessner, M. J. & Schuppler, M. (2014). Cell-wall deficient *L. monocytogenes* L-forms feature abrogated pathogenicity. *Front Cell Infect Microbiol* **4**, 60.

Serra, D. O., Richter, A. M., Klauck, G., Mika, F. & Hengge, R. (2013). Microanatomy at cellular resolution and spatial order of physiological differentiation in a bacterial biofilm. *MBio* **4**, e00103–e00113.

Srivastava, S. Y. & de Silva, A. M. (2009). Characterization of *Borrelia burgdorferi* aggregates. *Vector-Borne Zoonotic Dis* **9**, 323–329.

Stricker, R. B. & Johnson, L. (2011). Lyme disease: the next decade. *Infect Drug Resist* **4**, 1–9.

Takayama, K., Rothenberg, R. J. & Barbour, A. G. (1987). Absence of lipopolysaccharide in the Lyme disease spirochete, *Borrelia burgdorferi*. *Infect Immun* **55**, 2311–2313.

Thammasri, K., Rauhamäki, S., Wang, L., Filippou, A., Kivovich, V., Marjomäki, V., Naides, S. J. & Gilbert, L. (2013). Human parvovirus B19 induced apoptotic bodies contain altered self-antigens that are phagocytosed by antigen presenting cells. *PLoS ONE* **8**, e67179.

Whitmire, W. M. & Garon, C. F. (1993). Specific and nonspecific responses of murine B cells to membrane blebs of *Borrelia burgdorferi*. *Infect Immun* **61**, 1460–1467.

Winkler, W. (1899). Untersuchungen über das Wessen der Bakterien und deren einordnung im pilzsystem. *Zbl BaktII Abt Orig* **5**, 569–579.

Zhao, X., Zhang, K., Boquoi, T., Hu, B., Motaleb, M. A., Miller, K. A., James, M. E., Charon, N. W., Manson, M. D. & other authors (2013). Cryoelectron tomography reveals the sequential assembly of bacterial flagella in *Borrelia burgdorferi*. *Proc Natl Acad Sci U S A* **110**, 14390–14395.

Edited by: R. Lan

II

PLEOMORPHIC FORMS OF *BORRELIA BURGDORFERI* INDUCE DISTINCT IMMUNE RESPONSES

by

Leena Meriläinen, Heini Brander, Anni Herranen, Armin Schwarzbach and Leona Gilbert, 2015

Submitted manuscript

Pleomorphic forms of *Borrelia burgdorferi* induce distinct immune responses

Leena Meriläinen[a]*, Heini Brander[a], Anni Herranen[a], Armin Schwarzbach[b], and Leona Gilbert[a]

[a] Department of Biological and Environmental Sciences and NanoScience Center, University of Jyvaskyla, P.O Box 35, FI-40014 Jyvaskyla, Finland
[b] Arminlab, Zirbelstrasse 58, 86154 Augsburg, Germany

*Correspondence:
Leena Meriläinen
Department of Biological and Environmental Science/Nanoscience Center
Survontie 9
FIN-40014 University of Jyväskylä, Finland.
Phone: +358443363520
e-mail: leena.m.merilainen@jyu.fi

Keywords: *Borrelia burgdorferi*; pleomorphism; immune response; colocalization

Abstract

Borrelia burgdorferi is the causative agent of tick-borne Lyme disease. As a response to environmental stress *B. burgdorferi* can change its morphology to a round body form. The role of *B. burgdorferi* pleomorphic forms in Lyme disease pathogenesis has long been debated and unclear. Here, we demonstrated that round bodies were processed differently in differentiated macrophages, consequently inducing distinct immune responses compared to spirochetes in vitro. Colocalization analysis indicated that the F-actin participates in internalization of both forms. However, round bodies end up less in macrophage lysosomes than spirochetes suggesting that there are differences in processing of these forms in phagocytic cells. Furthermore, round bodies stimulated distinct cytokine and chemokine production in these cells. We confirmed that spirochetes and round bodies present different protein profiles and antigenicity. In a Western blot analysis Lyme disease patients had more intense responses to round bodies when compared to spirochetes. These results suggest that round bodies have a role in Lyme disease pathogenesis.

1. Introduction

Spirochete bacteria *Borrelia burgdorferi*, transmitted by *Ixodes* ticks, is the causative agent of Lyme disease [1] Innate immune responses initiated by phagocytic macrophages and dendritic cells are important in the clearance of a *B. burgdorferi* infection. Activated macrophages stimulate the adaptive immune response by the production of cytokines and chemokines, and presentation of processed bacterial antigens to naive T cells [2]. *B. burgdorferi* is engulfed into macrophages either by Fcγ-receptor mediated phagocytosis, conventional phagocytosis, or coiling phagocytosis [3]. The Fcγ-receptor mediated phagocytosis requires opsonization of the bacteria before internalization. *B. burgdorferi* does not have lipopolysaccharides (LPS) [4] that results in the recognition by Toll-like receptors (TLRs), such as TLR2/TLR1 heterodimer, on host cell surface [2] with cooperation of intracellular TLRs 7/8 and 9 on the endosomes [5-7]. They recognize pathogen-associated molecular patterns (PAMPs) on the *B. burgdorferi* surface, and initiate signaling cascades that lead to the formation of a phagocytic cup and spirochete internalization.

TLR mediated signaling cascades induce production of several cytokines and chemokines that determine the early immune responses in the host. The phagocytosis and degradation of the bacteria in the phagolysosomes activate TLR signaling within phagolysosomes and further promote cytokine production [5]. *B. burgdorferi* induce expression of multiple cytokines and chemokines in mouse [8] and human [9, 10] macrophages.

Borrelia burgdorferi is pleomorphic and can undergo the morphological transformation as a response to environmental factors [11-15]. Pleomorphic forms of *B. burgdorferi* have been observed in a handful of clinical samples [16-20]. In addition, the spinal fluid [21] and human serum [14] have shown to induce RBs that can revert back to motile spirochetes when placed into normal culture medium in vitro. Moreover, in preliminary studies RBs have displayed difference in biochemical characteristics [14], protein profiles, and antigenicity [11, 12, 18] when compared to the spirochetes. It has been suggested that the pleomorphic forms of *B.*

burgdorferi may explain the numerous Lyme disease symptoms and heterogeneous immune responses in individuals with Lyme disease [16]. Although the phenomenon and occurrence of pleomorphic bacteria are quite widely reported in many clinically important bacteria species such as *E. coli* [22], their role in Lyme disease pathogenesis is poorly understood. There is an essential need for immune studies examining the immune response to *B. burgdorferi* pleomorphic forms.

Here, we compared immune responses initiated by spirochetes and RBs. Macrophages internalized more spirochetes per cell and demonstrated higher lysosomal processing compared to RBs. The coiling phagocytosis for RBs could not be clearly demonstrated although involvement of F-actin in internalization of both forms was confirmed. Spirochetes and RBs stimulated distinct cytokine patterns in macrophages. Furthermore, there were differences in protein expression and antigenic properties between the two forms. Interestingly, Lyme disease patients displayed stronger reactivity against RB antigens. We confirmed that pleomorphic forms indeed induce a distinct immune response compared to spirochetes and they may have a role in Lyme disease pathogenesis.

2. Materials and methods

2.1. Bacterial strains and growth conditions

B. burgdorferi strain B31 was purchased from ATCC (ATCC 35210, Manassas, USA). The fluorescent infectious *B. burgdorferi* strain GCB726 with GFP was kindly provided by George Chaconas, University of Calgary, Canada. Cultures were grown, and RBs were induced as previously described [14].

2.2. Monocyte cell culturing and differentiation to macrophages

Human acute monocytic leukemia (THP-1) cell line was obtained from ATCC (ATCC TIB-202) and cultured in RPMI–1640 medium (Sigma) at 37 °C, 5% CO_2. The medium was supplemented with 10% heat-inactivated fetal bovine serum (FBS), 1% penicillin/streptomycin (pen/strep), 1% L-glutamine and 0.05 mM 2-mercaptoethanol (Bio-Rad, CA, USA). Monocytes were differentiated to macrophages using 200 nM phorbol 12-myristate 13-acetate (Sigma, MO) as previously described [23].

2.3. Phagocytosis and colocalization experiments

For analysis of phagocytosis index (PI) and colocalization of spirochetes and RBs with F-actin and lysosomes, coverslips with differentiated macrophages were transferred to medium without 1% pen/strep. In PI studies, *B. burgdorferi* B31 strain was used while colocalization experiments were performed with fluorescent *B. burgdorferi* GCB726 strain. Cells were kept on ice for 20 min prior addition of the bacteria to synchronize phagocytosis. Either 50 µl (10 x 10^6 bacteria) of *B. burgdorferi* spirochetes or 2 h induced RBs in RPMI medium without antibiotics with a multiplicity of infection (MOI) of 40 were added to cells. For PI analysis cells were incubated for 2 h at 37 °C. For colocalization studies, cells were incubated for 2 h, 8 h, or 24 h. After each time point, cells were washed twice with PBS and fixed with 4% paraformaldehyde/PBS for 20 min RT. Cells were immunolabeled using the previously

published protocol [24]. For PI analysis cells were immunolabeled with monoclonal mouse anti-*B. burgdorferi* OspA antibody (Santa Cruz Biotechnology, Dallas, USA) and with the secondary goat anti-mouse antibody conjugated with Alexa 488 (Invitrogen, Massachusetts, USA). For colocalization analysis with Lamp2, cells were immunolabeled similarly except rabbit anti-Lamp2 primary antibody and Alexa 555 or 594 were used. To study colocalization with F-actin cells were stained with Phalloidin-Tetramethylrhodamine B isothiocyanate (Santa Cruz Biotechnology) 1:1000 for 15 min. To inhibit phagocytosis in the colocalization experiments, macrophages were stimulated with spirochetes and RBs in the presence of 10 mM cytochalasin D (Sigma) that was added to the cells 30 min prior the bacteria. Cytochalasin D inhibits phagocytosis by disrupting actin polymerization. To prevent phagosome-lysosome fusion, 30 μM nocodazole was used to inhibit lysosomal pathway for *B. burgdorferi* and Lamp2 colocalization analysis. To allow phagocytosis nocodazole was added to the cells 30 min after the bacteria addition because nocodazole might inhibit phagocytosis in some amount. In both inhibition experiments, cells were fixed after 2 h incubation and immunolabeled/stained as explained above. As a last step, coverslips were mounted using Prolong Gold Antifade Reagent with DAPI (Life Technologies).

2.4. Confocal microscopy and image analysis

For determination of PI image stacks with 0.2 μm intervals from whole cells were acquired using Olympus confocal IX81microscope, 60x objective, 405 and 488 laser and DIC. The image stacks for colocalization analysis were obtained using Nikon A1R confocal microscope with resonant scanning, 60x objective, and 488 and 561 lasers. In both experiments altogether 40 and 30 cells, respectively, from three independent experiments, were randomly selected and optically sectioned. The brightness and contrast settings of all images, as well as quantification of *B. burgdorferi* engulfment by macrophages from animated multidimensional z-stacks, were applied using open source Fiji software (NIH, USA). The noise from green and red fluorescent images was suppressed using Gaussian blur filter with Sigma (radius) 0.8. The colocalization analysis was performed with open source BioImageXD software [25]. Three slices in total from the top, middle and bottom of each cell z-stack were chosen for quantification of colocalization with Manders coefficient. Thresholds were adjusted manually to eliminate background fluorescence signals. If necessary, a region of interest (ROI) was drawn to image to exclude other cells or bacteria outside the cell from the analysis. For each cell weighted arithmetic mean of coefficients from three slices were calculated. Statistical significances of colocalizations were calculated during analysis using Costes algorithm, and only coincidence probabilities of P = 1.00 was taken into account.

2.5. Cytokine and chemokine analysis

For cytokine and chemokine analysis, differentiated macrophages were exposed to spirochetes and RBs for 24 h. *E. coli* DH5α cells were used as a positive control for cytokine expression with the same MOI. The media was collected and centrifuged 16000g for 5 min. The analysis was performed using Proteome Profiler™ Human Cytokine Array Panel A Array kit (R&D Systems, Minneapolis, USA), according to the manufacturer's instructions. The kit simultaneously profiles by immunoblotting and chemiluminescence relative levels of 36 inflammation mediators: C5a, CD40 ligand, G-CSF, GM-CSF, CXCL1, CCL1, CD54, IFN-γ,

IL-1α, IL-1β, IL-1ra, IL-2, IL-4, IL-5, IL-6, IL-8, IL-10, IL-12 p70, IL-13, IL-16, IL-17, IL-17E, IL-23, IL-27, IL-32α, CXCL10, CXCL11, MCP-1, MIF, MIP-1α, MIP-1β, Serpin E1, RANTES, CXCL12, TNFα and sTREM-1. Samples were run as duplicates and experiments were performed twice. Immunoblot membranes were imaged with ChemiDoc XRS (Bio-Rad) and intensities were analyzed using ImageJ with Dot Blot Analyzer tool. The data was normalized to the positive control blots on the each membrane. Only those cytokine and chemokine responses that showed relative intensity values > 0.01 are reported in this study.

2.6. Two-dimensional gel electrophoresis

Protein profiles of spirochetes and RBs were analyzed with two-dimensional gel electrophoresis (2D PAGE). Cells treated with doxycycline (200 µg/ml, 48 h) were used as an indicator of outer membrane damage. Cell pellets (1–2x10^9 cells) were stored at -20°C until use. 2D PAGE was performed according to the ZOOM IPGRunner System manufacturing instructions (Invitrogen) with modifications. Cells were lysed by sonication for 15 s in a Lysis buffer [1x ZOOM 2D Protein solubilizer 2 (Invitrogen), 3 mM Tris base, 20 mM DL-dithiothreitol (DTT) and 1 x Protease inhibitor single-use cocktail (Thermo Scientific, Massachusetts, USA), pH 8.4]. DNA was removed by centrifugation 16 000 g for 1 min in QIAShredder microcentrifuge tubes (Qiagen, Hilden, Germany). The protein concentrations were determined using Nanodrop ND-1000 spectrophotometer (Thermo Scientific) and samples were stored at +4°C. The immobilized pH gradient (IPG) strips [broad range pH 3–10 (Invitrogen)] were equilibrated for 1 h at RT with the lysed samples (36 µg protein) in rehydration buffer [143 µl 1x ZOOM 2D Protein Solubilizer 2 (Invitrogen), 0.7 µl 2 M DTT, 0.8 µl Carrier ampholytes pH 3–10 (Invitrogen) and 0.5 µl 0.2% bromophenol blue in EtOH]. Isoelectric focusing was performed using a stepwise program 175 V for 15 min, 1500 V for 45 min, and 2000 V for 45 min. Samples were run on NuPAGE Novex 4–12% Bis-Tris ZOOM gels (Invitrogen) during SDS-PAGE. The strips were restrained on the gel with 0.5% agarose in Tris buffer (124 mM Tris, 960 mM glycine, 17.3 mM SDS in H_2O) and resolved in 1x NuPAGE MES SDS Running buffer (Invitrogen) 200 V for 45 min, with 0.5 ml NuPAGE Antioxidant (Invitrogen) in the upper chamber. Mark12 unstained standard (Invitrogen) was used as the molecular weight standard. Gels were stained with SilverQuest SilverStaining kit (Invitrogen) according to the manufacturer's instructions, except the sensitizing and staining times were doubled (20 and 30 min, respectively). Gels were fixed for 40 min or o/n at RT and imaged with QuantityOne Chemidoc XRS (Bio-Rad). Experiments were performed three times. The intensities of the protein spots were measured with open source software Flicker (Open2DProt). The corresponding protein intensities of spirochetes and RBs were normalized with the molecular standard and mean intensities were compared to examine whether protein expressions were decreased or increased with respect to RBs.

2.7. Western blot

Western blots of whole lysates from spirochetes and RBs were probed with Lyme patient sera to compare the antigenicity of these two forms. Doxycycline treated bacteria (200 µg/ml, 48 h) were used as a control for cell damage. Spirochetes and RBs were collected (2400 g, 15 min), resuspended in 2x SDS reducing loading buffer (0.5 M Tris-HCL, pH 6.8, 10% SDS,

17% β-mercaptoethanol, 0.2% bromophenol blue) and heated 95°C for 15 min. Protein concentrations were determined with Nanodrop ND-1000 spectrophotometer (Thermo-Scientific), and 20 µg of samples were resolved on 12% SDS-PAGE gels. High and low SDS Laemmli PAGE system molecular weight standards (Sigma) were used. Proteins were then transferred to nitrocellulose membranes (Whatmann, Sigma), blocked with 5% non-fat milk (1% TBS/0.2% Tween20), and incubated with 1:100 diluted Lyme or Lyme negative sera for 1 h RT. Seven pre-screened Lyme positive patients with sustained manifestations and three negative sera samples were used. Diagnosis was conducted through routine tests used in Borreliosis Centrum Augsburg. Informed consents from the donors were not collected because the data were analyzed anonymously. The German Federal Institute for Drugs and Medical Devices (http://www.bfarm.de) approved the usage of these samples (ethical approval number 95.10-5661-7066). After a series of washes with 1% TBS/0.2% Tween20, membranes were incubated with 1:500 secondary anti-human polyclonal IgG Fc-AP conjugate antibody (Novus Biologicals, Abingdon, UK) for 1 h RT. Developed membranes were imaged with Chemidoc XRS and protein band intensities were analyzed with ImageJ software. The intensities between spirochetes and RBs were compared. The intensity was considered higher in spirochetes or RBs if the difference was ≥ 25%.

2.8. Statistical analyses

All the statistical analyzes were performed using IBM SPSS Statistics. The comparison of phagocytosis between groups was tested with Pearsson's $\chi 2$-test. Non-parametric Mann-Whitney test was used for comparison of phagocytosis indexes. Colocalization and cytokine/chemokine data was analyzed with two-tailed unpaired t-test or with Mann-Whitney U-test. Differences were considered statistically significant when $P < 0.05$.

3. Results

3.1. Differentiated macrophages phagocytosed more spirochetes than RBs

After 2 h stimulation 75% and 62% of the differentiated macrophages associated with *B. burgdorferi* spirochetes or RBs, respectively, had phagocytosed bacteria (Table 1). Furthermore, the number of bacteria inside the cells (mean ± SD) at 2 h time point was quantified. Results demonstrated that macrophages stimulated with spirochetes engulfed significantly more bacteria per cell than cells associated with RBs ($P=0.045$) (Table 1). This data suggests that RBs are less internalized in macrophages than spirochetes.

3.2. F-actin is involved in the phagocytic uptake of both B. burgdorferi forms

The internalization of spirochetes and RBs into macrophages was analyzed from confocal z-stacks and micrographs. Furthermore, colocalization of *B. burgdorferi* spirochetes and RBs with F-actin in differentiated macrophages at different time points was examined. The goal was to determine if the same mechanisms are involved in the internalization of these two bacteria forms (Fig. 1). F-actin is enriched in the macrophage pseudopodia used for coiling phagocytosis, the predominant uptake mechanism of spirochetes in macrophages [26-28]. As shown in the Fig. 1A-F, F-actin was observed to accumulate in the area where bacteria were engulfed indicating the importance of F-actin in internalization of both *B. burgdorferi* forms. During phagocytosis, both spirochetes and RBs were surrounded by the F-actin (Fig. 1 A, B,

D) and colocalized with it as seen as yellow in Fig. 1A–F. Furthermore, F-actin was occasionally observed to wrap around the spirochetes that is characteristic for coiling phagocytosis. However, the similar long pseudopodia and wrapping of pseudopodia around the RBs was not observed although RBs were enclosed by F-actin and some coiling around them was detected (Fig. 1B, Fig. 1D). At 2 h time point, the colocalization percentage of spirochetes and RBs with F-actin was at its highest without statistical difference between these two forms. There was a minor decrease in the colocalization percentage at 8 h and 24 h time point, however; cells still internalized bacteria (Fig. 1G). Cytochalasin D was used as an inhibitor of phagocytosis for 2 h time point. Cytochalasin D inhibits actin polymerization that is essential for phagocytosis. Inhibition did not stop the uptake of the bacteria completely; nevertheless, it significantly decreased colocalization of both bacteria forms with F-actin (P=0.002 for spirochetes and P=0.005 for RBs) (Fig. 1G).

3.3. Spirochetes colocalize more with lysosomes than RBs

To investigate and compare processing of spirochetes and RBs in phagocytic cells, immunofluorescent colocalization analysis of these bacteria forms with lysosome-associated membrane protein 2 (Lamp2) at 2 h, 8 h, and 24 h time points was performed (Fig. 2A–F). At 2 h and 8 h time points there were no apparent difference in colocalization percentage between spirochetes and RBs, however; at 24 h post-stimulation the difference was significant (P=0.028) demonstrating the more substantial colocalization of spirochetes with lysosomes (Fig. 2G). Nocodazole was used to inhibit the microtubules and autophagosome-lysosome fusion and stop bacteria cargo to lysosomes. Nocodazole treatment significantly decreased colocalization of spirochetes (P=0.005) and RBs (P=0.000) with lysosomes suggesting that lysosomal pathway is important in *B. burgdorferi* processing (Fig. 2G). However, lower colocalization of RBs with lysosomes indicated that RBs might be processed additionally via some other than lysosomal pathway in macrophages.

3.4. RBs induce distinct cytokine response compared to spirochetes

The immune responses of differentiated macrophages stimulated with *B. burgdorferi* spirochetes or RBs were studied using a multiplex analysis of relative levels of excreted cytokines and chemokines. Expression levels of all cytokines induced by these two forms are presented in Fig. 3A–R. Out of 36 examined immune-modulating mediators, *B. burgdorferi* induced clear expression of 18 distinct compounds. There were 14 cytokines that displayed weak signal on the threshold level of the detection, and they were omitted from the analysis. Chemokines MIP-1β and RANTES demonstrated relatively the highest expression of all studied mediators for both forms (Fig. 3O and 3Q, respectively). Spirochetes and RBs stimulated production of similar types of cytokines. However, there were significant differences in expression levels of seven specific ones. Spirochetes stimulated significantly higher excretion of IL-1β (P=0.012), IL-1ra (P=0.000), IL-6 (P=0.022), MIF (P=0.015), MIP-1β (P=0.028) and RANTES (P=0.001) compared to RBs (Fig. 3E-G, 3M, 3O, 3Q, respectively). Remarkably, RBs expressed a significantly elevated level of MCP-1 (P=0.032) (Fig. 3L). Exposure to spirochetes and RBs decreased the IL-8 expression of the cells

significantly compared to media control (Fig. 3H). Exposure of cells to *E. coli* did not have a similar decrease in expression (Fig. 3H).

3.5. Spirochetes and RBs have differences in protein profiles and antigenicity

Protein profiles of spirochetes and RBs were compared using two-dimensional gel electrophoresis. In total 77 different protein spots were distinguished from the gels with molecular weights ranging between 3–200 kDa (Fig. S1 A–B). Corresponding proteins of spirochetes and RBs that displayed higher than 25% difference in mean relative intensity values are presented in Fig. S1 A–B and Table 2. Out of these 27 proteins, the expression of 15 proteins was increased in RBs, whereas, the expression decreased in 12 proteins when compared to spirochetes. The 15 proteins that displayed higher relative intensity in RBs were in the molecular range of 15–40 kDa. Proteins that expressed higher intensity in spirochetes were mostly larger, ranging from about 97 kDa to ≥ 200 kDa. There were two proteins with molecular weights of 4 and 21 kDa that were expressed less in spirochetes (spots 27 and 17, respectively, Fig. S1 A–B, Table 2).

The antigenicity of spirochetes and RBs were compared using western blots probed with seven Lyme patients' sera (Fig. S1 C). The intensities of bands on each membrane were compared between spirochetes and RBs (Table 3). All the tested positive sera were reactive against both spirochetes and RBs; however, there were differences in reactivity against some antigens. For instance, only five and two patients out of seven had IgG antibodies against 58 kDa and 60 kDa antigens, respectively (Table 3). In general, patients with sustained manifestations of Lyme disease reacted stronger against RBs compared to spirochetes. Interestingly, there were four antigens, 21, 39, 60, and 66 kDa, which were predominantly more immunoreactive compared to spirochetes (Table 3). Patients reacted against these particular RB antigens more often than the similar ones in spirochetes suggesting that patients indeed react differently against spirochetes and RBs, and RBs have different antigenic properties compared to spirochetes.

4. Discussion

Macrophages are critical to fighting off *B. burgdorferi* infections in mice and humans [29-31, 28]. It has been implied that the pleomorphic forms of this bacterium may help in the evasion from the immune system [32]. Our study demonstrated that the induced pleomorphic forms are recognized and engulfed by differentiated macrophages in vitro, however; macrophages engulfed significantly more spirochetes than RBs per cell (Table 1). This result indicates a difference in the uptake of these two forms.

Macrophages form F-actin rich pseudopodia when they interact and phagocytose *B. burgdorferi* spirochetes [26, 27]. Actin polymerization required for phagocytosis is mediated by CR3 ($\alpha M\beta_2$) and Fcγ receptors [26]. However, it is reported that internalization of unopsonized *B. burgdorferi* is independent of the Fc receptor [33]. Furthermore, many studies have demonstrated *B. burgdorferi* internalization without opsonization [5, 34, 8, 35, 36]. Here, we demonstrated that F-actin participates in the uptake of *B. burgdorferi* both

345 spirochetes and RBs without opsonization suggesting that F-actin is important also in the Fcγ
346 independent phagocytosis (Fig. 1). In addition, the cytochalasin D significantly diminished
347 the colocalization of F-actin with both bacteria forms supporting this observation (Fig. 1G).
348 Although the cell were synchronized in the beginning of the experiments, the standard
349 deviations (SD) for colocalization were rather high due to the different rate and timing of
350 phagocytosis between the cells.
351
352 Coiling phagocytosis is employed by approximately 60–70% of the macrophage cells for
353 engulfment of *B. burgdorferi* spirochetes [28]. Our results support the previous findings,
354 where coiling phagocytosis is demonstrated for the spirochete uptake (Fig. 1A). However,
355 such an extensive coiling and wrapping was not seen in RBs (Fig. 1B, 1D). F-actin
356 accumulated in the phagocytosis site of macrophages, surrounded RBs and colocalized with
357 them, nevertheless, within this study it remained unclear whether actual coiling phagocytosis
358 occurred with RBs. RBs are nonmotile and they have completely different morphology
359 compared to spirochetes that might explain why macrophages did not grow such a long and
360 thin pseudopods and coil so profusely. There is also a possibility that spirochetes and RBs are
361 internalized differently in macrophages: while spirochete uptake occurs via coiling
362 phagocytosis, RBs internalization might rather utilize conventional phagocytosis.
363
364 After internalization with phagocytosis, bacteria are usually transported via the endocytic
365 pathway to lysosomes and finally processed antigens are presented to T-cells by MHC II class
366 molecules. The colocalization of *B. burgdorferi* spirochetes with immunolabeled lysosomal
367 proteins [20, 35, 31] as well as LysoTracker stained acidic compartments [36] has been
368 previously reported. In those studies, colocalization was observed from early 10 min time
369 points up to 5 h of stimulation. Nevertheless, the quantification of actual colocalization was
370 performed in only one study [31], where 45% of the spirochetes colocalized with lysosomal
371 endopeptidase enzyme cathepsin L at 10 min time point and 57% after 5 h of incubation.
372 Here, to compare lysosomal processing of spirochetes and RBs in macrophages,
373 colocalization analysis was executed at three different time points. The colocalization of
374 spirochetes and RBs with Lamp2 remained at the same level at all three time points 2 h, 8 h,
375 and 24 h (Fig. 2G). In this study, the colocalization percentage of spirochetes with lysosomes
376 was found smaller than in the previous study [31]. This difference may be due to the different
377 analysis methods: in the previous study colocalization was analysed using kinetic
378 compartmental analysis, while in this study modern image analysis combined with Costes
379 algorithm for statistical significances was used. Interestingly, RBs colocalized less with
380 lysosomes compared to spirochetes at all time points, and the difference was significant after
381 24 h post-stimulation (Fig. 2G). This result indicates that spirochetes and RBs are processed
382 differently in macrophages. It is suggested that coiling phagocytosis could lead to a
383 presentation of antigens via MCH I molecules [37]. If spirochetes and RBs are phagocytosed
384 differently that could explain their different processing in macrophages.
385
386 Cytokines are thought to have an important role in Lyme disease pathogenesis. The
387 examination of cytokine profiles induced by *B. burgdorferi* spirochete and RBs indicated the
388 production of immune-modulating mediators consistent with the cytokine analysis of CH3

389 and C57 mouse bone marrow-derived macrophages stimulated with *B. burgdorferi* [8].
390 Cytokines and chemokines expressed in our analysis (Fig. 3) as well as in previous mouse
391 study were G-CSF, GM-CSF, IL-1β, IL-6, CXCL1, CXCL10, MCP-1, MIP-1α, MIP-1β,
392 RANTES and TNF-α. Furthermore, the phagocytosis of spirochetes by human macrophages
393 is reported to increase production of IL-1β, IL-6, IL-10, IFNγ, MCP-1 cytokines and MIP-1α,
394 MIP-1β, TNFα, and CXCL10 chemokines [10]. Anti-inflammatory IL-10 has an important
395 role as a regulator of inflammatory responses in Lyme disease [38] and IFNγ correlates
396 positively with the Lyme disease severity in humans [39]. However, in this study neither
397 spirochetes nor RBs induced IL-10 or IFNγ expression at a level that could be detected. In
398 addition, we highlighted six cytokines with immunological relevance that has not been fully
399 evaluated in Lyme disease (Fig. 3). The expression of CD54 (Fig. 3D), IL-16 (Fig. 3I), MIF
400 (Fig. 3M) and Serpin E1 (Fig. 3P) indicated that there is an enhancement of adhesion,
401 attraction and activation of immune cells. With respect to IL-8, significant decrease in
402 production compared to media control for both spirochete and RB stimulated macrophages
403 (Fig. 3H) could imply a cell specific response.
404
405 Furthermore, all of the expressed cytokines, except the IL-23 and MCP-1, were produced in
406 higher levels when cells were stimulated with spirochetes. MCP-1 regulates the migration and
407 infiltration of monocytes, T-cells, and NK-cells, and it potentially has a role in polarization of
408 naïve T cells to Th2 type [40]. MCP-1 expression is required for the development of
409 experimental Lyme arthritis in mice [41], and it is thought to be associated with other
410 autoimmune diseases as well [42]. The higher expression levels of MCP-1, stimulated by *B.*
411 *burgdorferi* RBs, could propose an involvement of the RBs in Lyme arthritis. In this study,
412 RBs demonstrated decreased macrophage phagocytosis, differences in phagocytosis
413 mechanisms and lysosomal processing compared to spirochetes. These differences in the
414 entry and processing could correspond to the lower cytokine and chemokine production in
415 general as well as to different cytokine profiles of spirochetes and RBs. The lower expression
416 of these cytokines by RBs could suggest suppressive immune response against these forms, or
417 immune control dysfunction.
418
419 The protein profiling of spirochetes and RBs have performed earlier with RPMI serum
420 starved [12] and 1 d H_2O induced RBs [11]. These studies reported protein spots with
421 molecular weights less than 97 kDa. Here, we observed protein spots ranging from 3.5 kDa to
422 higher than 200 kDa from both spirochetes and RBs (Fig. S1 A–B, Table 2). Our results
423 correspond to the genome data of *B. burgdorferi* B31 that the bacterium has proteins of
424 molecular weights from 3.3 kDa to 254.2 kDa [43]. However, the 15 proteins detected with
425 increased intensities in RBs were between the molecular weights of 15–40 kDa. Three
426 proteins with higher protein expression in RBs (spots 11, 18 and 19 in Table 2) were
427 determined corresponding to previously reported [12]. In another study [11] 6–16 kDa
428 proteins were examined with mass spectrometry and the differences between spirochetes and
429 1 d H_2O induced RBs were not found. In contrast to their results, we observed two 15 kDa
430 proteins in RBs (spots 24 and 26 in Table 2) with elevated expression when compared to

spirochetes. This difference may be due to the different exposure times to H_2O, because the longer exposure time used may have decreased the protein expression.

In former Western blot analysis [12] 41 kDa (flagellar protein FlaB) and 46 kDa proteins exhibited less reactivity in 48 h serum starved RBs when probed with sera from two infected monkeys and one Lyme patient. In our study, all tested sera reacted against 41 kDa and 45 kDa antigen. These sizes correspond to very immunogenic antigens flagellar protein (FlaB) and VlsE, respectively, as previously reviewed [44]. However, two patients reacted more against 41 kDa flagella on spirochetes, three against RBs and three had equal response to both (Table 3). Furthermore, four patients reacted more against RB VlsE. These discrepancies to previous findings may be due to the variability of patients' reactivity against this specific antigen, or in the distinct induction method of RBs. In addition, the number of tested sera was higher in our study.

Interestingly, the bands with a molecular weight of 39, 60, and 66 kDa demonstrated predominantly higher intensity in RBs compared to spirochetes. This supports the 2D PAGE results where smaller intensity spots displayed higher intensity in RBs. The 39, 60, and 66 kDa bands correspond to a laminin binding protein BmpA [45], heat shock protein GroEL [46] and p66 [47], respectively. These bands have been previously reported for *B. burgdorferi* B31 western blots probed with patients' sera [48]. Nonetheless, their reactivity against RBs has not been demonstrated before. The role of pleomorphic forms in Lyme disease has been previously criticized [49], nonetheless, there is a lack of studies connecting RBs to Lyme pathogenesis. Overall, this data implies that patients react differently against *B. burgdorferi* spirochetes and RBs suggesting that RBs may have a role in Lyme pathogenesis. Different antigenicity between spirochetes and RBs could add value for diagnostic purposes.

Conclusively, these results imply that *B. burgdorferi* RBs have access to immune cells and have the ability to stimulate an immune response. However, there are differences in phagocytosis and processing of these two pleomorphic *B. burgdorferi* forms in macrophages. In addition, the immune response differs from spirochetes especially with lower expression of IL-1β, IL-1ra, MIF, MIP-1β and RANTES. Conversely, RBs stimulate a significantly higher expression amount of MCP-1. Spirochetes and RBs have differences in protein expression and they have different antigenic properties as seen in patients IgG responses. These results indicate that RBs may have the ability to induce distinct immune response compared to spirochetes and that they could be associated with different clinical symptoms seen in patients. We suggest that pleomorphic RBs should be included in the Lyme disease diagnostic tools. The recognition and detection of pleomorphic forms are detrimental to the proper diagnosis and treatment of *B. burgdorferi* infections.

Acknowledgments

We thank Lassi Paavolainen for valuable advice with the colocalization analysis and Laura Pitkänen for technical assistance. This study was supported by the Schwartz Foundation and Jenny and Antti Wihuri Foundation.

Conflict of interest

The authors declare that they have no competing interests.

References

[1] Burgdorfer W, Barbour AG, Hayes SF, Benach JL, Grunwaldt E, Davis JP. Lyme disease-a tick-borne spirochetosis? Science 1982;216:1317-9.

[2] Hirschfeld M, Kirschning CJ, Schwandner R, Wesche H, Weis JH, Wooten RM, et al. Cutting edge: inflammatory signaling by *Borrelia burgdorferi* lipoproteins is mediated by toll-like receptor 2. J Immunol 1999;163:2382-6.

[3] Cervantes JL, Hawley KL, Benjamin SJ, Weinerman B, Luu SM, Salazar JC. Phagosomal TLR signaling upon *Borrelia burgdorferi* infection. Frontiers in cellular and infection microbiology 2014;4:55.

[4] Takayama K, Rothenberg RJ, Barbour AG. Absence of lipopolysaccharide in the Lyme disease spirochete, *Borrelia burgdorferi*. Infect Immun 1987;55:2311-3.

[5] Cervantes JL, Dunham-Ems SM, La Vake CJ, Petzke MM, Sahay B, Sellati TJ, et al. Phagosomal signaling by *Borrelia burgdorferi* in human monocytes involves Toll-like receptor (TLR) 2 and TLR8 cooperativity and TLR8-mediated induction of IFN-beta. Proc Natl Acad Sci U S A 2011;108:3683-8.

[6] Petzke MM, Brooks A, Krupna MA, Mordue D, Schwartz I. Recognition of *Borrelia burgdorferi*, the Lyme disease spirochete, by TLR7 and TLR9 induces a type I IFN response by human immune cells. J Immunol 2009;183:5279-92.

[7] Shin OS, Isberg RR, Akira S, Uematsu S, Behera AK, Hu LT. Distinct roles for MyD88 and Toll-like receptors 2, 5, and 9 in phagocytosis of *Borrelia burgdorferi* and cytokine induction. Infect Immun 2008;76:2341-51.

[8] Gautam A, Dixit S, Embers M, Gautam R, Philipp MT, Singh SR, et al. Different patterns of expression and of IL-10 modulation of inflammatory mediators from macrophages of Lyme disease-resistant and -susceptible mice. PLoS One 2012;7:e43860.

[9] Shin JJ, Strle K, Glickstein LJ, Luster AD, Steere AC. *Borrelia burgdorferi* stimulation of chemokine secretion by cells of monocyte lineage in patients with Lyme arthritis. Arthritis Res Ther 2010;12:R168.

[10] Strle K, Drouin EE, Shen S, Khoury JE, McHugh G, Ruzic-Sabljic E, et al. *Borrelia burgdorferi* stimulates macrophages to secrete higher levels of cytokines and chemokines than *Borrelia afzelii* or *Borrelia garinii*. J Infect Dis 2009;200:1936-43.

[11] Al-Robaiy S, Dihazi H, Kacza J, Seeger J, Schiller J, Huster D, et al. Metamorphosis of *Borrelia burgdorferi* organisms--RNA, lipid and protein composition in context with the spirochetes' shape. J Basic Microbiol 2010;50 Suppl 1:S5-17.

[12] Alban PS, Johnson PW, Nelson DR. Serum-starvation-induced changes in protein synthesis and morphology of *Borrelia burgdorferi*. Microbiology 2000;146 (Pt 1):119-27.

[13] Brorson O, Brorson SH. A rapid method for generating cystic forms of *Borrelia burgdorferi*, and their reversal to mobile spirochetes. APMIS 1998;106:1131-41.

[14] Merilainen L, Herranen A, Schwarzbach A, Gilbert L. Morphological and biochemical features of *Borrelia burgdorferi* pleomorphic forms. Microbiology 2015;161:516-27.

[15] Murgia R, Cinco M. Induction of cystic forms by different stress conditions in *Borrelia burgdorferi*. APMIS 2004;112:57-62.

519 [16] Aberer E, Kersten A, Klade H, Poitschek C, Jurecka W. Heterogeneity of *Borrelia*
520 *burgdorferi* in the skin. Am J Dermatopathol 1996;18:571-9.
521 [17] Brorson O, Brorson SH, Henriksen TH, Skogen PR, Schoyen R. Association between
522 multiple sclerosis and cystic structures in cerebrospinal fluid. Infection 2001;29:315-9.
523 [18] Hulinska D, Bartak P, Hercogova J, Hancil J, Basta J, Schramlova J. Electron
524 microscopy of Langerhans cells and *Borrelia burgdorferi* in Lyme disease patients. Zentralbl
525 Bakteriol 1994;280:348-59.
526 [19] MacDonald AB. Concurrent Neocortical Borreliosis and Alzheimer's Disease
527 Demonstration of a Spirochetal Cyst Form. Ann NY Acad Sci 1988;539:468–70.
528 [20] Montgomery RR, Lusitani D, de Boisfleury Chevance A, Malawista SE. Human
529 phagocytic cells in the early innate immune response to *Borrelia burgdorferi*. J Infect Dis
530 2002;185:1773-9.
531 [21] Brorson O, Brorson SH. In vitro conversion of *Borrelia burgdorferi* to cystic forms in
532 spinal fluid, and transformation to mobile spirochetes by incubation in BSK-H medium.
533 Infection 1998;26:144-50.
534 [22] Glover WA, Yang Y, Zhang Y. Insights into the molecular basis of L-form formation
535 and survival in *Escherichia coli*. PLoS One 2009;4:e7316.
536 [23] Daigneault M, Preston JA, Marriott HM, Whyte MK, Dockrell DH. The identification of
537 markers of macrophage differentiation in PMA-stimulated THP-1 cells and monocyte-derived
538 macrophages. PLoS One 2010;5:e8668.
539 [24] Thammasri K, Rauhamaki S, Wang L, Filippou A, Kivovich V, Marjomaki V, et al.
540 Human parvovirus B19 induced apoptotic bodies contain altered self-antigens that are
541 phagocytosed by antigen presenting cells. PLoS One 2013;8:e67179.
542 [25] Kankaanpaa P, Paavolainen L, Tiitta S, Karjalainen M, Paivarinne J, Nieminen J, et al.
543 BioImageXD: an open, general-purpose and high-throughput image-processing platform.
544 Nature methods 2012;9:683-9.
545 [26] Linder S, Heimerl C, Fingerle V, Aepfelbacher M, Wilske B. Coiling phagocytosis of
546 *Borrelia burgdorferi* by primary human macrophages is controlled by CDC42Hs and Rac1
547 and involves recruitment of Wiskott-Aldrich syndrome protein and Arp2/3 complex. Infect
548 Immun 2001;69:1739-46.
549 [27] Naj X, Hoffmann AK, Himmel M, Linder S. The formins FMNL1 and mDia1 regulate
550 coiling phagocytosis of *Borrelia burgdorferi* by primary human macrophages. Infect Immun
551 2013;81:1683-95.
552 [28] Rittig MG, Krause A, Haupl T, Schaible UE, Modolell M, Kramer MD, et al. Coiling
553 phagocytosis is the preferential phagocytic mechanism for *Borrelia burgdorferi*. Infect
554 Immun 1992;60:4205-12.
555 [29] Hoffmann AK, Naj X, Linder S. Daam1 is a regulator of filopodia formation and
556 phagocytic uptake of *Borrelia burgdorferi* by primary human macrophages. FASEB J
557 2014;28:3075-89.
558 [30] Liu N, Montgomery RR, Barthold SW, Bockenstedt LK. Myeloid differentiation antigen
559 88 deficiency impairs pathogen clearance but does not alter inflammation in *Borrelia*
560 *burgdorferi*-infected mice. Infect Immun 2004;72:3195-203.

561 [31] Montgomery RR, Nathanson MH, Malawista SE. The fate of *Borrelia burgdorferi*, the
562 agent for Lyme disease, in mouse macrophages. Destruction, survival, recovery. J Immunol
563 1993;150:909-15.
564 [32] Miklossy J, Kasas S, Zurn AD, McCall S, Yu S, McGeer PL. Persisting atypical and
565 cystic forms of *Borrelia burgdorferi* and local inflammation in Lyme neuroborreliosis. J
566 Neuroinflammation 2008;5:40.
567 [33] Montgomery RR, Nathanson MH, Malawista SE. Fc- and non-Fc-mediated phagocytosis
568 of *Borrelia burgdorferi* by macrophages. J Infect Dis 1994;170:890-3.
569 [34] Cruz AR, Moore MW, La Vake CJ, Eggers CH, Salazar JC, Radolf JD. Phagocytosis of
570 *Borrelia burgdorferi*, the Lyme disease spirochete, potentiates innate immune activation and
571 induces apoptosis in human monocytes. Infect Immun 2008;76:56-70.
572 [35] Montgomery RR, Malawista SE. Entry of *Borrelia burgdorferi* into macrophages is end-
573 on and leads to degradation in lysosomes. Infect Immun 1996;64:2867-72.
574 [36] Moore MW, Cruz AR, LaVake CJ, Marzo AL, Eggers CH, Salazar JC, et al.
575 Phagocytosis of *Borrelia burgdorferi* and *Treponema pallidum* potentiates innate immune
576 activation and induces gamma interferon production. Infect Immun 2007;75:2046-62.
577 [37] Rittig MG, Haupl T, Krause A, Kressel M, Groscurth P, Burmester GR. *Borrelia*
578 *burgdorferi*-induced ultrastructural alterations in human phagocytes: a clue to pathogenicity?
579 J Pathol 1994;173:269-82.
580 [38] Lazarus JJ, Meadows MJ, Lintner RE, Wooten RM. IL-10 deficiency promotes increased
581 *Borrelia burgdorferi* clearance predominantly through enhanced innate immune responses. J
582 Immunol 2006;177:7076-85.
583 [39] Salazar JC, Pope CD, Sellati TJ, Feder HM, Jr., Kiely TG, Dardick KR, et al.
584 Coevolution of markers of innate and adaptive immunity in skin and peripheral blood of
585 patients with erythema migrans. J Immunol 2003;171:2660-70.
586 [40] Gu L, Tseng S, Horner RM, Tam C, Loda M, Rollins BJ. Control of TH2 polarization by
587 the chemokine monocyte chemoattractant protein-1. Nature 2000;404:407-11.
588 [41] Brown CR, Blaho VA, Loiacono CM. Susceptibility to experimental Lyme arthritis
589 correlates with KC and monocyte chemoattractant protein-1 production in joints and requires
590 neutrophil recruitment via CXCR2. J Immunol 2003;171:893-901.
591 [42] Deshmane SL, Kremlev S, Amini S, Sawaya BE. Monocyte chemoattractant protein-1
592 (MCP-1): an overview. Journal of interferon & cytokine research : the official journal of the
593 International Society for Interferon and Cytokine Research 2009;29:313-26.
594 [43] Fraser CM, Casjens S, Huang WM, Sutton GG, Clayton R, Lathigra R, et al. Genomic
595 sequence of a Lyme disease spirochaete, *Borrelia burgdorferi*. Nature 1997;390:580-6.
596 [44] Aguero-Rosenfeld ME, Wang G, Schwartz I, Wormser GP. Diagnosis of lyme
597 borreliosis. Clin Microbiol Rev 2005;18:484-509.
598 [45] Simpson WJ, Schrumpf ME, Schwan TG. Reactivity of human Lyme borreliosis sera
599 with a 39-kilodalton antigen specific to *Borrelia burgdorferi*. J Clin Microbiol 1990;28:1329-
600 37.
601 [46] Carreiro MM, Laux DC, Nelson DR. Characterization of the heat shock response and
602 identification of heat shock protein antigens of *Borrelia burgdorferi*. Infect Immun
603 1990;58:2186-91.

[47] Bunikis J, Noppa L, Bergstrom S. Molecular analysis of a 66-kDa protein associated with the outer membrane of Lyme disease Borrelia. FEMS Microbiol Lett 1995;131:139-45.
[48] Ma B, Christen B, Leung D, Vigo-Pelfrey C. Serodiagnosis of Lyme borreliosis by western immunoblot: reactivity of various significant antibodies against *Borrelia burgdorferi*. J Clin Microbiol 1992;30:370-6.
[49] Lantos PM, Auwaerter PG, Wormser GP. A systematic review of *Borrelia burgdorferi* morphologic variants does not support a role in chronic Lyme disease. Clin Infect Dis 2014;58:663-71.

643 **Figure Legends**
644
645 **Fig. 1.** Differentiated macrophages utilize coiling phagocytosis with F-actin rich pseudopodia
646 to engulf both *B. burgdorferi* spirochetes and round bodies (RB). Confocal micrographs of
647 differentiated THP-1 macrophages stimulated with green fluorescent *B. burgdorferi* (Bb) A)
648 spirochetes for 2 h, B) 2 h H_2O RB for 2 h C) spirochetes for 8 h, D) RBs for 8 h, E)
649 spirochetes for 24 h, and F) RBs for 24 h with MOI 40. Cells were stained with phalloidin to
650 indicate F-actin on macrophages (red). White squares depict the zoomed area on the left
651 corner of the merged images. All image slices are from the center of the cell. Scale bars 10
652 μm. G) Mean colocalization percentages ± SD (n=30) of F-actin with spirochetes or RBs after
653 2 h, 8 h, and 24 h. Cytochalasin D (CytoD) was used as inhibitor for phagocytosis. Inhibited
654 colocalization was analysed after 2 h stimulation. **P < 0.01.
655
656 **Fig. 2**. *B. burgdorferi* spirochetes colocalize more with lysosomes than round bodies (RBs).
657 Confocal micrographs of differentiated THP-1 macrophages stimulated with green fluorescent
658 *B. burgdorferi* (Bb) A) spirochetes for 2 h, B) 2 h H_2O RB for 2 h C) spirochetes for 8 h, D)
659 RBs for 8 h, E) spirochetes for 24 h, and F) RBs for 24 h with MOI 40. Cells were
660 immunolabeled with Lamp2 antibody and Alexa 555 or 594 (red) for confocal imaging. White
661 squares depict the zoomed area on the left corner of the merged images. All image slices are
662 from the center of the cell. Scale bars 10 μm. G) Mean colocalization percentages ± SD
663 (n=30) of spirochetes and RBs with Lamp2 at timepoints 2 h, 8 h, and 24 h. Nocodazole was
664 used to inhibit phagosome-lysosome fusion at timepoint 2 h. *P <0.05, **P < 0.01, ***P <
665 0.001.
666
667 **Fig. 3.** Immune mediator expression of differentiated macrophages exposed to *B. burgdorferi*
668 spirochetes (S) and round bodies (RB). *B. burgdorferi* spirochetes, 2 h H_2O RB and *E. coli*
669 DH5α cells with MOI of 50 were incubated with differentiated THP-1 cells for 24 h.
670 Untreated immune cells incubated only with culture media (M) were included as a negative
671 control, while *E. coli* DH5α cells (Ec) with MOI of 50 were used as a positive control for
672 macrophage cytokine and chemokine expression. Mean cytokine production of 18 excreted
673 cytokines (A–R) ± SD (n=2). *P <0.05, **P < 0.01, ***P < 0.001.
674
675 **Supplementary Figure Legend**
676
677 **Fig. S1.** Spirochetes and round bodies (RB) display differences in protein profiles and
678 immunoreactivity. Representative two-dimensional electrophoresis gels from whole cell
679 lysates of A) *B. burgdorferi* B31 spirochetes and B) 2 h H_2O RB. Proteins spots with
680 intensities that differ more than 25% with respect to comparing spirochetes and RBs are
681 indicated with numbers (1–27) in silver stained gels. Molecular weights are indicated on the
682 left side of the images. C) Representative western blots of spirochetes (S) and RBs with Lyme
683 patients' sera (left; n=7) and Lyme negative sera (right; n=3). Doxycycline treated bacteria
684 (200 μg/ml, 48 h) were used as a control for damaged cells.

Figure 1.

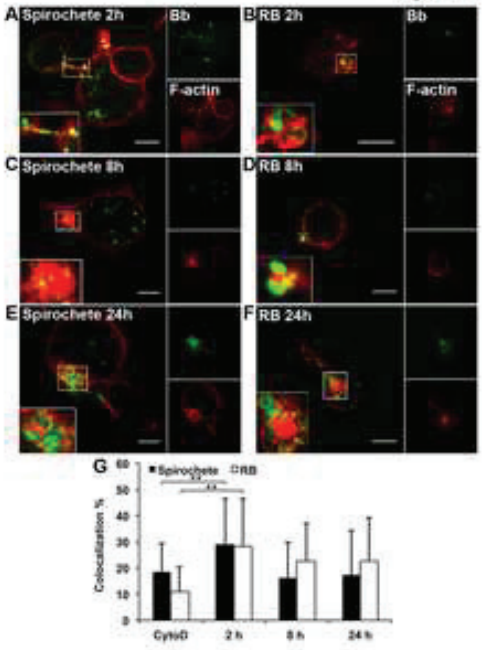
A Spirochete 2h
Bb
F-actin
B RB 2h
Bb
F-actin
C Spirochete 8h
D RB 8h
E Spirochete 24h
F RB 24h
G
Spirochete
RB
Colocalization %
CytoD
2 h
8 h
24 h

Figure 2.

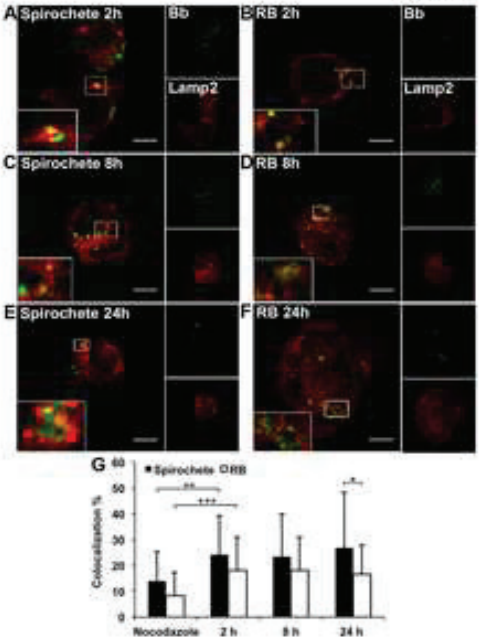
A Spirochete 2h
Bb
Lamp2
B RB 2h
Bb
Lamp2
C Spirochete 8h
D RB 8h
E Spirochete 24h
F RB 24h
G
Spirochete
RB
Colocalization %
Nocodazole
2 h
8 h
24 h

Figure 3.

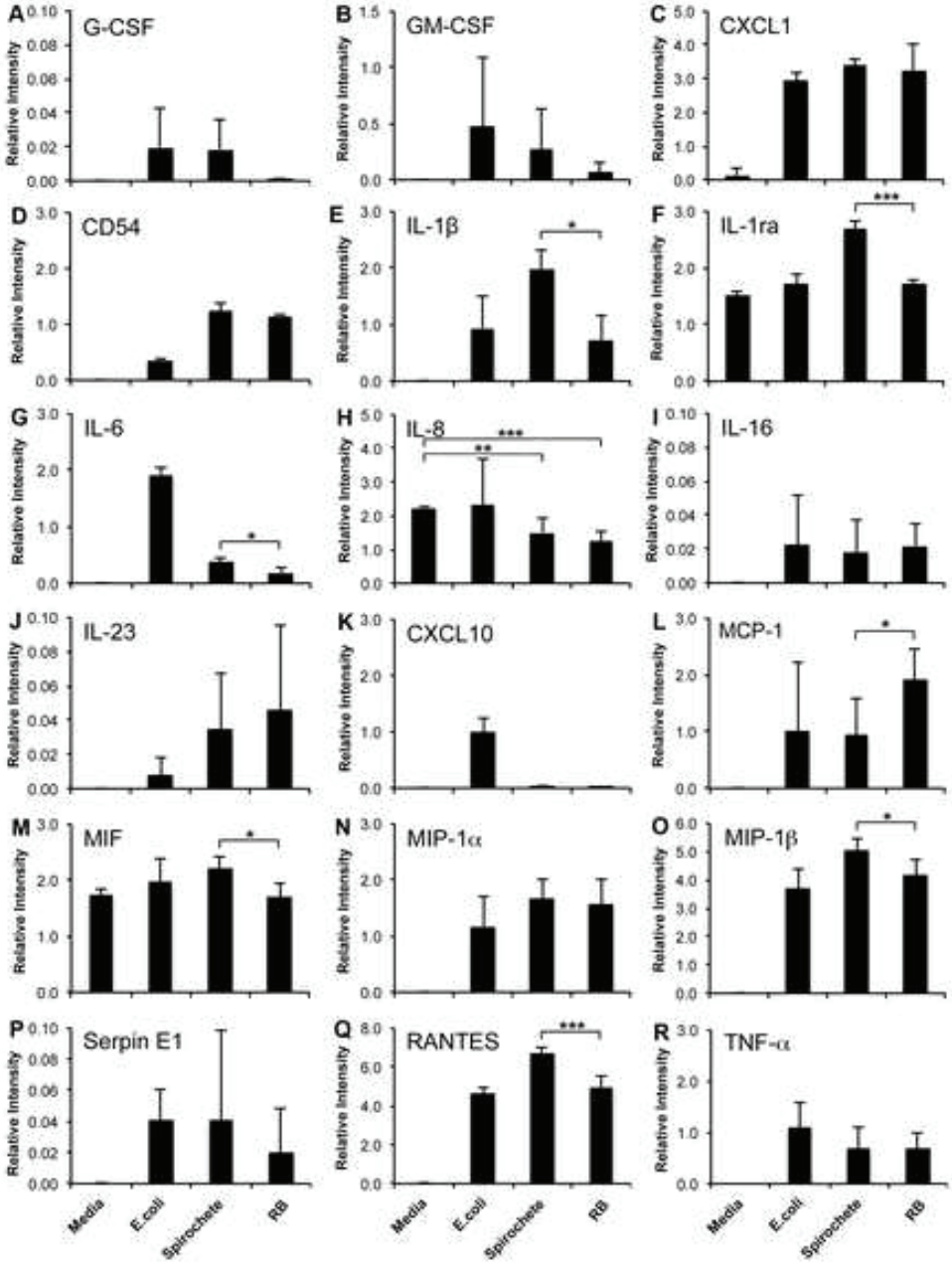
A
G-CSF
B
GM-CSF
C
CXCL1
D
CD54
E
IL-1β
F
IL-1ra
G
IL-6
H
IL-8
I
IL-16
J
IL-23
K
CXCL10
L
MCP-1
M
MIF
N
MIP-1α
O
MIP-1β
P
Serpin E1
Q
RANTES
R
TNF-α
Relative Intensity
Media
E.coli
Spirochete
RB

Figure S1.

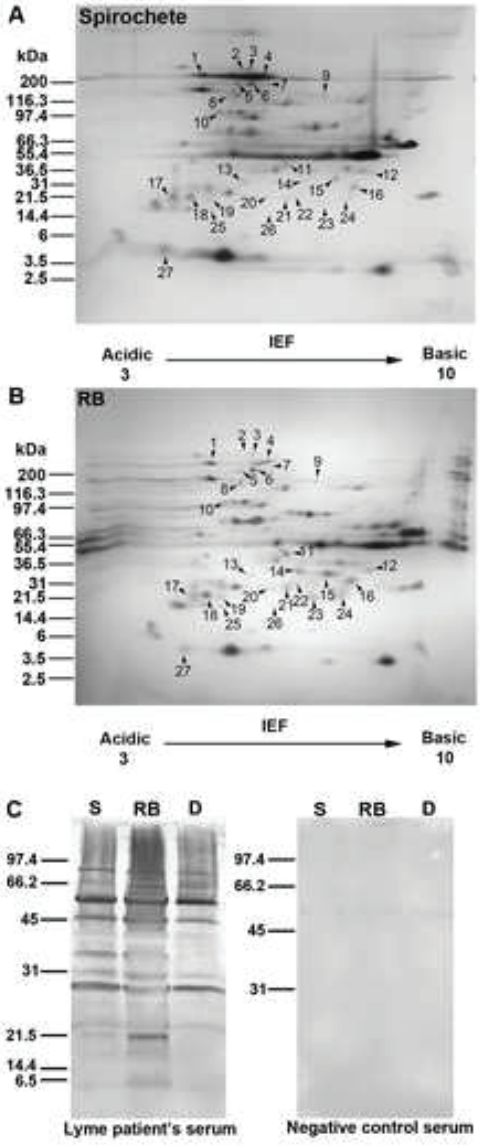
A
Spirochete
kDa
200
116.3
97.4
66.3
55.4
36.5
31
21.5
14.4
6
3.5
2.5
Acidic
3
IEF
Basic
10
B
RB
C
S
RB
D
97.4
66.2
45
31
21.5
14.4
6.5
Lyme patient's serum
Negative control serum

Table 1. Phagocytosis percentages and indexes of *B. burgdorferi* associated differentiated macrophages.

Total	n	Phagocytosed cells% (N)	PhI ± SD
Macrophages and spirochetes	40	75% (30)	3.0 ± 1.8 [a]
Macrophages and RBs	40	62% (25)	2.3 ± 1.8

[a] $P < 0.05$ (Mann-Whitney U test). Comparison analysis of phagocytic index between macrophages exposed to spirochetes and 2 h H_2O round bodies (RBs).

Table 2. Protein profile differences of *B. burgdorferi* spirochetes (S) and round bodies (RB).

Spot	~Mw (kDa)	S	RB	Difference%	Spot	~Mw (kDa)	S	RB	Difference%
1	>200	+	-	31.5	**15**	33	-	+	41.5
2	>200	+	-	45.2	**16**	31	-	+	27.7
3	>200	+	-	49.3	**17**	21	+	-	35.7
4	>200	+	-	58.8	**18**	21	-	+	39.9
5	200	+	-	47.5	**19**	21	-	+	34.0
6	200	+	-	26.2	**20**	27	-	+	33.9
7	200	+	-	37.6	**21**	27	-	+	49.9
8	120	+	-	27.5	**22**	27	-	+	42.2
9	160	+	-	34.9	**23**	18	-	+	38.4
10	97	+	-	33.4	**24**	18	-	+	35.4
11	40	-	+	36.5	**25**	15	-	+	29.7
12	33	-	+	32.6	**26**	15	-	+	33.7
13	33	-	+	26.6	**27**	4	+	-	28.7
14	33	-	+	51.6					

Table 3. Comparison of spirochete (S) and round body (RB) Western blots probed with Lyme patient's serum.

Mw (kDa)	Reactive sera (n = 7)	Higher intensity (>25%) against S	Higher intensity (>25%) against RB	No difference between S and RB
93	6	0	4	2
66	5	0	5	0
60	2	0	2	0
58	5	0	3	2
45	7	0	4	3
41	7	2	3	2
39	6	1	5	0
36	6	0	4	2
34	7	1	3	3
31	6	1	3	2
30	6	1	2	3
28	5	1	2	2
23	7	0	2	5
21	1	0	1	0
18	6	1	2	3

III

AN IMPROVED AND NOVEL MULTIPLEX ELISA FOR LYME DISEASE DIAGNOSIS

by

Kanoktip Puttaraksa, Leena Meriläinen, Ana Campillo, Armin Schwarzbach, Paula Garcia-Nogales and Leona Gilbert, 2015

Submitted manuscript

An Improved and Novel Multiplex ELISA for Lyme Disease Diagnosis

Kanoktip Puttaraksa*, Leena Meriläinen*, Ana Campillo†, Armin Schwarzbach‡, Paula Garcia-Nogales†, Leona Gilbert*
*University of Jyvaskyla, Department of Biological and Environmental Sciences and NanoScience Center, Jyvaskyla, Finland; †Applied Research using OMIC Sciences, S.L. (AROMICS), Department of Research and Development, Barcelona, Spain; and ‡ArminLabs, Laboratory for Tick-borne Diseases, Augsburg, Germany

This work was supported by the Schwartz Foundation, and the European Union (EU) Seventh Framework Programme for research and technological development (FP7/2007-2011) [grant agreement number 262411].

The running title: Novel Multiplex ELISA for Lyme Disease
Key words: ELISA, *Borrelia burgdorferi*, round bodies, Lyme disease, Tick-borne diseases

Address correspondence and reprint requests to Kanoktip Puttaraksa (MSc.), University of Jyvaskyla, Department of Biological and Environmental Science and NanoScience center, P.O. Box 35, FI-40014 University of Jyvaskyla, Finland. E-mail address: kanoktip.k.thammasri@jyu.fi

Abbreviations used in this article: LD, Lyme disease; RBs, round bodies; Bb B31, *B. burgdorferi sensu stricto* B31; Bb 297, *B. burgdorferi sensu stricto* 297; Ba, *B. afzelii*; Bg, *B. garinii.*

Abstract

The use of recombinant antigens of *Borrelia burgdorferi* has been reported as a strategy to improve the accuracy and standardization of the serological approach for Lyme disease (LD). Accordingly, a novel multiplex ELISA was developed by using the specific antigens include *B. burgdorferi* peptides/proteins from the different disease stages of LD, pleomorphic round body forms (RBs) of *B. burgdorferi,* and tick-borne co-infections. We hypothesized that the assessment of antibodies against specific antigens by the multiplex ELISA could enhance the accuracy of LD diagnosis. Sera of LD patients (n = 54) and healthy donors (n = 15) from Germany, Spain, and Finland, were tested and compared between the multiplex ELISA and the standard two-tier assays. The multiplex ELISA exhibited high sensitivity (98.15%), specificity (100%), PPV (100%), and NPV (93.75%); whereas, the conventional two-tier test had lower sensitivity (87.04%) and NPV (68.18%), but the similar values for specificity (100%) and PPV (100%). Patients' antibody responses indicated reactivity to all three common European *B. burgdorferi* subspecies, RBs, recombinant peptides, and co-infections. The potential antigens including C2, C6, OspE-1, OspE-2, LFA-1, *Ehrlichia* and RBs demonstrated improved LD diagnosis. Interestingly, IgM and IgG antibodies against RBs were detected at high percentages but independent from other antigens indicated by Cohen's kappa analysis.

Therefore, RBs are the relevant novel antigens to be used in LD diagnosis. In conclusion, the novel multiplex ELISA assay has enhanced performance than the conventional two-tier tests; therefore, this is a model for developing a single-step and thorough tick-borne diseases diagnostic kit.

Introduction

Borrelia burgdorferi sensu lato is a causative agent of Lyme disease (LD) and is transmitted to humans through the bite of an infected tick (1, 2). Three main subspecies including *B. burgdorferi sensu stricto* (Bb), *B. afzelii* (Ba), and *B. garinii* (Bg) have been frequently cultured from Lyme patients (2, 3). Nevertheless, ticks may carry various other pathogens including bacteria (e.g. *Rickettsia, Ehrlichia*), protozoa (e.g. *Babesia*), and viruses (e.g. tick-borne encephalitis virus). Indeed, multiple pathogens can be transmitted through a single tick bite and subsequently cause co-infections (4, 5).

Diagnosis of LD is based on the history of a tick bite, exposure to the ticks in the endemic area of the disease, clinical features, and serological examinations (6). The standard LD diagnosis approach is the two-tier test that first requires enzyme immunoassay (EIA) or immunofluorescence assay (IFA), followed by the confirmation of the positive or equivocal response with a Western immunoblot (7). Most existing commercial serodiagnostic kits commonly use mixtures of whole-cell lysates, whole-cells combined with purified classical proteins, e.g. flagella antigen (p41), outer surface protein C (OspC), or the variable surface lipoprotein E (VlsE) as an antigen (8). The recombinant synthetic invariant region C6 derived from the VlsE is commonly included in the tests (8).

The disadvantages of the two-tier test are time consumption, high costs, not standardized, and the requirement of technical experience. Furthermore, the high possibility of low sensitivity and specificity in the two-tier testing has been reported particularly in the early infection state (8, 9). The new commercial immunoassay approach focused on the use of purified, recombinant, or synthetic peptides of *B. burgdorferi* as the source of antigens. The implementation of the recombinant antigens enhanced the test's sensitivity and specificity (8, 10). Also, it has been reported that *B. burgdorferi* could escape from the host's defense mechanisms and alter its antigenic properties by changing its morphology into the RBs form (11-14). Therefore, we developed a single-step diagnostic test to detect the immune reactions to specific antigens regarding different LD stages, *B. burgdorferi* genospecies, pleomorphic forms, and tick-borne co-infections to increase sensitivity and specificity of the immunoassay. This test could provide a model for the improvement of tick-borne diagnostics in the future.

Materials and Methods

Serum samples

Retrospective well-characterized sera (n = 69) were obtained from a highly specialized LD clinic, BCA (Borreliose Centrum Augsburg GmbH & Co. KG, Augsburg, Germany).

Patients and healthy donors were recruited from Spain, Germany, and Finland. Serum samples from LD patients (n = 54) and negative controls (n = 15) from the donors had been subjected to clinical examination followed by the commercially available anti-*Borrelia* ELISA tests (Euroimmun, Luebeck, Germany and Virotech Sekisui Diagnostics, Rüsselsheim, Germany). Positive samples were confirmed using the anti-*Borrelia* immunoblot (Euroimmun). Patients were categorized into three groups; early localized infection (n = 5), later disseminated infection or post treatment LD syndrome (PTLDS) without co-infection (n = 34), and PTLDS with co-infections (n = 15), based on clinical manifestations and serological results (Supplemental data, Table SI). This study was conducted under the approval of Federal Institute for Drugs and Medical Devices in Germany (No.95.10-5661-7066).

Antigens

Fifteen antigens under six antigen groups were used (Supplemental data, Table S2). Full lysates of *B. burgdorferi* spirochetes and pleomorphic RBs, the recombinant proteins/peptides typical for indicating different LD stages, as well as peptides of tick-borne co-infections, were used as antigens in the multiplex ELISA assay. Recombinant antigens were purchased from the commercial companies as stated in the Table S2. The full lysate of *Escherichia coli* (*E. coli*) DH5α strain was used to discard possible detection of cross-reactivity since proteins and peptides in this study were generated in *E. coli*.

Bacteria culturing and lysate preparation

Bb B31 and Bg were obtained from ATCC (ATCC, Manassas, USA). Bb 297 and Ba were kindly provided by Seppo Meri (Haartman Institute, Helsinki, Finland). Cultures were grown in Barbour-Stoenner-Kelly medium (BSK-II) without gelatin (15), supplemented with 6% rabbit serum (Sigma-Aldrich, St. Louis, USA) at 37°C. Induction of RBs of Bb B31 was performed according the previously published protocol (13). A total of 50-100 x 10^6 low passage spirochetes and H_2O induced RBs were centrifuged 5000 x g for 10 min. *E. coli* was cultured in Lysogeny Broth (LB) medium and incubated at 37°C for 2.5 h with shaking 250 rpm. The optical densities (OD) were measured at 600 nm and cells were centrifuged 13000 x g for 5 min, stored at -80°C until used. The pellets were suspended with 100 µL of PBS and denatured by heating at 99°C for 15 min. The protein concentration of lysates was measured by Nanodrop 1000 spectrophotometer at 280 nm.

Enzyme-linked immunosorbent assay (ELISA)

Antigens 1.0 mg/mL were diluted 1:100 in carbonate buffer (0.1M Na_2CO_3/0.1M $NaHCO_3$, pH 9.5). Antigens were placed into the 96-well plate (Thermo Fisher Scientific, MA, USA) 100 µL/well as duplicates. The blank control (only carbonate buffer) and positive control, either human IgG or IgM (Sigma-Aldrich), were included in every plate. Antigen coated plates were incubated overnight at 4°C and washed three times with 250 µL of PBS-T buffer (phosphate buffered saline (PBS) / 0.05% Tween® 20, Sigma-Aldrich). Plates were blocked with 2% bovine serum albumin-PBS (BSA, Sigma-

Aldrich) and incubated overnight at 4°C. Serum samples 1:200 in 1% BSA-PBS were added to the plates, to the blank and positive controls only 1% BSA-PBS were added. Plates were incubated for 2 h at room temperature (RT) and washed five times with PBS-T. A volume of 100 µL horseradish peroxidase (HRP) conjugated mouse anti-human IgG (Abcam, Cambridge, UK) 1:10000 or IgM (Novus Biologicals, Colorado, USA) 1:1000 in 1% BSA-PBS was added and plates were incubated for 1.5 h at RT. Wells were washed five times with PBS-T before adding 100 µL TMB substrate (Thermo Fisher Scientific) and incubated at RT in dark for 5 and 30 min for anti-IgG and anti-IgM, respectively. The reaction was stopped by the addition of 100 µL 2M H_2SO_4. The OD was measured using Victor^{TM}X4 Multilabel Plate Reader 2030 (PerkinElmer, Massachusetts, USA) at 450 nm for 0.1 sec.

The cut-off value of each antigen was obtained by calculation of mean absorbance of the negative sera plus three times the standard deviation (SDs) of the mean (mean + 3SDs) (16). Absorbance values from different experiments were normalized to ensure the comparability of OD index values (ODI). ODI of each antigen was achieved from its mean absorbance value divided by the cut-off. The borderline values were accounted as negative to avoid the false positive results.

Statistical analysis

The accuracy of the commercially two-tier test and the novel multiplex ELISA assay was validated by matching the coincident results to the reference diagnosis. The sensitivity and the specificity were calculated by sensitivity = true positives (TP)/(TP + false negatives (FN)), and specificity = true negatives (TN)/(TN + false positives (FP)). Furthermore, the positive (PPV) and the negative predictive values (NPV) were calculated by PPV = TP/(TP+FP) and NPV = TN/(TN+FN) (16).

Results were analyzed using the Microsoft Excel 2011 and IBM SPSS Statistics version 22. The differences in seropositivity to each antigen between patient groups were determined using the Mann-Whitney U test. The agreement of immune responses between each antigen pair was evaluated by the Cohen's kappa analysis.

Results

The novel multiplex ELISA improved the accuracy of LD diagnosis

The performances between two tests, the novel multiplex ELISA and the standard two-tier tests, were compared (Fig. 1). The IgM seropositivity with the two-tier test (44.44%) was lower than the multiplex ELISA (66.67%) (Fig. 1*A*). Furthermore, IgG seropositivity was slightly lower by the two-tier test (75.93%) than with the multiplex ELISA (88.88%) (Fig. 1*B*). In both assays, negative controls were 100% IgM and IgG seronegative.

The percentages of IgM and IgG seropositivity against each antigen in different patient groups by the multiplex ELISA were examined (Table I). The early localized group presented anti-RBs and anti-Bg IgG antibodies at a significantly ($p < 0.05$) higher than the PTLDS groups. PTLDS patients without co-infections were detected to show higher levels of IgM and IgG antibodies to many antigens with no significant differences when compared to the other groups. The titer of IgG antibodies against autoimmune,

lymphocyte function-associated antigen 1 (LFA-1) and myelin basic protein (MBP), and co-infections, *Babesia microti* (BM) and *Ehrlichia*, antigens in PTLDS with co-infections group were higher than others although not statistically significant. However, the titer of anti-Bg IgM antibody in this group was significantly ($p < 0.05$) higher than in the early localized group, and anti- outer surface protein E (OspE) IgG antibody was higher than in the PTLDS group.

To compare the accuracy of the two-tier and the multiplex ELISA assays, the sensitivity and specificity of these assays were determined (Table II). Serological reactions, either IgM or IgG positive, in the controls and LD patients by those two assays were compared to the clinical diagnosis by the specialized LD clinic as the reference (Table SI). The sensitivity of the two-tier test was 87.04% (47/54) whereas the ELISA assay was higher being 98.15% (53/54). There was no false positive recognized in the negative controls: the specificity of both assays was 100% (15/15). Comparison of PPV and NPV between the two-tier and the multiplex ELISA tests were consequently determined. The PPV was 100% for both assays whereas the NPV was 68.18% by the two-tier test and 93.75% by the multiplex ELISA assay.

Agreement of selected antigens in the multiplex ELISA

The Cohen's kappa statistic was applied to evaluate the agreement between antigens in the multiplex ELISA (Table III). The kappa (κ) coefficient value provides a quantitative measurement of the reliability and agreement between variables in the study. A value of 1 represents perfect agreement; whereas, 0 indicates poor agreement (17, 18). High agreement value indicated high immunological responses dependency of those antigens in the same patient's sample. Good agreement was demonstrated between C2, OspE-1, OspE-2 and *Ehrlichia* ($\kappa = 0.514 – 0.824$), and between C6 and OspE-2 ($\kappa = 0.547$) in the IgM test (Table III*A*). Antigens associated with early and disseminated infection, C2, C6, and OspE-2 depended on each other ($\kappa = 0.483 – 0.776$) in the IgG test (Table III*B*). Furthermore, IgG antibodies against LFA-1, *Ehrlichia*, and MBP depended on all early and disseminated infection antigens ($\kappa = 0.420 – 0.773$). Variation of agreement levels between the *B. burgdorferi* spirochetes to other antigen types was presented. Interestingly, immune responses to RBs were independent from other antigens; however, it slightly depends on C6 and Bb B31 spirochetes ($\kappa = 0.226 – 0.410$). These results are in harmony with the serological analysis where some patients were found to have IgM or IgG positive responses against only the RBs or with other antigens (Table SI).

European LD patients have antibody responses against three main *B. burgdorferi* subspecies and RBs

All three genospecies are pathogenic in European LD patients (Fig. 2). The level of IgM antibodies against Bg was the highest (55%), while other subspecies were detected at the lower levels, anti-RBs (18%), anti-Bb B31 and 297 (11%), and anti-Ba (5%) (Fig. 2*A*). Interestingly, the percentages of anti-RBs were higher than anti-Bb B31 spirochetes in the IgM test. The seropositivity of IgG antibodies against Bb B31 and RBs were the highest (27% for both), whereas, other strains were present with the lower, anti-Bb 297 (14%), anti-Ba (17%), and anti-Bg (15%) (Fig. 2*B*).

Discussion

The present retrospective study demonstrated the potential use of multiple antigens and antigen types in the serological assay for LD diagnosis. Various specific antigens from three species of *B. burgdorferi* and tick-borne co-infections were used in the novel multiplex ELISA assay. A selection of antigens is important since it will indicate the immunological differences in the patients. VlsE peptide is the most commonly used antigen in LD diagnosis due to its role in the survival of *B. burgdorferi* (19). Immune responses to invariable regions of VlsE have been detected in the early, and persistently infected patients indicating that these peptides are broadly antigenic in *B. burgdorferi* infection (19). Antigenicity of recombinant conserved invariant regions of VlsE, particularly C6, has been assessed previously in humans, monkeys and mice (20-22). In the present study, the commercially two-tier kits used the full sequence of VlsE whereas the novel ELISA contained the specific invariant regions, C2 and C6 peptides. Patients were either IgM/IgG seropositive to VlsE, 36 positives by the two-tier test, and 40 positives by the multiplex ELISA (Table SI). The commercial kits indicated only IgG positivity to VlsE in those patients, whereas, the multiplex ELISA characterized of IgM/IgG positivity to C2/C6 in them (Table SI). Therefore, the use of conserved regions VlsE in the ELISA enhanced the sensitivity of the test. The ability of *B. burgdorferi* to maintain infection indicates the capability of bacteria to evade host immune response. OspE, the surface component of *B. burgdorferi*, is known to participate in evasion from the complement system (23) and anti-OspE antibodies indicate disseminated infection (24). Antibodies against OspE sequences (1 and 2) in the current study were highly expressed in Lyme patients, particularly in the group of PTLDS with co-infections (80–87%) as shown in Table I. Results provide evidence that OspE is a potential antigen for LD diagnosis, and different sequences have similar antigenicity.

Prolonged disseminated *B. burgdorferi* infection may trigger autoimmunity by the mimicry of amino acid sequence homology with the self-antigens, and consequently activate multi-organ system disorders (25, 26). The initiation of the autoimmunity in *B. burgdorferi* infection begins with a cross-reactivity response between the outer surface protein A and a self-antigen, LFA-1 (25). Therefore, immune responses to LFA-1 imply the development of autoimmune disorder (26). The cross-reactivity of *B. burgdorferi* and other self-antigens such as collagen I and MBP have been reported in LD patients with autoimmune diseases (27). Antibodies against LFA-1 and MBP were detected in every patient group; however, the highly positive was PTLDS with co-infections group (Table I). Also, the multiplex ELISA includes two common co-infections of LD, BM and *Ehrlichia* (5, 28). Distinguishing between these infections is important for the treatment strategy. Most PTLDS with co-infections patients were IgM/IgG positive to either BM or *Ehrlichia* antigens (14/15) as expected (Table SI).

The full lysate of the most common *B. burgdorferi* subspecies cause of LD in Europe, Bb, Ba, and Bg (29), were included in the developed ELISA assay. The European LD patients in the present study revealed immune reactions to all three subspecies (Fig. 2). Anti-Bg IgM antibodies and anti-Bb B31 IgG antibodies were the most frequencies established in these patients. It is interesting that Bb B31 have highest IgG incidences since Ba and Bg are thought to be more common (Fig. 2*B*). Furthermore, it was

demonstrated that some patients were reactive against more than one *B. burgdorferi* species (Table SI). In additional, pleomorphic RBs were included in the ELISA assay as a novel antigen candidate. *B. burgdorferi* spirochetes could transform into RBs in unfavorable conditions that may help the bacteria to escape from the host's immune system (11-14). High RBs specific antibody response was detected in every stage of LD patients (Table I). However, the immune reaction to RBs was independent of other antigens (Table III). Consequently, patients identified as negative by the conventional diagnostic two-tier kits possibly react to RBs. Obviously, pleomorphic RBs of all three subspecies *B. burgdorferi*, particularly Bb B31 and Bg, should be considered as antigens in serodiagnostic tools.

In conclusion, the novel multiplex ELISA assay has better performance than the conventional two-tier test with higher sensitivity, specificity, PPV, and NPV (Table II). The high accuracy and strength of this novel multiplex ELISA is in its usability as a single test for LD diagnosis. Based on the immune responses evidenced in patients, C2, C6, OspE-1, OspE-2, LFA-1, *Ehrlichia*, and RBs of *B. burgdorferi* were the potential antigens to use in LD diagnostic tool. Some antigens commonly used in the commercial kits, such as p41 and OspC, would be wise alternative options to increase the sensitivity of the test, particularly for early localized infection. In additional, other common co-infections in LD patients such as *Chlamydia pneumoniae*, *Mycoplasma pneumoniae*, and *Yersinia* are plausible to include in the test . Furthermore, a serodiagnostic tool that can differentiate the disease stages, genospecies of *B. burgdorferi sensu lato*, pleomorphic forms, and co-infections in a single test is very useful for timely and accurate patient diagnosis. Prompt diagnosis and correct treatment are necessary for the improvement of Lyme disease patients' quality of life.

Acknowledgements

We thank the researchers and clinicians of BCA (Borreliose Centrum Augsburg GmbH & Co. KG, Augsburg, Germany) for providing and diagnosing the sera samples and also Seppo Meri (Haartman Institute, Helsinki, Finland) for providing Bb 297 and Ba strains used in the present study.

Disclosures

The authors have no financial conflicts of interest.

References

1. Johnson, R. C., G. P. Schmid, F. W. Hyde, A. G. Steigerwalt, and D. J. Brenner. 1984. Borrelia-Burgdorferi Sp-Nov - Etiologic Agent of Lyme-Disease. *Int. J. Syst. Evol. Microbiol.* 34: 496-497.
2. Wang, G., A. P. van Dam, I. Schwartz, and J. Dankert. 1999. Molecular typing of Borrelia burgdorferi sensu lato: taxonomic, epidemiological, and clinical implications. *Clin. Microbiol. Rev.* 12: 633-653.
3. Baranton, G., D. Postic, I. Saint Girons, P. Boerlin, J. C. Piffaretti, M. Assous, and P. A. Grimont. 1992. Delineation of Borrelia burgdorferi sensu stricto, Borrelia

garinii sp. nov., and group VS461 associated with Lyme borreliosis. *Int. J. Syst. Bacteriol.* 42: 378-383.

4. Parola, P., and D. Raoult. 2001. Ticks and tickborne bacterial diseases in humans: an emerging infectious threat. *Clin. Infect. Dis.* 32: 897-928.
5. Brouqui, P., F. Bacellar, G. Baranton, R. J. Birtles, A. Bjoersdorff, J. R. Blanco, G. Caruso, M. Cinco, P. E. Fournier, E. Francavilla, M. Jensenius, J. Kazar, H. Laferl, A. Lakos, S. Lotric Furlan, M. Maurin, J. A. Oteo, P. Parola, C. Perez-Eid, O. Peter, D. Postic, D. Raoult, A. Tellez, Y. Tselentis, B. Wilske, A. R. Escmid Study Group on Coxiella, Bartonella, and D. European Network for Surveillance of Tick-Borne. 2004. Guidelines for the diagnosis of tick-borne bacterial diseases in Europe. *Clin. Microbiol. Infect.* 10: 1108-1132.
6. Wormser, G. P., R. J. Dattwyler, E. D. Shapiro, J. J. Halperin, A. C. Steere, M. S. Klempner, P. J. Krause, J. S. Bakken, F. Strle, G. Stanek, L. Bockenstedt, D. Fish, J. S. Dumler, and R. B. Nadelman. 2006. The clinical assessment, treatment, and prevention of lyme disease, human granulocytic anaplasmosis, and babesiosis: clinical practice guidelines by the Infectious Diseases Society of America. *Clin. Infect. Dis.* 43: 1089-1134.
7. Centers for Disease Control and Prevention. 1995. Recommendations for test performance and interpretation from the Second National Conference on Serologic Diagnosis of Lyme Disease. *MMWR Morb. Mortal. Wkly. Rep.* 44: 590-591.
8. Aguero-Rosenfeld, M. E., G. Wang, I. Schwartz, and G. P. Wormser. 2005. Diagnosis of lyme borreliosis. *Clin. Microbiol. Rev.* 18: 484-509.
9. Branda, J. A., M. E. Aguero-Rosenfeld, M. J. Ferraro, B. J. B. Johnson, G. P. Wormser, and A. C. Steere. 2010. 2-Tiered Antibody Testing for Early and Late Lyme Disease Using Only an Immunoglobulin G Blot with the Addition of a VlsE Band as the Second-Tier Test. *Clin. Infect. Dis.* 50: 20-26.
10. Wilske, B., V. Fingerle, and U. Schulte-Spechtel. 2007. Microbiological and serological diagnosis of Lyme borreliosis. *FEMS Immunol. Med. Microbiol.* 49: 13-21.
11. Alban, P. S., P. W. Johnson, and D. R. Nelson. 2000. Serum-starvation-induced changes in protein synthesis and morphology of Borrelia burgdorferi. *Microbiology* 146 (Pt 1): 119-127.
12. Al-Robaiy, S., H. Dihazi, J. Kacza, J. Seeger, J. Schiller, D. Huster, J. Knauer, and R. K. Straubinger. 2010. Metamorphosis of Borrelia burgdorferi organisms--RNA, lipid and protein composition in context with the spirochetes' shape. *J. Basic Microbiol.* 50 Suppl 1: S5-17.
13. Merilainen, L., A. Herranen, A. Schwarzbach, and L. Gilbert. 2015. Morphological and biochemical features of Borrelia burgdorferi pleomorphic forms. *Microbiology* 161: 516-527.
14. Gruntar, I., T. Malovrh, R. Murgia, and M. Cinco. 2001. Conversion of Borrelia garinii cystic forms to motile spirochetes in vivo. *APMIS* 109: 383-388.
15. Barbour, A. G. 1984. Isolation and cultivation of Lyme disease spirochetes. *Yale J Biol Med* 57: 521-525.

16. Crowther, J. R. 2001. The ELISA guidebook. Humana Press, Totowa, NJ.
17. Viera, A. J., and J. M. Garrett. 2005. Understanding interobserver agreement: the kappa statistic. *Fam Med* 37: 360-363.
18. McHugh, M. L. 2012. Interrater reliability: the kappa statistic. *Biochem Med* 22: 276-282.
19. McDowell, J. V., S. Y. Sung, L. T. Hu, and R. T. Marconi. 2002. Evidence that the variable regions of the central domain of VlsE are antigenic during infection with lyme disease spirochetes. *Infect. Immun.* 70: 4196-4203.
20. Liang, F. T., and M. T. Philipp. 1999. Analysis of antibody response to invariable regions of VlsE, the variable surface antigen of Borrelia burgdorferi. *Infect. Immun.* 67: 6702-6706.
21. Embers, M. E., M. B. Jacobs, B. J. Johnson, and M. T. Philipp. 2007. Dominant epitopes of the C6 diagnostic peptide of Borrelia burgdorferi are largely inaccessible to antibody on the parent VlsE molecule. *Clin. Vaccine Immunol.* 14: 931-936.
22. Liang, F. T., A. L. Alvarez, Y. Gu, J. M. Nowling, R. Ramamoorthy, and M. T. Philipp. 1999. An immunodominant conserved region within the variable domain of VlsE, the variable surface antigen of Borrelia burgdorferi. *J. Immunol.* 163: 5566-5573.
23. Hellwage, J., T. Meri, T. Heikkila, A. Alitalo, J. Panelius, P. Lahdenne, I. J. Seppala, and S. Meri. 2001. The complement regulator factor H binds to the surface protein OspE of Borrelia burgdorferi. *J. Biol. Chem.* 276: 8427-8435.
24. Metts, M. S., J. V. McDowell, M. Theisen, P. R. Hansen, and R. T. Marconi. 2003. Analysis of the OspE determinants involved in binding of factor H and OspE-targeting antibodies elicited during Borrelia burgdorferi infection in mice. *Infect. Immun.* 71: 3587-3596.
25. Trollmo, C., A. L. Meyer, A. C. Steere, D. A. Hafler, and B. T. Huber. 2001. Molecular mimicry in Lyme arthritis demonstrated at the single cell level: LFA-1 alpha L is a partial agonist for outer surface protein A-reactive T cells. *J. Immunol.* 166: 5286-5291.
26. Gross, D. M., T. Forsthuber, M. Tary-Lehmann, C. Etling, K. Ito, Z. A. Nagy, J. A. Field, A. C. Steere, and B. T. Huber. 1998. Identification of LFA-1 as a candidate autoantigen in treatment-resistant Lyme arthritis. *Science* 281: 703-706.
27. Vojdani, A., F. Hebroni, Y. Raphael, J. Erde, and B. Raxlen. 2009. Novel Diagnosis of Lyme Disease: Potential for CAM Intervention. *Evid Based Complement Alternat Med* 6: 283-295.
28. Loa, C. C., M. E. Adelson, E. Mordechai, I. Raphaelli, and R. C. Tilton. 2004. Serological diagnosis of human babesiosis by IgG enzyme-linked immunosorbent assay. *Curr. Microbiol.* 49: 385-389.
29. Rauter, C., and T. Hartung. 2005. Prevalence of Borrelia burgdorferi sensu lato genospecies in Ixodes ricinus ticks in Europe: a metaanalysis. *Appl. Environ. Microbiol.* 71: 7203-7216.

Figure Legends

FIGURE 1. Performances of the novel multiplex ELISA assay compared with the conventional two-tier test. Serological responses in Lyme patients (n = 54) and negative controls (n = 15) tested by the commercial two-tier test and the multiplex ELISA assay were assessed. Percentages of serological positive (black panel), borderline (gray panel), and negative (white panel) of the IgM (*A*) and IgG (*B*) tests were presented. Samples with seropositive antibodies against any antigen were considered as positive; borderlines were considered as negative.

FIGURE 2. Proportion of immunity against *B. burgdorferi* genospecies and morphological forms in LD patients. The IgM (*A*) and IgG (*B*) seropositivity to full lysates spirochetes *B. burdorferi sensu stricto* B31 (Bb B31), *B. burdorferi sensu stricto* 297 (Bb 297), *B. afzelii* P12 (Ba), and *B. garinii* Fuji P1 (Bg) as well as pleomorphic round bodies (RBs) of Bb B31 were identified in LD patients. Percentages were calculated by dividing the number of samples that were positive to the particular antigen with the total responses of IgM (38 responses) and IgG (98 responses) tests.

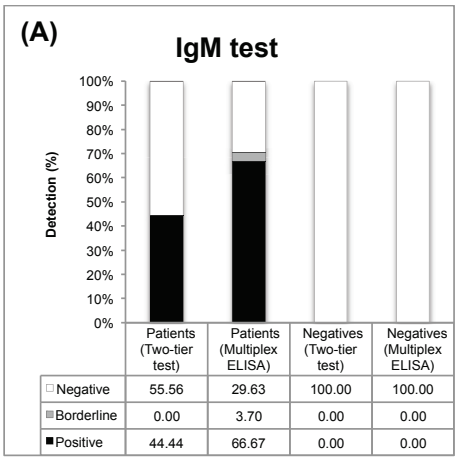
(A)
IgM test
Detection (%)
100%
90%
80%
70%
60%
50%
40%
30%
20%
10%
0%
Patients (Two-tier test)
Patients (Multiplex ELISA)
Negatives (Two-tier test)
Negatives (Multiplex ELISA)
Negative 55.56 29.63 100.00 100.00
Borderline 0.00 3.70 0.00 0.00
Positive 44.44 66.67 0.00 0.00

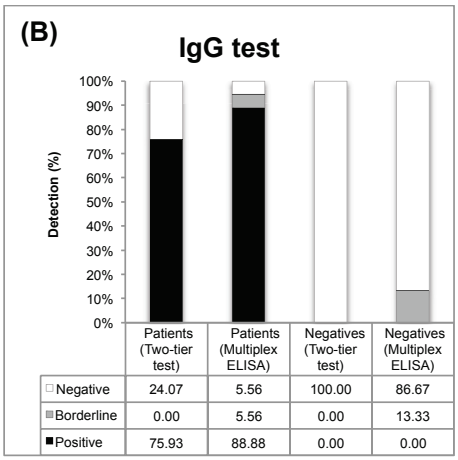
(B)
IgG test
Detection (%)
100%
90%
80%
70%
60%
50%
40%
30%
20%
10%
0%
Patients (Two-tier test)
Patients (Multiplex ELISA)
Negatives (Two-tier test)
Negatives (Multiplex ELISA)
Negative 24.07 5.56 100.00 86.67
Borderline 0.00 5.56 0.00 13.33
Positive 75.93 88.88 0.00 0.00

FIGURE 1.

Table I. Percentage of seropositive responses against the multiplex antigens obtained in the different stages of LD patients. Difference seropositive against specific multiplex antigens in three stages of LD patients. Percentages of seropositive IgM and IgG antibodies against specific antigens by the multiplex ELISA were established and compared in the different disease stages of LD. The Mann-Whitney U test was used to determine the different seropositivity to each antigen between patient groups; the level of statistical significance was considered at $p < 0.05$.

Antigen types	Multiplex antigens[a]	Percentage of seropositive response					
		Early localized LD patients (n = 5)		PTLDS[b] without co-infection patients (n = 34)		PTLDS[b] with co-infection patients (n = 15)	
		IgM	IgG	IgM	IgG	IgM	IgG
Early infection	**C2**	0	100	18	62	20	73
	C6	0	80	6	50	0	67
Disseminated infection	**OspE-1**	0	40	24	44	27	80
	OspE-2	0	60	15	47	0	87[2]
Autoimmune conditions	**LFA-1**	0	60	29	50	47	67
	Collagen I	0	40	3	32	7	13
	MBP	0	20	24	38	27	60
Co-infections	**BM**	20	40	27	32	20	60
	Ehrlichia	0	40	21	44	13	60
***Borrelia* genospecies/ pleomorphic forms (Full lysates)**	**Bb B31**	0	80	12	38	0	60
	RBs	0	100[2, 3]	18	44	7	40
	Bb 297	0	20	12	27	0	27
	Ba	0	60	6	29	0	27
	Bg	0	80[2, 3]	38	21	53[1]	27
Negative control	***E. coli***	0	40	6	12	7	13

- Significant different was determined at $p < 0.05$; [1] greater than early localized LD patients, [2] greater than PTLDS LD patients without co-infection, [3] greater than PTLDS LD patients with co-infections

[a] Antigen's abbreviations: C2 = invariant region C2 peptide 19-mer derived from variable surface lipoprotein E (VlsE), C6 = invariant region C6 peptide 25-mer derived from VlsE, OspE-1 = conserved region of outer surface protein E 1 (peptide), OspE-2 = conserved region of outer surface protein E 2 (peptide), LFA-1 = leukocyte function-associated antigen 1 protein (peptide), Collagen I = human collagen type I protein, MBP = myelin basic protein, BM = *Babesia microti* peptide, *Ehrlichia* = *Ehrlichia* peptide, Bb B31 = spirochetes of *Borrelia burgdorferi sensu stricto* B31, RBs = round bodies form of *Borrelia burgdorferi sensu stricto* B31, Bb 297 = spirochetes of *Borrelia burgdorferi sensu stricto* 297, Ba = spirochetes of *Borrelia afzelii* P12, Bg = spirochetes of *Borrelia garinii Fuji* P1, *E. coli* = *Escherichia coli* strain DH5α

[b] PTLDS = post treatment Lyme Disease syndrome

Table II. Accuracy of the multiplex ELISA assay compared to the conventional two-tier test for LD diagnosis. Sensitivity, specificity, PPV, and NPV were determined to access the reliability of the diagnostic tests. Prevalence of IgM/IgG reactions in characterized sera samples (n = 69) of 15 negative controls and 54 Lyme patients were compared to the reference clinical diagnosis by the specialized LD clinic.

Assays	Sensitivity[a] (%)	Specificity[a] (%)	PPV[a] (%)	NPV[a] (%)
Two-tier	87.04	100	100	68.18
Multiplex ELISA	98.15	100	100	93.75

- Seropositive samples were considered by any samples positive for either IgM or IgG antibodies for at least one antigen. The number of true positive, true negative, false positive, and false negative was counted from Table S1.

[a] Sensitivity = true positive/(true positive + false negative) x 100%, Specificity = true negative/(true negative + false positive) x 100%, Positive predictive value (PPV) = true positive/(true positive + false positive), and Negative predictive value (NPV) = true negative/(true negative + false negative)

493 **Table III.** Immunological response agreement of an antigen to another antigen used in the multiplex ELISA. Cohen's kappa statistic was used to
494 define the similarity immune responses to each antigen pair in Lyme patients (n = 54). Kappa (κ) coefficient values of IgM (*A*) and IgG (*B*)
495 antibodies were illustrated.

(A) IgM test	C2	C6	OspE-1	OspE-2	LFA-1	Collagen I	MBP	BM	*Ehrlichia*	Bb B31	RBs	Bb 297	Ba	Bg
C6	0.323	-	-	-	-	-	-	-	-	-	-	-	-	-
OspE-1	0.824	0.237	-	-	-	-	-	-	-	-	-	-	-	-
OspE-2	0.676	0.547	0.526	-	-	-	-	-	-	-	-	-	-	-
LFA-1	0.607	0.154	0.674	0.363	-	-	-	-	-	-	-	-	-	-
Collagen I	-0.065	-0.038	-0.068	-0.056	-0.071	-	-	-	-	-	-	-	-	-
MBP	0.118	0.085	0.143	0.256	0.021	0.237	-	-	-	-	-	-	-	-
BM	0.321	0.216	0.220	0.359	0.358	0.074	0.220	-	-	-	-	-	-	-
Ehrlichia	0.733	0.323	0.706	0.514	0.607	-0.065	0.118	0.208	-	-	-	-	-	-
Bb B31	0.229	0.649	0.156	0.395	0.080	-0.052	0.016	0.138	0.229	-	-	-	-	-
RBs	0.122	0.410	0.182	0.253	-0.021	-0.061	0.182	0.158	0.122	0.297	-	-	-	-
Bb 297	0.229	0.649	0.156	0.395	0.080	-0.052	0.156	0.270	0.229	0.460	0.498	-	-	-
Ba	0.323	1.000	0.237	0.547	0.154	-0.038	0.085	0.216	0.323	0.649	0.410	0.649	-	-
Bg	0.418	0.025	0.481	0.202	0.549	0.025	0.221	0.273	0.418	-0.046	-0.146	-0.046	0.025	-
E. coli	0.091	0.372	0.049	0.194	0.006	0.372	0.341	0.176	0.091	0.237	0.133	0.237	0.372	0.086

(B) IgG test	C2	C6	OspE-1	OspE-2	LFA-1	Collagen I	MBP	BM	*Ehrlichia*	Bb B31	RBs	Bb 297	Ba	Bg
C6	0.687	-	-	-	-	-	-	-	-	-	-	-	-	-
OspE-1	0.362	0.292	-	-	-	-	-	-	-	-	-	-	-	-
OspE-2	0.483	0.505	0.776	-	-	-	-	-	-	-	-	-	-	-
LFA-1	0.652	0.586	0.628	0.773	-	-	-	-	-	-	-	-	-	-
Collagen I	0.237	0.097	0.162	0.144	0.329	-	-	-	-	-	-	-	-	-
MBP	0.508	0.420	0.447	0.603	0.672	0.286	-	-	-	-	-	-	-	-
BM	0.203	0.387	0.485	0.507	0.419	-0.009	0.353	-	-	-	-	-	-	-
Ehrlichia	0.452	0.447	0.556	0.632	0.705	0.285	0.516	0.627	-	-	-	-	-	-
Bb B31	0.233	0.447	0.408	0.559	0.336	0.059	0.218	0.702	0.481	-	-	-	-	-
RBs	0.087	0.226	-0.110	0.044	-0.107	0.134	-0.229	0.105	0.038	0.407	-	-	-	-
Bb 297	0.277	0.412	0.272	0.388	0.438	0.105	0.402	0.129	0.397	0.397	0.095	-	-	-
Ba	0.283	0.438	0.233	0.341	0.324	0.113	0.373	0.483	0.437	0.662	0.287	0.594	-	-
Bg	0.173	0.305	0.089	0.281	0.188	0.169	0.128	0.314	0.285	0.586	0.586	0.199	0.645	-
E. coli	0.148	0.229	-0.011	0.148	0.176	0.192	0.297	0.148	0.163	0.315	0.239	0.440	0.549	0.515

- Interpretation of Kappa value: < 0 Less than chance agreement, 0.01–0.20 Slight agreement, 0.21– 0.40 Fair agreement, 0.41–0.60 Moderate agreement, 0.61–0.80 Substantial agreement, 0.81–0.99 Almost perfect agreement (17).

- Antigen's abbreviations: C2 = invariant region C2 peptide 19-mer derived from variable surface lipoprotein E (VlsE), C6 = invariant region C6 peptide 25-mer derived from VlsE, OspE-1 = conserved region of outer surface protein E 1 (peptide), OspE-2 = conserved region of outer surface protein E 2 (peptide), LFA-1 = leukocyte function-associated antigen 1 protein (peptide), Collagen I = human collagen type I protein, MBP = myelin basic protein, BM = *Babesia microti* peptide, *Ehrlichia* = *Ehrlichia* peptide, Bb B31 = spirochetes of *Borrelia burgdorferi sensu stricto*

B31, RBs = round bodies form of *Borrelia burgdorferi sensu stricto* B31, Bb 297 = spirochetes of *Borrelia burgdorferi sensu stricto* 297, Ba = spirochetes of *Borrelia afzelii* P12, Bg = spirochetes of *Borrelia garinii Fuji* P1, *E. coli* = *Escherichia coli* strain DH5α

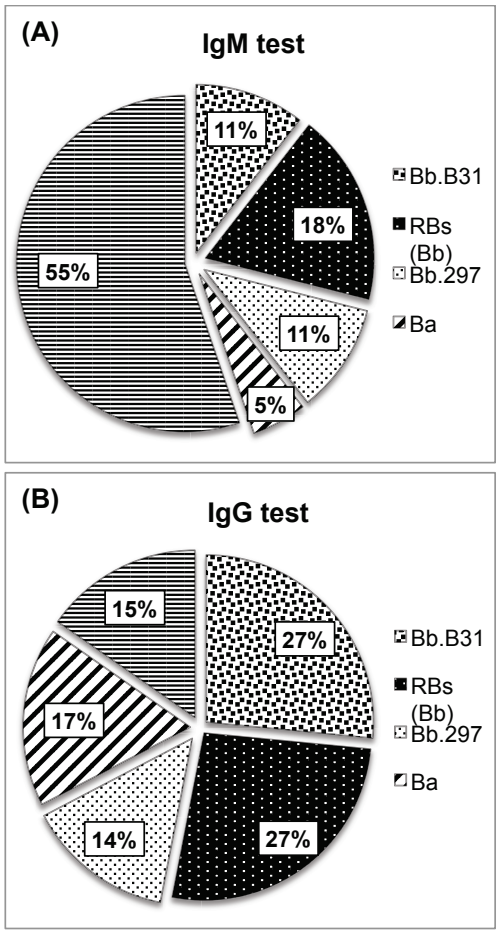
(A)
IgM test
11%
18%
55%
11%
5%
Bb.B31
RBs (Bb)
Bb.297
Ba
(B)
IgG test
15%
27%
17%
14%
27%
Bb.B31
RBs (Bb)
Bb.297
Ba

FIGURE 2.